1-1-1968

Determination of bond strengths by kinetic and thermochemical methods.

William D. K. Clark
University of Windsor

DETERMINATION OF BOND STRENGTHS BY KINETIC AND THERMOCHEMICAL METHODS

BY

WILLIAM D. K. CLARK

A DISSERTATION

Submitted to the Faculty of Graduate Studies through the
Department of Chemistry in Partial Fulfillment
of the Requirements for the Degree of
Doctor of Philosophy at the
University of Windsor

Windsor, Ontario

1968

THIS DISSERTATION HAS BEEN EXAMINED AND APPROVED BY:

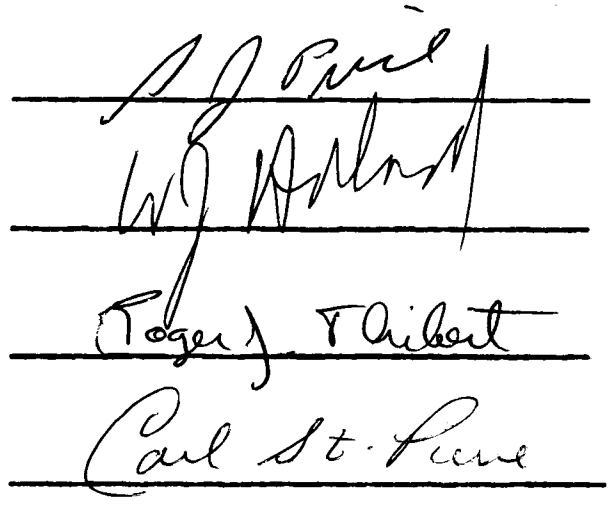

To Joyce

A patient, understanding, and
loving wife.

ABSTRACT

A. Pyrolysis of Ethylbenzene

The pyrolysis of ethylbenzene has been studied in a toluene carrier flow system from 910°K to 1089°K using total pressures from 20.4 mm to 37.9 mm with toluene/ethylbenzene ratios of 37 to 170. Benzene was also used as carrier. The products from the pyrolysis included methane, ethylene, hydrogen, benzene, and styrene. First-order rate constants

$$C_6H_5CH_2CH_3 \longrightarrow C_6H_5CH_2 + CH_3 \qquad [1]$$

for reaction [1], calculated from the methane produced, were independent of pressure, contact time, surface, carrier, and the carrier to ethylbenzene ratio. A least squares treatment of the data gave

$$\log_{10}k_1 = 14.7 - (70,100/2.3RT).$$

This is in excellent agreement with the results obtained by Esteban, Kerr, and Trotman-Dickenson using primarily an aniline carrier technique. The activation energy may be equated to $D[C_6H_5CH_2\text{-}CH_3]$.

Ethylbenzene decomposed mainly by reaction [1]. However, under the experimental conditions used, reactions [2] and [3] accounted for

$$C_6H_5CH_2CH_3 \longrightarrow C_6H_6 + C_2H_4 \qquad [2]$$

$$C_6H_5CH_2CH_3 \longrightarrow C_6H_5C_2H_3 + H_2 \qquad [3]$$

1 to over 50% of the decomposition. Reaction [2] is largely a heterogeneous process, while [3] occurred in the gas phase. Secondary radical attack on the ethylbenzene was of minor importance.

B. Thermochemistry

The enthalpy of reaction [4] in chloroform solution at 25°C and 1 atmosphere pressure

$$In(CH_3)_3,c + 3Br_2(soln.) \longrightarrow InBr_3(soln.) + 3CH_3Br(g) \quad [4]$$

is -162.5 kcal/mole. The enthalpy of reaction [5] under identical conditions

$$In(CH_3)_3,c, + 2Br_2(soln.) \longrightarrow CH_3InBr_2(soln.) + 2CH_3Br(g) \quad [5]$$

is -124.7 kcal/mole. With the enthalpy of reaction [4], $\Delta H^{\circ}_{f298}[In(CH_3)_3,c] = 29.5$ kcal/mole, which with the enthalpy of reaction [5], gives $\Delta H^{\circ}_{f298}[CH_3InBr,c] = -85.5$ kcal/mole, and with $\Delta H_{sublimation}[In(CH_3)_3,c] = 11.6$ kcal/mole gives $\Delta H^{\circ}_{f298}[In(CH_3)_3,g] = 41.1$ kcal/mole. Combining this last value with $\Delta H^{\circ}_{f298}[CH_3,g] = 33.2$ kcal/mole and $\Delta H^{\circ}_{f298}[In,g] = 58.2$ kcal/mole gives $\bar{E}(In-CH_3) = 38.9$ kcal/mole. From previous kinetic studies, $D[(CH_3)_2In-CH_3 + D\ In-CH_3] = 87.9$ kcal/mole. Hence $D[CH_3In-CH_3] = 28.8$ kcal/mole.

In preparation for more refined studies on metal alkyl compounds, the calibration of a rotating bomb calorimeter was carried out. A thermistor was used as the temperature sensing element. The relationship between temperature and

resistance could be represented by the three equations

$$\ln R = \frac{A}{T} + B \qquad [6]$$

$$\frac{1}{\ln R} = CT + D \qquad [7]$$

and

$$\ln R = \frac{A^1}{T+\theta} + B^1 \qquad [8]$$

to about the same degree of accuracy. The variation of temperature with time for the calorimeter followed the equation

$$\frac{dT}{dt} = u + g(T_j - T). \qquad [9]$$

Numerical techniques were used to test equations [6] through [9], and to evaluate $\int_{t_1}^{t_2} T dt$ in the calculation of the temperature rise for combustion experiments. The degradative oxidation of trimethylindium was not amenable to quantitative thermochemical study.

ACKNOWLEDGEMENTS

I would like to take this opportunity to acknowledge with the deepest gratitude Dr. S. J. W. Price whose help, guidance, and encouragement made this work possible.

I would also like to thank Messrs. Otto and Peter Brudy and the Central Machine Shop at this university for their excellent work in the construction of the rotating bomb calorimeter.

I am also grateful to the National Research Council of Canada for the bursary and studentships awarded to me during the course of this work.

TABLE OF CONTENTS

	Page
DEDICATION	ii
ABSTRACT	iii
ACKNOWLEDGEMENTS	vi
LIST OF TABLES	ix
LIST OF FIGURES	x
TABLE OF NOMENCLATURE	xii
CHAPTER	
I Introduction	
Introductory Concepts and Definitions	1
Determination of Bond Dissociation Energies	3
Determination of Heats of Formation	5
Numerical Methods and Computer Technique	6
II Theoretical Considerations	
Kinetic Determination of Bond Energies	8
Calorimetric Determination of Bond Energies	12
Numerical Methods of Analysis	33
III Pyrolysis of Ethylbenzene	
Preparation of Materials	41
Apparatus and Procedure	41
Results and Discussion	50
IV Reaction Calorimetry of Trimethylindium	
Preparation of Materials	79
Apparatus and Procedure	81
Results and Discussion	90
V Rotating Bomb Calorimetry of Trimethylindium	
Preparation of Materials	96
Apparatus and Procedure	96
Results and Discussion	107

CHAPTER Page

VI Suggestions for Further Research

Trimethylindium 135
Trimethylthallium 136
Trimethylgallium 137

APPENDIX 138

BIBLIOGRAPHY 154

VITA AUCTORIS 158

LIST OF TABLES

Table		Page
1.	Pyrolysis of Ethylbenzene, Fundamental Data and the First Order Rate Constant	52
2.	Pyrolysis of Ethylbenzene, Products of the Reaction	55
3.	Pyrolysis of Ethylbenzene, Product Ratios With Respect to Ethylbenzene and Methane	58
4.	Pyrolysis of Benzene, Fundamental Data, Products, and First-Order Rate Constants	67
5.	Rate Constants for the Molecular Breakdown of Ethylbenzene	72
6.	Reaction of Trimethylindium With Various Substances	92
7.	Enthalpy of Reaction of Trimethylindium with Bromine in Chloroform Solution	92
8.	Calibration of Thermistors against Calibrated Thermometers	109
9.	Test for the Polynomial Curve-fitting Program	111
10.	Polynomial Curve Fits to the Thermistor Calibration Data	112
11.	Data for the Plot of dT/dt vs T	119
12.	Results of Tests to Evaluate the Best Method of Numerical Integration	124
13.	Determination of the Energy Equivalent of the Calorimeter	126
14.	Convergence of Values in the Calibration Program .	128
15.	Heat of Combustion of Auxiliary Materials	130

LIST OF FIGURES

Figure		Page
1.	Time-temperature curve for a bomb-calorimetric experiment	26
2.	Schematic diagram of toluene carrier flow system	42
3.	Ethylbenzene injection system	45
4.	Placement of heating windings on furnace block for temperature profile control	46
5.	A typical temperature profile	46
6.	Schematic diagram of the injection system used for gas analysis	49
7.	Arrhenius plot of the first-order rate constants for the pyrolysis of ethylbenzene	63
8.	Arrhenius plot of the first-order rate constants for the pyrolysis of benzene	68
9.	Arrhenius plot of the first-order rate constant for reaction [12]	73
10.	Arrhenius plot of the first-order rate constant for reaction [11]	74
11.	Apparatus for the production of trimethylindium	80
12.	Reaction calorimeter for trimethylindium study	82
13.	Circuit diagram for the electrical calibration of the reaction calorimeter used in the trimethylindium study	83
14.	Storage vessel for the 1N bromine in chloroform solution	84
15.	Vessel for release of indium tribromide into chloroform	86
16.	Variation of the heat of reaction of trimethylindium with bromine in chloroform solution at 25°C	89

Figure Page

17. Photograph of the rotating bomb calorimeter 94

18. Photograph of the calorimeter bucket 98

19. Diagram of the bomb head 105

20. Thermistor calibration: plot of 1/lnR vs T 115

21. Thermistor calibration: plots of lnR vs 1/T, B, and lnR vs 1/(T+θ), A 116

22. Thermistor calibration: plot of T vs lnR 117

23. Characterization of the calorimeter: plot of dT/dt vs T 118

24. Test curve generated from two hyperbolas for evaluation of the best method of numerical integration 122

TABLE OF NOMENCLATURE

ΔH_f^o	Standard heat of formation at 298°K
$\Delta H_{process}$	Heat of process indicated
D	Bond Dissociation Energy
K	Transmission coefficient
k	Boltzmann's constant
k_i	Rate constant for process i
h	Planck's constant
T	Absolute temperature
F(T)	Total partition function
f_i	Partition function of degree of freedom i
m	Mass of a molecule
R	Universal gas constant
A,B,C	Moments of inertia of a molecule
ν	Vibrational frequency
E_{exp}	Experimental activation energy
$\bar{E}$	Mean or average bond dissociation energy
E	Internal energy
H	Enthalpy
P	Pressure
V	Volume
C_i	Heat capacity at constant thermodynamic variable i
S	Entropy

C_{sf}	Energy equivalent of the calorimetric system
q_i	Heat from ignition energy
q_n	Heat from formation of nitric acid
$q_{substance}$	Heat from combustion of substance
E_c	Heat of combustion

CHAPTER I

INTRODUCTION

Introductory Concepts and Definitions

The strength of the chemical bond is of prime importance for the quantitative treatment of chemical reactions. The exothermicity of endothermicity of a chemical process is determined by which bonds are formed and which bonds are broken. This liberation or absorption of energy in conjunction with structural considerations of the products and reactants determines the feasibility of chemical reaction. The rupture of a particular bond in one molecule and the stability of the seemingly same bond in another molecule gives information as to the differences in electronic configuration of the two cases and sheds new light on the existing theories of valence. The contrast in the dissociation energies in the N-N bond in nitrogen tetroxide and the N-N bond in the nitrogen molecule (12.9 kcal and 225.0 kcal respectively (1)) illustrates dramatically the differences in the binding forces between the nitrogen atoms. Therefore, the concept of a bond energy is important in the areas of chemical kinetics and is integrally related in the concept of the chemical bond.

The dissociation energy, $D(R_1\text{-}R_2)$, in the molecule (or radical) M is the endothermicity of the reaction in which M

is decomposed into two fragments R_1 and R_2 formed by breaking the bond R_1-R_2 (2), provided the recombination of R_1 and R_2 proceeds with zero activation energy.

$$M \longrightarrow R_1 + R_2 - D(R_1\text{-}R_2) \text{ kcal/mole.} \quad [1]$$

The endothermicity is computed for the reactants and products in the gaseous phase, at zero pressure and at 0° K.

The heat of atomization of a molecule is equal to the sum of the dissociation energies of all the bonds that have to be broken to leave a molecule as separate atoms (2). In the case of water:

$$H_2O \longrightarrow H + OH - D(H\text{-}OH)$$

$$OH \longrightarrow H + OH - D(O\text{-}H)$$

The heat of atomization is D(H-OH) + D(O-H). The dissociation energies of a bond between any two given atoms but referred to different fragments will not usually be equal. For example:

$$D(H\text{-}OH) = 118 \text{ kcal/mole},$$

$$D(O\text{-}H) = 100 \text{ kcal/mole}.$$

The average bond energy, $\bar{E}$, for the molecule AX_n is defined as 1/n of its heat of atomization. Therefore in the case of the water molecule, the average bond energy from above is 109 kcal/mole.

Thermochemical measurements allow the determination of the heats of formation of a substance in its standard state from elements in this standard state (3). As such, for a compound ABC, it is the heat of the reaction A + B + C $\longrightarrow$ ABC where A, B, and C are elements in their standard states.

The usual standard state for elements is defined as their most stable form which exists at 298°K and unit fugacity (4). In such a state, the elements are considered to have zero enthalpy. For water again,

$$H_2(g) + O_2(g) \xrightarrow[1\ atm]{298^\circ K} H_2O\ (l),$$

$$H^\circ_{f_{298}}(H_2O,l) = H_{rxn} + H^\circ_{f_{298}}(H_2, g) + H^\circ_{f_{298}}(O_2, g),$$

$$H^\circ_{f_{298}}(H_2O,l) = H_{rxn},$$

as the values of the heat of formation of oxygen and hydrogen in their standard states are zero.

From heat of formation data for products and reactants, it is also possible to arrive at average bond energies. For the process,

$$H_2O(g) \longrightarrow 2H(g) + O(g)$$

the heat of the reaction is the heat of atomization and as two bonds are broken,

$$\bar{E} = H_{rxn}/2 \qquad [2]$$

Therefore bond dissociation energies and heats of formation of atoms or radicals are integrally related.

Determination of Bond Dissociation Energies

Methods of estimating bond dissociation energies by investigating the process of bond-breaking may be divided into three groups, according to the form in which energy is supplied to the molecule being dissociated (5). Methods where the energy is supplied in the form of radiation are based on the investigation of absorption spectra, predissociation phenomena, photodecomposition, and photosensitized

decomposition. The application of the first two methods is limited to simple molecules due to the complexity of the spectra involved. The latter two methods only give an upper limit for the respective bond dissociation energies.

The electron impact method has the energy supplied by a beam of electrons. Again, this method only gives an upper limit to the dissociation energy. The form of the dissociation is into ions rather than atoms or radicals and leads to difficulty sometimes in the interpretation of the ionization potential (5).

The third group includes all methods in which energy supplied to the molecule is thermal energy. These methods consist of two subgroups: the equilibrium method and the kinetic method.

The equilibrium method (2) is based on the measurement of the equilibrium constant of the gaseous reaction

$$R_1R_2 \longrightarrow R_1 + R_2 \quad [3]$$

where R_1 and R_2 are the radicals or atoms formed by the rupture of the bond in question. This method is particularly suited for studies of the dissociation energies of diatomic molecules, but is found lacking for the cases where R_1, R_2 are radicals. The equilibrium in this latter case is disrupted by the attack of the radicals on the parent species, and/or reactions between R_1 and R_2 which lead to products other than the parent molecule.

In the kinetic method, the assumption is made that the reverse process in reaction [1] has zero activation energy.

This assumption has strong experimental evidence for small radicals and atoms (6). As a result, the activation energy for the unimolecular dissociation process is equated to the dissociation energy of the R_1-R_2 bond (5). The required activation energy can be computed from the temperature coefficient of the unimolecular dissociation rate constant which is the slope of a plot of the log of the rate constant vs reciprocal temperature. The accuracy of the desired value depends on the accuracy of the rate constant, and the length of the temperature range. Systemic errors in the values of the rate constants due to side reactions of the radicals R_1 and R_2 can be minimized with the suppression of such reactions by a radical scavenger.

Determinations of Heats of Formation

Heats of reaction, and hence heats of formation are measured calorimetrically. The type of calorimeter used depends upon the type of reaction involved, the amount of heat exchanged, and the duration of the reaction (7). Most calorimetric methods have in common the measurement of the temperature rise of a known amount of calorimetric fluid which has exchanged heat with the reaction or process under study. The energy equivalent or heat capacity of these calorimetric systems is determined by calibration with either electrical energy or a reaction of known heat content.

The flame calorimeter (7,8) measures the heat generated by the combustion of various vapours or gases in oxygen at constant pressure. The apparatus is best suited to permanent

gases or substances with very high vapour pressure.

The reaction calorimeter is the term used for the apparatus which measures the heat liberated when a substance reacts with something other than oxygen. Common reactions employed include hydrogenation, hydrohalogenation, halogenation, and hydrolysis. The apparatus is usually of a constant pressure type and may operate under isothermal or adiabatic conditions. The amount of energy liberated in the reaction is of the order of several hundred calories. While this type of calorimetry will often allow reaction of compounds which do not undergo suitable reactions with oxygen, necessary auxiliary data is sometimes difficult to find.

The bomb calorimeter is the oldest and best characterized of all the calorimeters known (7). It is a constant volume apparatus in which substances react with oxygen at moderate pressures to form simple compounds. The amount of energy released is usually several thousand calories. The heat of formation values for the products commonly formed are well established, and the instrumentation for measuring the energy released is quite adequate.

Numerical Methods and Computer Technique

One of the newest tools at the chemist's disposal is the digital computer. The high speed and accuracy of this machine reduce hours of tedious work to seconds, and carries it out error free. The adaptation of the methods of numerical analysis from the desk calculator to the digital computer allows the solution of problems and processing of data in

many different ways in order to see which is the best.

For instance, gas kinetic data can be sorted according to the various parameters involved so that the distribution of products can be seen more readily in terms of pressure increases or variations in temperature. The area under a portion of a time-temperature curve in a calorimetric experiment can be found and this alleviates square counting or the use of approximate treatments of data. A set of data can perhaps be better fit by something other than a linear equation. A polynomial curve fitting program would try polynomials of various degrees and evaluate the standard deviation with each so that a judgment could be made as to which fit the data best.

The digital computor is a powerful aid if for no other reason than its unfailing accuracy and speed.

CHAPTER II

THEORETICAL CONSIDERATIONS

Kinetic Determination of Bond Energies

a) Limits of the Kinetic Method

Transition state theory (9) predicts that the rate constant for a unimolecular dissociation is

$$k = K \frac{kT}{h} \frac{F^*(T)}{Fa(T)} e^{-D/RT} \qquad [4]$$

where a denotes the initial state and * that of the activated complex. The total partition functions F*(T) and Fa(T) can be separated into translational, rotational, and vibrational contributions.

The translational partition function

$$f_t(T) = (2\pi mkT)^{3/2}/h^3 \qquad [5]$$

will be the same for the normal molecule and the activated complex. The rotational partition function will be

$$f_r(T) = \frac{8\pi^2 IkT}{\sigma h^2} \qquad [6]$$

for a linear molecule and for a non-linear molecule

$$f_r(T) = \frac{8\pi^2 (2\pi kT)^{3/2} (ABC)^{1/2}}{h^3} \qquad [7]$$

Likewise the rotational partition function for the normal molecule and activated complex will be similar.

If each mode of internal vibration behaves as a harmonic

oscillator, the expression for the rate constant becomes

$$k_1 = K \frac{\sigma a}{\sigma *} \frac{kT}{h}\left(\frac{A*B*C*}{AaBaCa}\right)^{1/2} \frac{\prod^{3n-7}(1-e^{-h\nu*/k})^{-1}}{\prod^{3n-6}(1-e^{-h\nu a/k})} e^{\frac{-D}{RT}} \quad [8]$$

At relatively low temperatures such that $h\nu \gg kT$, the terms $(1-e^{-h\nu/kT})$ tend to unity and k_1 becomes

$$k_1 = K \frac{\sigma a}{\sigma *} \left(\frac{A*B*C*}{AaBaCa}\right)^{1/2} \frac{kT}{h} e^{-D/RT} \quad [9]$$

If the temperature is relatively high such that $h\nu \ll kT$ and the terms $(1-e^{-h\nu/kT})$ may be replaced by $kT/h\nu$,

$$k_1 = K \frac{\sigma a}{\sigma *} \left(\frac{A*B*C*}{AaBaCa}\right)^{1/2} \frac{\prod^{3n-6}\nu a}{\prod^{3n-7}\nu *} e^{-D/RT} \quad [10]$$

For the case $h\nu \gg kT$ (equation 9), taking the logarithms of both sides and differentiating with respect to T gives

$$\frac{d \ln k_1}{dT} = \frac{D}{RT^2} \quad [12]$$

Therefore, the Arrhenius activation energy, $E_{exp} = D$. Using the same operations for the case $h\nu \ll kT$ gives

$$\frac{d \ln k_1}{dT} = \frac{D + RT}{RT^2} \quad [11]$$

Therefore $E_{exp} = D + RT$. Hence

$$D \leqslant E_{exp} \leqslant D + RT \quad [13]$$

The magnitude of RT at 1000°K is less than 2 kcal so that the bond dissociation energy may be measured as accurately as the experimental activation energies. Also in the

preceeding discussion, it should be noted that the rate constants measured are those in the pressure independent region of the reaction.

b) Toluence Carrier Technique

In order to measure the activation energy for the process

$$R_1R_2 \longrightarrow R_1 + R_2 \qquad [3]$$

accurately, it is necessary to be able to determine the rate of the primary dissociation with accuracy. The first prerequisite to accomplish this is that the bond under study is considerably weaker than any other bonds in the molecule.

The primary dissociation process is followed by subsequent reactions of the radicals either with themselves or undecomposed molecules. A direct measure of radical concentration would only give the steady state concentration which is not proportional to the time of reaction (2).

The use of a flow system in which reactants pass through the furnace in a very short time so that the radicals have no time for subsequent reactions provides some means of isolating the primary step. The radicals are counted by some method as they leave the furnace. However, even very high flow rates would not likely prevent some reaction and would probably lead to problems of thermal equilibrium.

The estimation of the rate of initial dissociation is best accomplished by removing the radicals by the use of a scavenger. However, the removal of radicals, except by recombination, produces radicals and thus there is a danger

of a chain reaction. The kinetics of a chain process are very complex and would lead to difficulty in determining the initial rate of decomposition.

Toluene overcomes the threat of possible chain processes by producing benzyl radicals on reaction with other radicals. Under the experimental conditions usually employed, benzyl radicals are stable and either pass out of the hot zone to dimerize in a cooler region, or combine in the hot zone with other free radicals. Radicals, R, produced in an initial bond break, react with toluene as follows:

$$R + C_6H_5CH_3 \longrightarrow C_6H_5CH_2 + RH \qquad [14]$$

If reaction [14] represents the only appreciable fate of R, then the measurement of the rate of formation of RH allows one to calculate the rate determining initial decomposition as reaction [14] is fast.

The main limitations of the method are that the bond being broken in the compound under investigation must be much weaker than the C-H bond in the side chain of toluene, preferably by at least 10 kcal (10). The radicals produced must react rapidly with toluene to produce a stable molecule (2). The toluene carrier technique may be used at temperatures where toluene itself decomposes if the products coming from the fragmentation of the studied compound are identifiable. Even if the products are not distinguishable, suitable corrections for the decomposition of the toluene can be made (11). However, any extensive decomposition of toluene would cause problems due to the inability to pump

away the products rapidly enough.

Calorimetric Determination of Bond Energies

a) General Introduction

In a thermochemical investigation, the experimenter attempts to determine the quantity of energy associated with a unit amount of a given chemical reaction or physical process (8). As part of this investigation, it is necessary to determine the energy and the extent of the process under study, the nature of the thermodynamic property involved, the temperature of the process, and corrections needed to refer the reaction to some standard or reference states.

In order to attach significance to the measured energy associated with a reaction or process, it is necessary to describe the given reaction or process adequately with respect to all factors which may influence the value of the energy. Among these factors are temperature, pressure, state of the material, and concentration. Each factor should be specified with an accuracy warranted by its effect on the value of the energy. With the products and reactants of the reaction so defined, it becomes a simple matter to correct each quantity to its thermodynamic standard state. Tabulation of standard state data allows calculation of new standard state data from measured heats of reactions.

In addition to adequately specifying the given process or reaction, it is important to specify the thermodynamic property which is measured, as either the change in internal energy, ΔE, or the change in heat content or enthalpy, ΔH.

According to the first law of thermodynamics, for any process

$$\Delta E = q + w + u \qquad [15]$$

where q is the heat energy absorbed, w is the PV work done on the system and u is any other energy absorbed by the system. Usually u is zero as it deals with energy terms due to changes in the motion of the entire system, variations in electric or magnetic field strength etc., which are usually constant.

For a process at constant volume, V, $P\Delta V = 0$. Therefore $\Delta E = q$, the heat absorbed by a process occurring in a calorimeter at constant volume.

For a process at constant pressure, $w = -P\Delta V$. Substituting in equation [15] gives

$$\Delta E = q - P\Delta V \qquad [16]$$

Hence

$$\Delta E + P\Delta V = q \qquad [17]$$

and

$$\Delta E + \Delta PV = \Delta(E + PV) = q \qquad [18]$$

Defining

$$E + PV = H, \qquad [19]$$

one can write

$$\Delta H = q. \qquad [20]$$

Therefore for a process in a calorimeter at constant pressure, the heat absorbed by the process is the change in enthalpy, ΔH. For any specified process, the difference between the value of ΔH and ΔE may be evaluated from the

relation

$$\Delta H = \Delta E + \Delta PV. \qquad [21]$$

The thermochemical experiment consists of two parts: the calorimetric part, which involves the determination of the quantity of energy evolved by the reaction or process; and the chemical part, which involves the measurement of the amount of the given reaction or process.

In the calorimetric part, the energy equivalent of the calorimeter is determined either by use of a known amount of electrical energy or a known amount of chemical reaction with a well characterized reaction heat. The energy equivalent is defined as the known amount of energy divided by the temperature rise it produces. It is therefore evident, that for the same calorimeter, an equal temperature rise produced by a reaction of unknown energy, will have released the same energy.

In the chemical part, the prime interest is in determining the nature and completeness of the chemical reaction studied. The reaction should preferably produce a very limited number of products in well defined thermodynamic states. It is then possible to determine the completeness of the reaction by measuring the amount of one of the reactants consumed, or more often by measuring the amount of the products. For example in the following combustion:

$$C_6H_{14}(liq) + 9\tfrac{1}{2}O_2(g) \longrightarrow 6CO_2(g) + 7H_2O(liq)$$

it is easier to measure the CO_2 produced than the hexane consumed as the latter may contain small amounts of dissolved

air and moisture which require corrections. Since the stoichiometry of hydrocarbon combustion is well known, there is no need to determine the quantity of water produced.

As most calorimetric investigations are not carried out at the temperature commonly used in the definition of the standard state of a substance, namely 298°K, some means must be found of correcting for the variation of the heat of reaction with temperature. For any process at constant pressure

$$\Delta H = H \text{ products} - H \text{ reactants}$$

and differentiating with respect to temperature,

$$\frac{\partial \Delta H}{\partial T} = \frac{\partial H \text{ products}}{\partial T} - \frac{\partial H \text{ reactants}}{\partial T} \qquad [22]$$

By definition, the change in enthalpy with respect to temperature at constant pressure is the heat capacity at constant pressure. Therefore

$$\frac{\partial \Delta H}{\partial T} = (C_p) \text{ products} - (C_p) \text{ reactants} = \Delta Cp \qquad [23]$$

and in a similar manner for a constant volume process,

$$\frac{\partial \Delta E}{\partial T} = \Delta C_v . \qquad [24]$$

Therefore it is only necessary to know the difference in heat capacities of the products and reactants in order to determine the variation of the heat of reaction with temperature.

Also, the calorimetric investigation may not be done at the defined pressure in the standard state definition. From the first and second laws of thermodynamics

$$dE = TdS - PdV \qquad [25]$$

Therefore

$$\frac{\partial E}{\partial T} dT + \frac{\partial E}{\partial P} dP = T \frac{\partial S}{\partial T} dT + T \frac{\partial S}{\partial P} dP - P \frac{\partial V}{\partial T} dT - P \frac{\partial V}{\partial P} dP$$

and

$$\left(\frac{\partial E}{\partial P} - T \frac{\partial S}{\partial P} + P \frac{\partial V}{\partial P}\right) dP + \left(\frac{\partial E}{\partial T} - T \frac{\partial S}{\partial T} + P \frac{\partial V}{\partial T}\right) dT = 0$$

The only way for the relation to hold is if the bracketed expressions are zero. Therefore the internal energy change as a function of pressure is given by

$$\frac{\partial E}{\partial P} = T \frac{\partial S}{\partial P} - P \frac{\partial V}{\partial P} . \qquad [26]$$

As

$$\frac{\partial S}{\partial P} = - \frac{\partial V}{\partial T},$$

therefore

$$\frac{\partial E}{\partial P} = -T \frac{\partial V}{\partial T} - P \frac{\partial V}{\partial P} \qquad [27]$$

and it is necessary to find $\partial V/\partial T$ and $\partial V/\partial P$ data for the quantities concerned. Similarly for the enthalpy

$$H = E + PV \qquad [19]$$

and $\frac{\partial H}{\partial P} = \frac{\partial E}{\partial P} + P \frac{\partial V}{\partial P} + V.$

Upon substitution and simplification,

$$\frac{\partial H}{\partial P} = -T \frac{\partial V}{\partial T} + V. \qquad [28]$$

The temperature which is assigned to a reaction is determined by the temperatures at which the reactants and products enter and leave the calorimeter (8). If all of the reactant material is in the calorimeter at the beginning

of the experiment at temperature T_A, and all of the product material is in the calorimeter at the end of the experiment at temperature T_B, one has the choice of choosing T_A or T_B as the assigned temperature. If the energy equivalent of the calorimeter is taken as that of the final system, or initial system, the assigned temperatures are respectively T_A and T_B.

b) Moving Bomb Calorimetry

The most well developed area of thermochemistry is the degradative oxidation of organic compounds containing the elements carbon, hydrogen, and oxygen (7). The reaction is carried out at constant volume under a pressure of 25 to 30 atmospheres of oxygen. The reaction vessel is a corrosion resistant steel tubular vessel of about 350 ml. internal volume with a screw-on cap containing valves for the introduction and emission of gases. This vessel is termed a bomb. The bomb, containing the sample, is immersed in a can of water, the temperature of which rises when the sample is ignited by electrical means. The bomb and can of water are surrounded by a constant temperature bath. From the measured temperature rise of the water in the can, and a previous determination of the energy equivalent of the system, the amount of heat liberated by the combustion of the sample can be found.

The limiting part of a thermochemical investigation is the chemical rather than the calorimetric part (12). For compounds containing only carbon, hydrogen, and oxygen it is

not difficult to obtain data to specify the mass, purity, and nature of the primary reactant, and the masses, chemical nature, and states of the products. However, for compounds containing other elements than the above three, such as sulphur, halogen, or metal, the products frequently cannot be defined rigorously as to their chemical nature, physical state, or concentration.

The combustion of an organometallic compound in a conventional static bomb calorimeter results in the production of inorganic compounds of the metal as well as the usual products from the organic part of the molecule. The inorganic species can be quite complex usually yielding more than one compound, each of which may be formed in different allotropic modifications. The chemical species and allotropic modifications may be in ill-defined physical states. For example, the heat content of amorphous material usually depends on the conditions of formation. Also differences in particle size of crystalline material results in varying heat content for the different sizes (12).

The rotating-bomb or moving-bomb calorimeter provides a means for producing a final state of the bomb process that is easy to characterize both chemically and thermodynamically (12). A suitable solution is placed in the bomb so that the solid products of combustion can be dissolved. A means is available for imparting rotation to the bomb after the combustion reaction is finished, and assures the rapid solution of the solid products in the bomb. The final state

then consists of a gas phase and a liquid phase containing the metal in a single oxidation state, with both phases homogeneous and in equilibrium with one another.

Several rules must be observed in selecting a suitable initial solution (13):

i) The solution should preferably be acid or neutral to minimize the solubility of carbon dioxide. However an alkaline solution, if used, should dissolve all the carbon dioxide produced in the bomb.

ii) The solution should not react with the interior of the bomb or its fittings.

iii) The solution should dissolve the solid products of combustion within a reasonable time, preferably only a few minutes after the bomb rotation is started.

iv) If side reactions occur, such as the oxidation of a reducing agent used to reduce the metal to a certain oxidation state, thermochemical data of adequate accuracy for the required corrections should be available.

v) Established analytical methods of adequate accuracy should be available to determine the extent of all side reactions. Side reactions producing gaseous products should be avoided.

c) Organometallic Compounds and Comparison Experiments

In all accurate combustion calorimetry, the investigator must correct the heat evolution he measures, which is for the actual process in the bomb, to the idealized combustion reaction with all reactants and products in their

standard states. The rotating bomb method while overcoming the major problem of final state definition presents some minor complexities in the corrections to standard states.

The physical constants needed for the corrections peculiar to organometallic compounds (13) include:

i) values for the initial and final bomb solutions as functions of composition of the following properties: density, vapour pressure, solubility of bomb gases, $\partial E/\partial P$, and heat capacity;

ii) values of the heat of dilution of substances that are in aequeous solution;

iii) thermochemical data needed to apply corrections for all side reactions; and

iv) all data needed in correcting for unusual experimental details - for example, the heat capacity of materials present in the combustion but not in the calibration experiments.

As a relatively large volume of solution, about 50 ml, is used in the rotating-bomb method, the dissolving of the bomb product gases, particularly the carbon dioxide in the solution represents a large thermal correction. However, the solubility and heat of solution of carbon dioxide seldom are known with the desired accuracy or not at all for a particular multicomponent system. Also as a unique multicomponent system is present, the experimental values may not be available for all the needed physical constants of the solution, such as $\partial E/\partial P$ and heat capacity.

In addition, the calibration of the calorimeter is usually done by the combustion of a certain weight of benzoic acid which has a certified heat of combustion. One of the conditions in using the benzoic acid is that the bomb contains only one cc. of water. The use of a 50 cc. multicomponent solution requires the use of an uncertain correction.

To overcome these minor difficulties, a comparison experiment is performed. The comparison experiment involves the combustion of a combination of benzoic acid and a hydrocarbon oil to yield the same amounts of energy and carbon dioxide as in the actual experiment. Also, a sample of an inorganic compound of the metal which is soluble in the bomb solution is placed in a second crucible and spilled into the solution when the rotation is started. This procedure serves to give a final state identical to that of the actual experiment.

After correction for the heat of combustion of the organic sample, the results of the comparison experiment yield a value of the heat of solution of the inorganic compound in the initial bomb solution to form the final solution. By combination of thermochemical equations, which may include those for small dilution effects, the combustion reaction may be referred to the inorganic compound of the metal as product, with the latter in a physical state for which the heat of formation is well known. Because the final states of the comparison and actual experiment are nearly identical, the corrections to standard states, including the

important term for the solution of carbon dioxide in the final bomb solution, are nearly the same for both experiments. Therefore errors in corrections caused by inaccurate data cancel in the final values of the heat of combustion as referred to the inorganic compound of the metal. Similarly, errors, that occur because the calorimetry is different than that in the calibration experiments with benzoic acid, will be nearly the same, and then effectively cancel in the final value of the heat of combustion.

To avoid corrections due to oxidation or solution of the bomb interior, the interior surfaces of the bomb as well as the crucible used for holding the sample must be inert to the conditions used. A platinum lined interior, with platinum fittings, and a platinum crucible offer extreme inertness to both oxidation and solution. However, the combustion of organometallic compounds sometimes leads to the formation of molten metal or molten metal oxides which can splatter and damage the thin platinum liner, or alloy with the crucible. In this case, alternative materials such as liners and crucibles of nickel-chromium alloy or stainless steel may be preferable. Crucibles of refractory materials such as fused silica, alumina, or porcelin could also be used satisfactorily. Attack by certain bomb solutions on these materials would require thermochemical corrections.

Volatile materials and those that are hygroscopic or sensitive to oxygen must be enclosed in a container before being introduced to the bomb. Some organometallic compounds

suffer from all three problems.

Glass ampoules are unsatisfactory for organometallic compounds (13). Molten glass from the ampoule can react with solid combustion products to give thermochemical effects of unknown magnitude. The molten glass, on cooling, can envelop solid combustion products, which would then go undissolved in the bomb solution.

Fused silica ampoules and polyester or polyhydrocarbon bags overcome the difficulties encountered with glass ampoules. However, fused silica ampoules, like fused silica crucibles may introduce corrections due to reaction with solid combustion products or dissolution in the bomb liquid. Polyester or polyhydrocarbon bags combust completely and leave nothing to react with or envelop solid combustion products.

Even with the employment of the moving-bomb method, using a suitable solution, and enclosing the sample in polyester bags, the problem of incomplete reaction may still plague the combustion of an organometallic compound (20). Incomplete combustion means that either not all of the sample reacted, or that carbon was not completely oxidized to carbon dioxide. No general recommendation to achieve complete combustion can be given. Some techniques which can be tried (20) include variation of the oxygen pressure in the bomb; changes in the size, shape, or weight of the crucible; use of a perforated crucible to allow better access of oxygen; installation of a baffle across the top of the crucible to impede

the escape of burning sample; or some combination of these measures. The use of an auxiliary combustant, such as a hydrocarbon oil, may be used to accelerate a sluggish combustion or temper a violent one.

If no variation in technique will produce a complete combustion, recourse must be made to measuring the amount of unreacted material and determining the carbon monoxide formed. If this alternate proves too unsatisfactory, the compound will have to be studied in a reaction calorimeter.

d) Calibration of the Bomb with Benzoic Acid

Benzoic acid has been chosen as a calorimetric standard substance (14) because it a) can be obtained in a stable solid form b) can be purified relatively easily, c) is not noticeably volatile at ordinary room temperatures, d) does not absorb moisture from the atmosphere, e) burns quantitatively in the bomb, and f) can be compressed in tablets.

The certified value of the benzoic acid can be used (14) if it is combusted under the following conditions:

a) The combustion reaction is referred to 298°K.

b) The sample is burned in a bomb of constant volume in pure oxygen at an initial pressure of 30 atmospheres at 298°K.

c) The number of grams of sample burned is equal to three times the internal volume of the bomb in litres.

d) The number of grams of water placed in the bomb prior to combustion is equal to three times the internal volume of the bomb in litres.

Small departures from the above conditions are allowed

but require the use of the correction factor

$$f = 1 + 10^{-6}\ 20(P-30)+42(Ms/V-3)+30(Mw/V-3)-45(T-298) \quad [29]$$

where P is the initial pressure in atmospheres of the oxygen at the temperature, T, to which the reaction is referred, Ms is the mass of benzoic acid in grams, Mw is the mass of water placed in the bomb in grams, and V is the internal volume of the bomb in litres. The value of the heat of combustion of benzoic acid as supplied by the Parr instrument company is 6318 calories per gram.

If the quantity of heat released by a sample of benzoic acid, q, produces a net temperature rise, ΔT, the energy equivalent of the calorimeter system, C, is defined as

$$C = \frac{q}{\Delta T} \quad [30]$$

Choosing the energy equivalent of the calorimeter to be that of the system after combustion, the temperature assigned to the reaction is the temperature prior to ignition, T_b (figure 1). Besides the heat from the benzoic acid, there are also contributions from the ignition energy, q_i, and the energy from the formation of nitric acid due to the presence of small amounts of nitrogen in the bomb, q_n. Therefore the energy equivalent of the system after combustion is

$$C_f = \frac{q + q_i + q_n}{T} \quad [31]$$

However to define a system which is invariant from calibration to calibration, it is necessary to exclude the energy equivalent of the products. Therefore

$$C_{sf} = C_f - C_{cf} \quad [32]$$

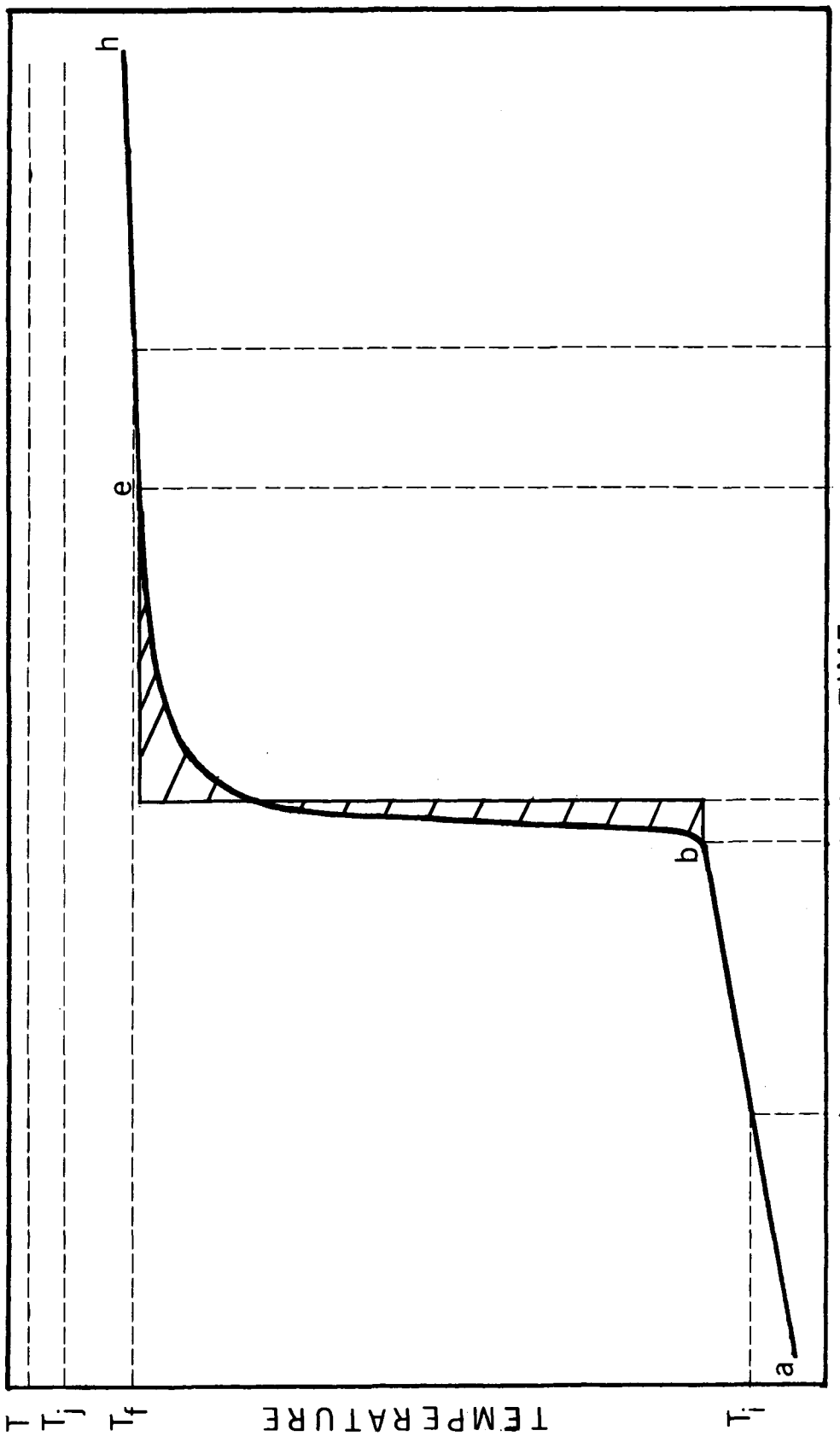

FIGURE 1: Time-temperature curve for a bomb-calorimetric experiment

where C_{cf} is calculated from the heat capacities of the crucible, oxygen, carbon dioxide, and water in the bomb at the end of the combustion with benzoic acid. Also included should be the specific heats and differences in mass of any other materials present in different amounts in the standard calorimeter system and the system as actually used.

e) Evaluation of the Corrected Temperature Rise

With an isothermal bomb calorimeter, the calculation of the corrected temperature rise involves two corrections: one is for the heat generated from the stirring of the calorimetric fluid; the other is for the heat exchanged between the calorimetric fluid and the constant temperature jacket. The stirring effect is considered constant, while heat exchange with the jacket is taken as proportional to the temperature difference between the jacket and the calorimeter fluid. In an actual combustion, these two effects and the heat from the reaction produce a time-temperature curve as shown in figure 1.

The portions of the curve ab, be, eh represent the time-temperature relations in the initial, main, and final periods respectively of the experiment. The main period is the section of the curve where the temperature increase is due largely to the energy of the combustion; the initial and final periods correspond to periods where the temperature rise is due to the stirring and exchange effects only. The temperature, T_j, is the jacket temperature and T_∞ is the convergence temperature which is the limiting value the

temperature would reach in infinite time if T_j and the rate of stirring remained constant.

The length of the initial and final periods is usually 10 to 20 minutes. In a rotating bomb calorimeter the final period may be about 40 minutes (15) in order to get all the products of combustion dissolved. The length of the main period depends on the lag of the bomb i.e. the time it takes for the generated heat to manifest itself in the form of a measured temperature rise. For a combustion experiment, the main period should be at least ten times the time required for the temperature rise to attain two-thirds of its final value (14). Also the temperature rise in the main period should be read at intervals of not more than 15 seconds if an accuracy of 0.01% in the corrected temperature rise is desired.(14).

The total rate of temperature rise due to the stirring and exchange affects (14) is

$$\frac{dT}{dt} = u + g(T_j - T) \qquad [33]$$

where u and g are constant. Since $dT/dt=0$ when $T=T_\infty$, therefore

$$T_j = T_\infty - u/g \qquad [34]$$

Substituting in equation [33]

$$\frac{dT}{dt} = g(T_\infty - T). \qquad [35]$$

If s_i and s_f represent the values of dT/dt at the mean temperatures T_i and T_f of the initial and final periods respectively, then

$$g = \frac{s_i - s_f}{T_f - T_i} \qquad [35a]$$

$$u = s_f + g(T_f - T_i), \qquad [35b]$$

and

$$T_\infty = \frac{s_i T_f - s_f T_i}{s_i - s_f} . \qquad [35c]$$

The correction ΔT which must be subtracted from the observed temperature rise, $(Te-T_b)$, to correct for the effects of stirring and heat exchange is obtained by integrating equations [33] or [35]:

$$\Delta T = u(te-t_b) + g\int_{t_b}^{t_e}(T_j - T)dt \qquad [36]$$

or

$$\Delta T = g\int_{t_b}^{t_e}(T_\infty - T)dt \qquad [37]$$

Equations [36] and [37] may be replaced by

$$\Delta T = [u + g(T_j - Tm)]\ (te-t_b) \qquad [38]$$

and

$$\Delta T = g(T_\infty - Tm)(te-t_b) \qquad [39]$$

respectively. Tm represents the mean temperature of the wall of the calorimeter in the main period. As no simple analytical expression of the relation between time and temperature in the main period of a combustion experiment exists (14), Tm must be found by graphical or numerical integration. If n temperatures Tr are measured (or interpolated from observed values) at equal time intervals, Δt, during the main period, then

$$Tm = \left(\sum_{r=2}^{m-1} Tr + \frac{T_b+Te}{2}\right)\frac{\Delta t}{te-t_b} \qquad [40].$$

The time intervals used must not be more than 15 seconds.

Dickinson's method (14) of obtaining the corrected temperature rise finds the time, t_x, (figure 1) such that

$$s_b(t_x-t_b) + s_e(te-tx) = g\int_{t_b}^{t_e}(T-T_\infty)dt = \Delta T \quad [41].$$

Dickinson showed that this relationship holds if the two shaded areas in figure 1 are equal. The time t_x is the time when the temperature rise has reached 60 per cent of its total amount (16), and is the point where the calorimeter ceases to be heated at a rate equivalent to that in the initial period, and begins to be heated (or cooled) at the rate as in the final period.

f) Calorimeter Design and Temperature Measurement

The determination of the corrected temperature rise is based on the validity of equation [33]. In order for this relationship to hold, the following features of calorimeter design (14) must be present: (a) no insulating material other than air can be used in the space between the calorimeter and the jacket; (b) the thickness of this air space must not exceed 12 mm. (for a 3^o maximum temperature difference between calorimeter and jacket); (c) evaporation of water from the calorimeter must be reduced to a minimum. By determining the variation of temperature with time at a number of temperatures, one can test whether equation [33] holds and these design features are effective.

The temperature scale used in bomb calorimetric experiments is unimportant (14), provided equation [33] holds for

the scale employed and both calibration and combustion determinations are done on the same scale. The commonly used temperature measuring instruments are mercury-in-glass thermometers, platinum resistance thermometers, thermistors, and thermocouples. Mercury-in-glass thermometers, particularly the Beckmann type, are suitable for work of moderate precision (17), but are usually replaced by one of the other three in high precision work. Both the platinum resistance thermometer and the thermocouple are used for work of the highest accuracy. The platinum resistance thermometer in particular, can be calibrated and used as a primary temperature standard due to its long term stability and reproducible performance. However, both instruments require expensive equipment due to the need of measuring very small changes in e.m.f. and resistance to a high degree of accuracy. The thermistor, with its large negative temperature coefficient of resistance, undergoes a much more marked change in resistance than a resistance thermometer for the equivalent temperature change. Therefore the thermistor is usable with relatively inexpensive auxiliary equipment. While the thermistor is very sensitive, small in bulk, and rapid in response, it suffers from a minor degree of instability and must be recalibrated periodically.

For the relatively small temperature range used in calorimetric work, the relationship given by Daniels et al (18) between the natural logarithm of the thermistor resistance R, and the absolute temperature, T, should be valid:

$$\ln R = \frac{A}{T} + B \qquad [42]$$

The constants A and B may be determined by a plot of $\ln R$ vs $1/T$.

g) Reaction Calorimetry

Compounds which will not combust completely with oxygen under the conditions used in bomb calorimetry can sometimes be made to react much more satisfactorily with other substances. The most desirable reaction is one which will proceed to completion in a few minutes at room temperature, with completely analyzable products.

A common type of apparatus of moderate precision used for reaction calorimetry (17) is the constant pressure calorimeter as described by Powell and Mortimer (19). It consists essentially of a small glass reaction vessel suspended in a liquid which is housed in a Dewar flask. The temperature rise of the liquid due to reaction in the vessel is measured by means of a Beckmann thermometer. The energy equivalent of the system is determined by electrical calibration as unlike bomb calorimetry, no standard reaction equivalent to the combustion of benzoic acid has been established. While the severest limitation of such a system is the very long time it takes to reach thermal equilibrium (17), it is very inexpensive, easily constructed and operated, and gives results with about ± 0.5 per cent accuracy (17).

The reaction best suited for the study of simple metal

alkyls seems to be halogenation. The iodination and bromination of the group II metal alkyls (17) and gallium trimethyl (19) have been investigated thermochemically and for the most part exhibit attack of the halogen on the metal-carbon bond. The problems of moisture and air sensitivity of these species requires their enclosure in glass ampoules prior to reaction.

A more recent type of reaction calorimeter results from the use of the rotating bomb calorimeter. The reaction of trimethylaluminum with acetic acid in toluene solution (20) was carried out in a regular rotating bomb calorimeter under about one atmosphere of dry nitrogen pressure. The trimethylaluminum was sealed into thin glass phials and placed in the platinum crucible. Upon rotation, the phials were broken and reaction initiated. Calibration was done in the usual fashion with benzoic acid. The accuracy attainable was as expected for this type of system.

Numerical Methods of Analysis

Numerical methods have two inherent forms of error. Truncation errors result from finite mathematical operations where an infinite process is needed to achieve the true value. Round-off error occurs due to the limitation of working with a fixed number of significant digits and having to chop values exceeding the number of digits allowed.

a) Evaluation of Integrals

The definite integral $\int_a^b f(x)dx$ sometimes cannot be

solved in a closed form; that is, a formula which is evaluated between the limits a and b and expressed in terms of simple algebraic functions to give the value of the integral, cannot be found. In this case, the interpretation that the value of the integral is the area under the curve $y = f(x)$ between the limits $x = a$, and $x = b$ is employed.

Numerical methods to evaluate the area under a curve are based on the generation of values of $f(x)$ at certain values of x and the approximation of $f(x)$ by some function in these smaller intervals. The approximation of $f(x)$ is integrable in closed form and these smaller areas are sumed to give the value of the integral. Usually, the more closely spaced are the values of x, that is, the smaller the intervals, the more closely approached is the true value of the integral.

In the case of experimentally derived points, there is no $f(x)$ from which to derive further points, and the intervals of x are usually not of equal magnitude. This second feature rules out the use of either of two common integration procedures, Simpson's Rule and the Trapezoid Rule (21), as they are derived for equally spaced intervals. However, the $m + 1$ pairs of observed values (x_i, y_i) where $i = 0, 1, 2, -----, m$, can be represented by a polynomial of degree m as given by Lagrange's interpolation formula (21):

$$y = \sum_{k=o}^{m} \frac{y_k P_k(x)}{P_k(x_k)}, \qquad [43]$$

where

$$P_k(x) = \frac{(x-x_0)(x-x_1) \text{ --- } (x-x_m)}{x-x_k} \qquad [44]$$

Lagrange's formula is derived for the case where the set of x_i do not form an arithmetic progression (21). Therefore the area under the curve formed by the set of points and represented by y, is given by

$$\int_{x_o}^{x_m} y\,dx = \sum_{k=0}^{m} \frac{y_k}{P_k(x_k)} \int_{x_o}^{x_m} P_k(x)\,dx. \qquad [45]$$

For m = 1,

$$\int_{x_o}^{x_1} y\,dx = \frac{x_1-x_0}{2} (y_0 + y_1), \qquad [46]$$

which is the area of a trapezoid formed by connecting adjacent points by a straight line.

For m = 2,

$$\int_{x_o}^{x_2} y\,dx = \frac{(x_2-x_0)^2}{6} \left[\frac{y_0}{P_0(x_0)} (3x_1-2x_0-x_2) + \frac{y_1}{P_1(x_1)} (x_0-x_2) + \frac{y_2}{P_2(x_2)} (2x_2+x_1-3x_1) \right]. \qquad [47]$$

When $x_1-x_0 = x_2-x_1$, this last equation reduces to the form of Simpson's rule.

Therefore, for a set of experimentally derived points, either equation [46] or equation [47] can be applied to successive sets of 2 or 3 points respectively and the results summed to obtain the value of the integral between the desired limits.

b) Systems of Linear Simultaneous Equations

Many physical problems can be represented by a set of simultaneous linear equations. Linear equations have each term in each equation containing only one unknown, and each unknown appears to the first power. An arbitrary set of n equations in n unknowns may have a unique solution, no solution, or an infinite number of solutions. A set of equations falling into the last two categories is said to be a singular set of equations. It is characterized by a determinant having a value of zero, or for practical purposes, a value close to zero. In the latter case, it is the accumulation of round-off error which produces an unreliable answer.

In general, there are two approaches to solving simultaneous linear equations: one is a direct and finite approach; the other is an indirect and infinite approach. The direct method theoretically produces an exact answer in a finite number of operations; the indirect method needs an infinite number of operations to produce an exact answer but can usually come very close with a finite number of steps.

The Gauss elimination method (22) uses finite techniques. For the case of three equations in three unknowns

$$\begin{aligned} a_{11}x_1 + a_{12}x_2 + a_{13}x_3 &= b_3 \\ a_{21}x_1 + a_{22}x_2 + a_{23}x_3 &= b_2 \\ a_{31}x_1 + a_{32}x_2 + a_{33}x_3 &= b_3 \end{aligned} \qquad [48]$$

two multipliers,

$$m_2 = \frac{a_{21}}{a_{11}} \qquad \text{and} \qquad m_3 = \frac{a_{31}}{a_{11}}$$

are defined. The first row is multiplied by m_2 and subtracted from the second equation. The first row is also multiplied by m_3 and subtracted from the third equation. The result is

$$a_{11}x_1 + a_{12}x_2 + a_{13}x_3 = b_1$$

$$0 + a'_{22}x_2 + a'_{23}x_3 = b'_2$$

$$0 + a'_{32}x_2 + a'_{33}x_3 = b'_3 .$$

Next a multiplier $m_x = a'_{32}/a'_{22}$ is defined and applied as above. The result is a triangular matrix with all elements below the diagonal equal to zero. Back substitution is carried out beginning with $a''_{33}x_3 = b''_3$ in order to solve for the x's. The product of the diagonal elements of the triangular matrix is the value of the determinant and thus this method offers an easy check for singularity.

An indirect method results if an attempt is made to refine the solution. The solution vector $x_1^{(o)}$, $x_2^{(o)}$, $x_3^{(o)}$ is multiplied by the matrix of coefficients and $b_1^{(o)}$, $b_2^{(o)}$, $b_3^{(o)}$ calculated. This new set of equations is subtracted from the original set and the result is

$$a_{11}\epsilon_1^{(o)} + a_{12}\epsilon_2^{(o)} + a_{13}\epsilon_3^{(o)} = B_1^{(o)}$$

$$a_{21}\epsilon_1^{(o)} + a_{22}\epsilon_2^{(o)} + a_{23}\epsilon_3^{(o)} = B_2^{(o)} \qquad [49]$$

$$a_{31}\epsilon_1^{(o)} + a_{32}\epsilon_2^{(o)} + a_{33}\epsilon_3^{(o)} = B_3^{(o)}$$

where

$$\epsilon_i^{(o)} = x_i - x_i^{(o)} \quad \text{and} \quad B_i = b_i - b_i^{(o)}$$

The $B_i^{(o)}$ are readily calcuable and reapplication of the elimination method gives the $\epsilon_i^{(o)}$'s. Therefore the refined solution is $x_i^{(1)} = x_i^{(o)} + \epsilon_i^{(o)}$. Continued use of the method should give a better solution until the effects of round-off error become too large. The method used for this 3 x 3 system is readily applicable to an n x n system.

If the system [48] is rewritten in the form

$$x_1 = \frac{1}{a_{11}} (b_1 - a_{12}x_2 - a_{13}x_3)$$

$$x_2 = \frac{1}{a_{22}} (b_2 - a_{21}x_1 - a_{23}x_3) \qquad [50]$$

$$x_3 = \frac{1}{a_{33}} (b_3 - a_{31}x_1 - a_{32}x_2)$$

an illustration of the indirect Gauss-Seidel method (21) can be shown. If $x_1^{(o)}$, $x_2^{(o)}$, $x_3^{(o)}$ represents an initial approximation to the solution, then the first equation of [50] can be solved for a new approximation to x_1:

$$x_1^{(1)} = \frac{1}{a_{11}} (b_1 - a_{12}x_2^{(o)} - a_{13}x_3^{(o)}).$$

With this new value for x_1 and the value $x_3^{(o)}$, a new value of x_2 can be found

$$x_2^{(1)} = \frac{1}{a_{22}} (b_2 - a_{21}x_1^{(1)} - a_{23}x_3^{(o)}).$$

Using the new values of x_1 and x_2

$$x_3^{(1)} = \frac{1}{a_{33}} (b_3 - a_{31}x_1^{(1)} - a_{32}x_2^{(1)}).$$

The cycle is repeated using the $x_i^{(1)}$'s as the initial solution and continued until the differences between successive values of x_i are less than some predetermined limit.

c) Curve Fitting by the Least Squares Method

It is usually desirable to have a functional relationship expressing the form of experimentally derived points. The form of the mathematical model which describes the set of points best indicates the correct interpretation of the process which generated the data.

The method of least squares (22) uses the criterion that for the equation best fitting a set of x, y data, the sum of the squares of the residuals, S, will be a minimum, where the residual is the difference between the experimentally obtained y and the y' obtained from the equation. In the case of testing a quadratic, $y_i' = c_1 + c_2x + c_3x^2$, the object will be to find c_1, c_2, c_3 in order to minimize S. Therefore

$$S = \sum_{i=1}^{n} (y_i - y_i') = \sum_{i=1}^{n} (y_i - c_1 - c_2x_i - c_3x_i^2)^2.$$

To minimize S considered as a function of c_1, the partial derivative of S with respect to c_1 is set equal to zero. The result is

$$nc_1 + (\sum x_i)c_2 + (\sum x_i^2)c_3 = \sum y_i$$

Similarly differentiating S with respect to c_2 and c_3 and equating to zero the set of normal equations for fitting a quadratic to the data is obtained:

$$nc_1 + (\sum x_i)c_2 + (\sum x_i^2)c_3 = \sum y_i$$

$$(\sum x_i)c_1 + (\sum x_i^2)c_2 + (\sum x_i^3)c_3 = \sum (x_i y_i) \quad [51]$$

$$(\sum x_i^2)c_1 + (\sum x_i^3)c_2 + (\sum x_i^4)c_3 = \sum (x_i^2 y_i)$$

This system is a set of simultaneous linear equations, and can be solved as in the preceding section for the c_i's. The same method is applicable for fitting a polynomial of any degree to a set of data. However, the effect of round-off error in the cases of higher degree polynomials usually puts a practical limit on the degree of the polynomial. Other forms of equations besides polynomials can be used, but sometimes the set of normal equations will not be linear and thus will present a much more difficult solution.

CHAPTER III

PYROLYSIS OF ETHYLBENZENE

a) Preparation of Materials

i) Toluene

The toluene used was toluene from sulfonic acid, Eastman Organic X325. It was dried by refluxing over sodium ribbon under vacuum and then degassed by bulb to bulb distillation.

ii) Benzene

The benzene used was Fisher Certified Reagent grade benzene supplied by the Fisher Scientific Company. It was treated in the same manner as the toluene.

iii) Ethylbenzene

The ethylbenzene used was supplied by Eastman Organic Chemicals. It was fractionally distilled and degassed before use.

All of the above materials were analyzed on a Perkin Elmer 800 Gas Chromatograph with flame ionization detector. In all cases, the major impurities were never greater than 1 part in 5000 of the liquid being analyzed.

b) Apparatus and Procedure

A toluene carrier flow system was used in this work. Figure 2 is a schematic of this apparatus.

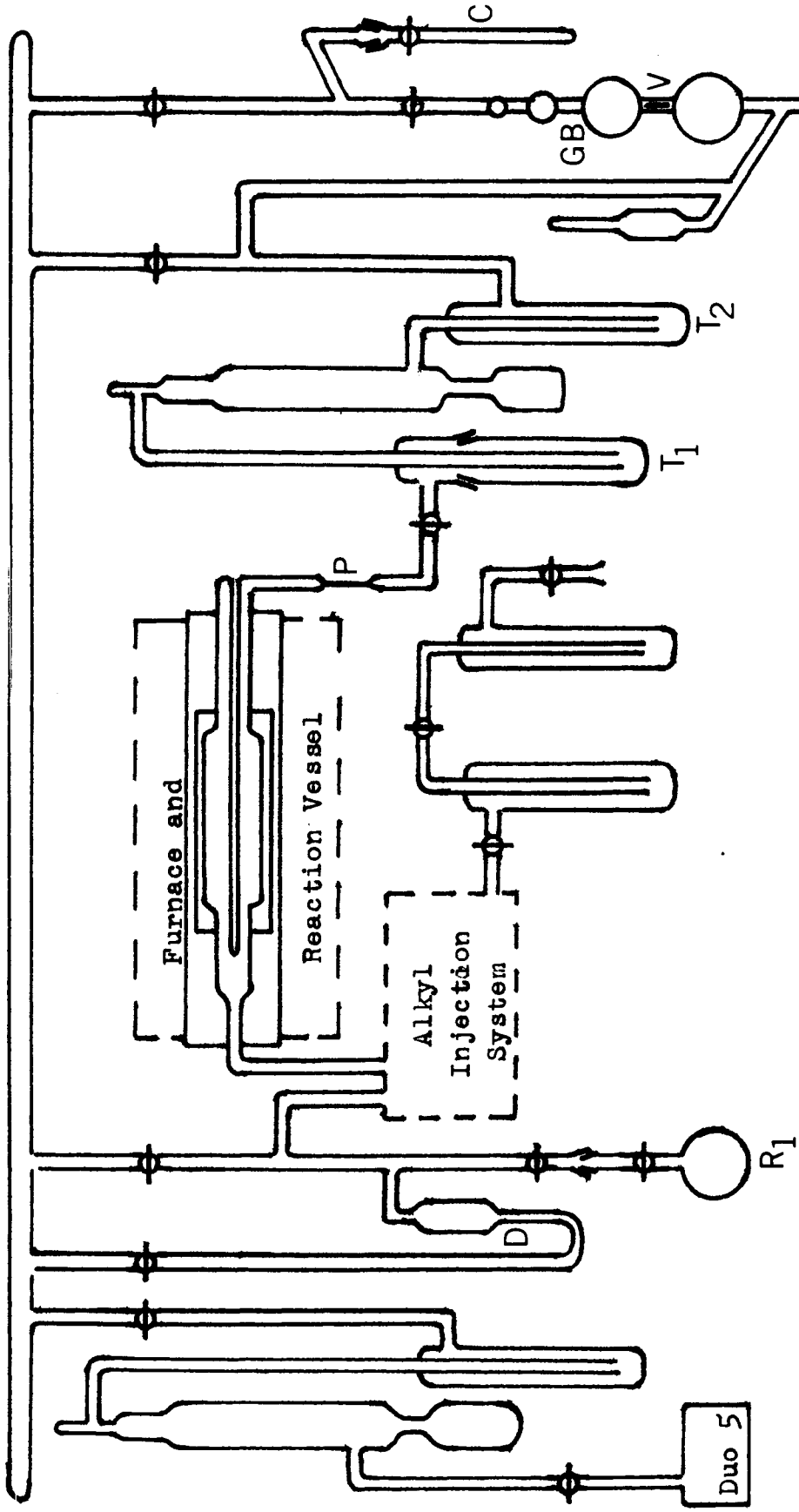

FIGURE 2: Schematic diagram of toluene carrier flow system.

The vacuum source of the system was a two-stage mercury diffusion pump backed by a two-stage oil-sealed rotary vane fore pump, Balzers Duo 5. All ground glass joints were lubricated with Dow Corning High Vacuum Silicone grease. Heated taps were lubricated with Apiezon T grease, while unheated taps were lubricated with Apiezon N grease.

The reaction vessels (figure 2) were fused quartz tubes 40 mm. O.D., and 6.5 to 8 inches long. Each end was sealed to 20 mm. O.D. quartz tubing which ended with graded quartz to pyrex seals. An axial thermocouple well of 10 mm. O.D. quartz tubing ran the length of the vessel.

An electric furnace was used to heat the reaction vessel. The furnace was constructed from a quartz cylinder 3 inches O.D., 24 inches long, and a wall thickness of one quarter inch. The quartz cylinder was wound with Chromel-A resistance ribbon 2 mm. wide and 0.2 mm. thick, having a resistance of 0.603 ohms per foot. The windings were cemented in place with Sauereisen Cement, No. 31. The heating element was tapped at seven points so that the profile could be adjusted by variable shunt resistors. An inconel liner 2.5 inches in diameter, 12 inches long, and 0.25 inches thick was centered inside the quartz cylinder to even out the temperature profile.

The quartz tube was centered horizontally in a box (12 x 12 x 24 inches) constructed of 0.25 inch asbestos sheeting with a 0.75 inch angle iron frame. The ends of the box had 3 inch diameter holes to accomodate the quartz tube. Powdered

alumina filling the rest of the box provided insulation. The furnace connected through a Variac to a 220 volt a-c power supply. The maximum operating temperature of the furnace was 1100° C.

A 10 ohm platinum resistance thermometer was mounted along the inside wall of the quartz tube as the sensing element for a Sunvic Resistance Thermometer Controller Type RT. 2. The measurement of the voltage across a movable Chromel-P-Alumel thermocouple which was inserted in the axial thermocouple well provided a means of monitoring the temperature in the reaction vessel. A Croydon Thermocouple Potentiometer Type P4 was used to measure the voltage. Over the length of the reaction vessel, the temperature was maintained within $\pm$ 2° C with a steep fall-off outside of this region (figure 5).

The toluene or benzene was stored in a detachable vessel R_1 so that it could be weighed before and after each run. A constant temperature water bath maintained the required toluene or benzene carrier pressure. The pressure of the carrier was read on a dioctylphthalate-mercury differential manometer (D in figure 2) with 7.5 magnification compared to a mercury manometer. The flow rate of the carrier through the reaction zone was controlled by the length and inside diameter of the sealed-in capillary at the outlet of the furnace (P in figure 2).

Ethylbenzene was likewise stored in a detachable vessel R_2. The injection system shown in figure 3 was used to

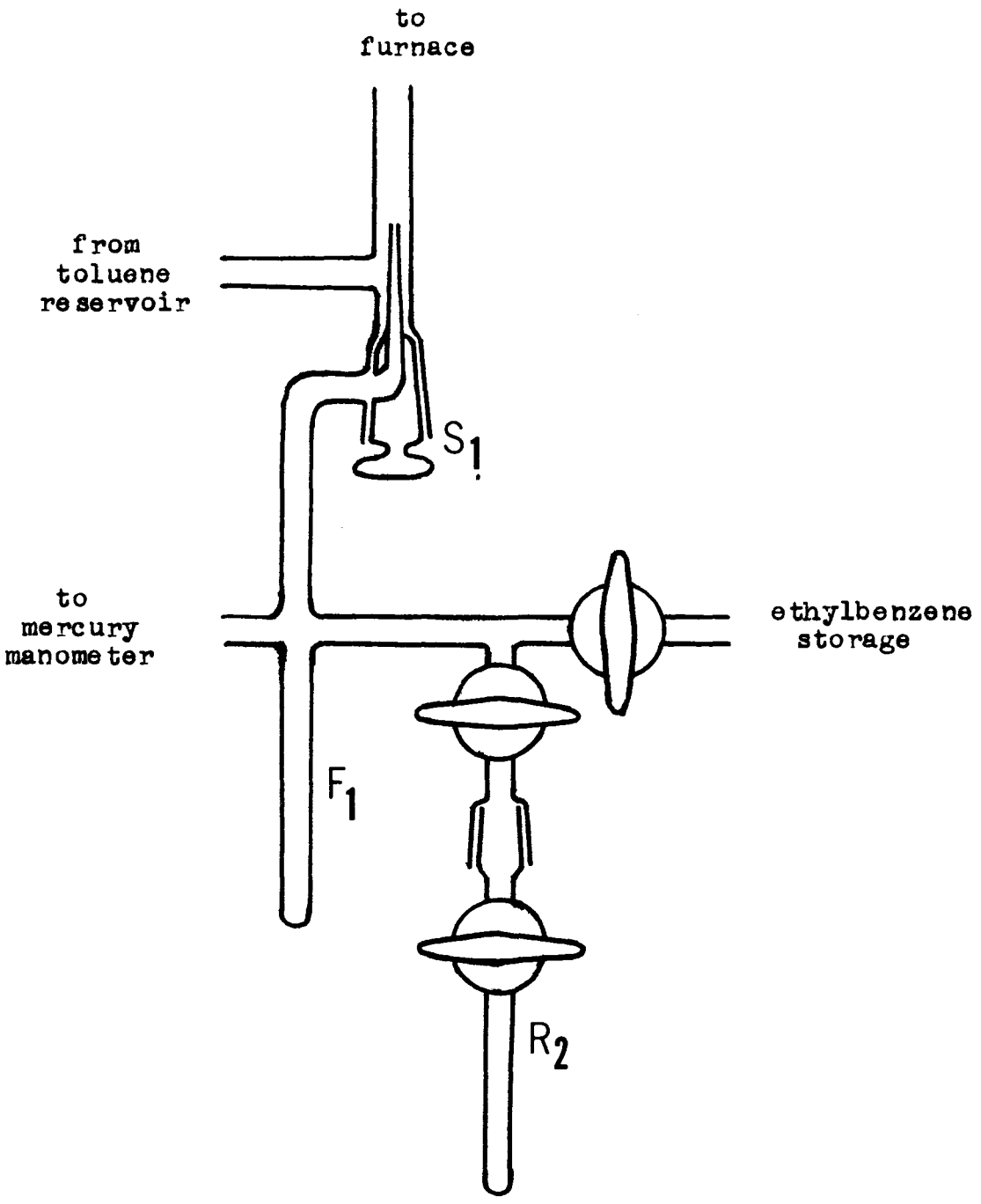

FIGURE 3: Ethylbenzene injection system

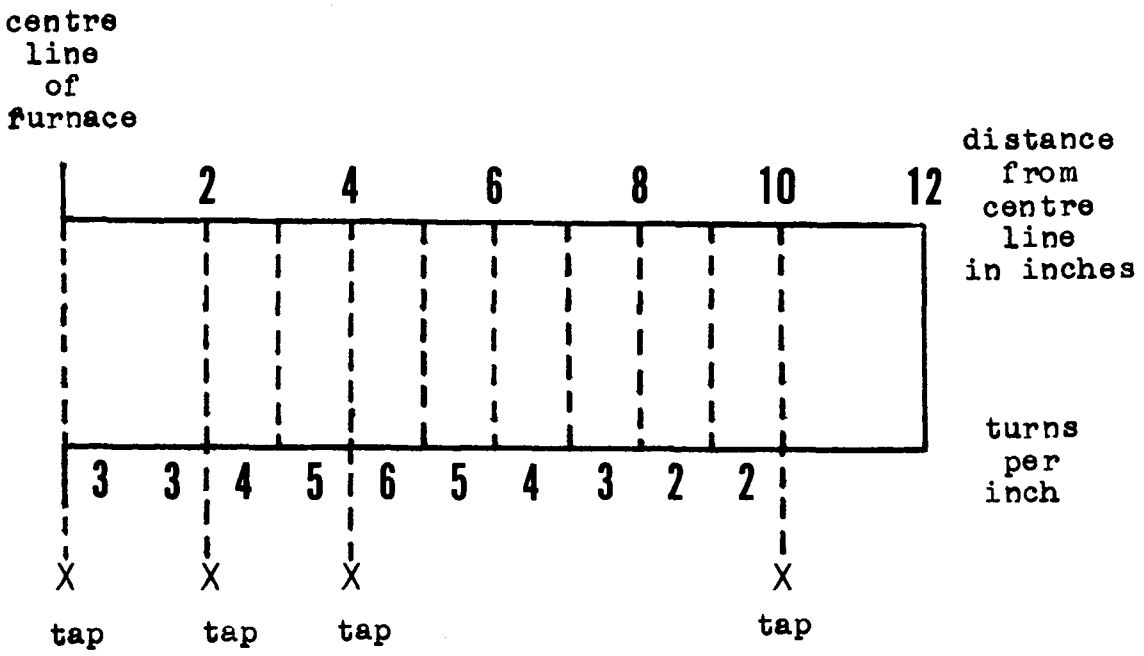

FIGURE 4: Furnace block with taps for changing the temperature profile.

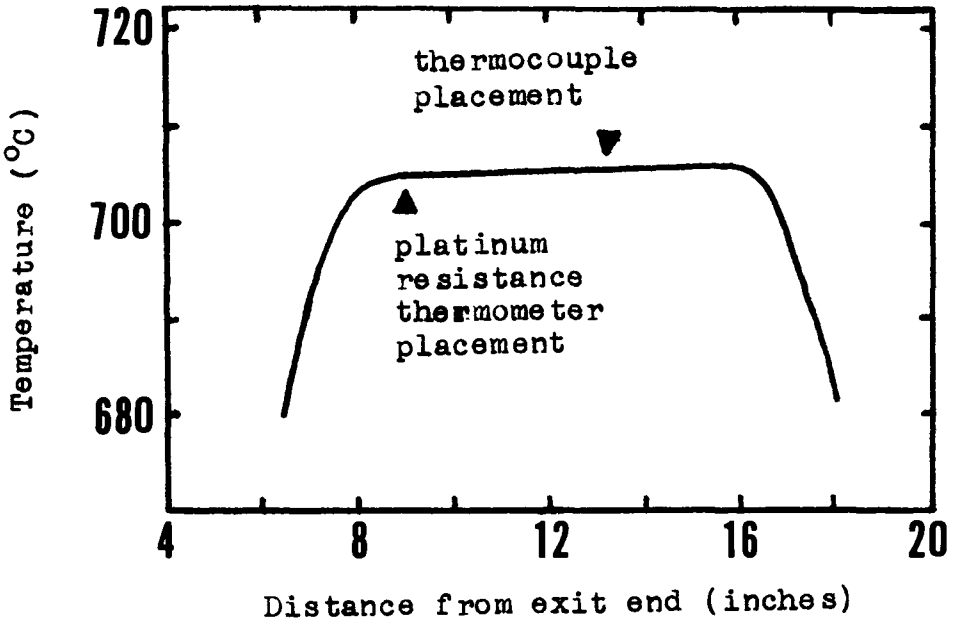

FIGURE 5: A typical temperature profile.

introduce the ethylbenzene into the stream of toluene or benzene vapour. A U-tube mercury manometer was employed to measure the ethylbenzene pressure which was maintained by a heated water bath.

All the tubing and vacuum taps leading to the furnace and from the furnace to the cold traps were wound with asbestos covered heating wire. Power from a Variac allowed the tubing to be heated as hot as 90° C. The heated windings prevented the condensation of any reactants or products in any part of the heated area.

The trap T_1, thermostated at -80° C with an acetone-dry ice sludge, collected the products liquid at room temperature. Trap T_2, thermostated at -110° C by means of a cooled ethanol bath, collected any liquid products not trapped by T_1. The Toepler pump, TP, was used to transfer the products which escaped T_1 and T_2 to the gas burette, GB, via the non-return valve, V. A sample of the gaseous products could be sealed into the collecting tube, C.

All runs were carried out by the following procedure. After the furnace had reached and maintained the desired temperature, and the vacuum was 10^{-4} mm or better, the carrier flow was commenced. In 3 to 5 minutes tap S_1 of the injection system was opened and the ethylbenzene admitted to the carrier stream. A certain amount of ethylbenzene had previously been distilled from R_2 to the finger F_1 and maintained at a pressure higher than that of the carrier stream. The flow of ethylbenzene was prolonged for

9 to 18 minutes followed by a 3 to 5 minute post-run of carrier alone.

The products trapped in T_1 were warmed to room temperature and transferred to a bottle for subsequent analysis. The pressure and volume of the gaseous products in the gas burette were measured and the temperature recorded. These products were transferred to the vessel C for subsequent analysis. The unused ethylbenzene was distilled from the finger F_1 to the reservoir R_2. The previously weighed containers of carrier and ethylbenzene, R_1 and R_2, were removed from the apparatus and reweighed.

During a run, the total pressure was recorded every minute, and the ethylbenzene pressure was checked every three minutes. The furnace temperature was recorded every three minutes and then averaged. The variation was never more than two degrees over the period of the run.

The gaseous products were analysed using a Perkin Elmer 154 gas chromatograph equipped with a $\frac{1}{4}$ inch, 6 foot silica gel column. The column was maintained at 80° C and a helium flow rate of 20 cc per minute was used. A nitrogen carrier was used when a hydrogen analysis was desired. Figure 6 is a schematic diagram of the injection system used for the gaseous product analysis. The sample vessel, C , was placed in a position with a steel bar resting on the break seal and this region evacuated. The U tube between C_2 and C_3 was also evacuated and then isolated. Using a magnet, the steel bar was raised and dropped onto the break seal. A portion

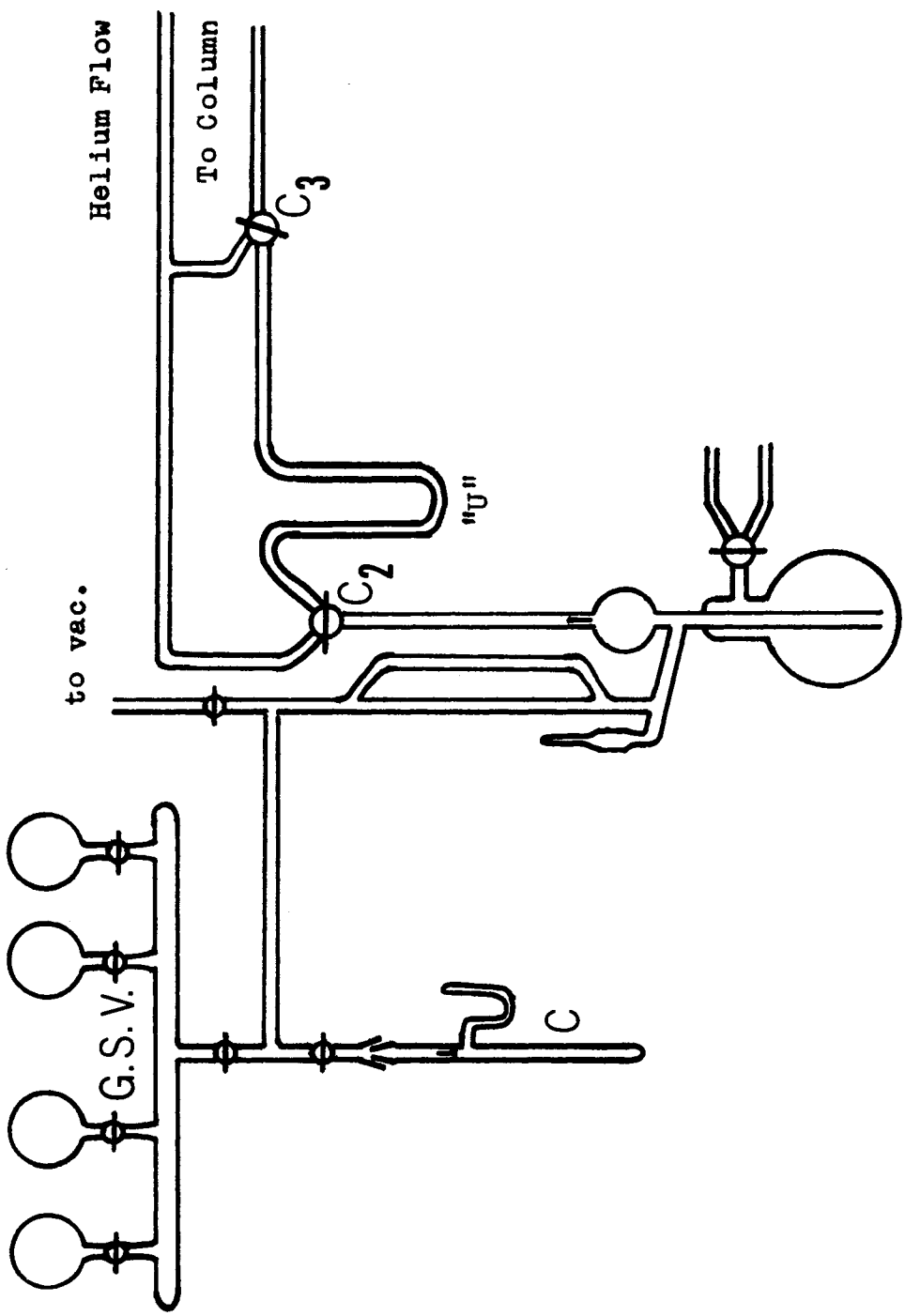

FIGURE 6: Schematic diagram of the injection system used for gas analysis.

of the gas sample was then transferred to the gas buret and the pressure measured. C_2 was then opened and the mercury level raised to transfer the sample to the U tube. C_2 was then turned to allow the helium flow to enter the U tube simultaneously as C_3 was turned to connect the U tube to the column. Calibration curves were constructed using pure gases from the gas storage vessels (G.S.V.) with each set of analysis so that peak heights could be used for analysis.

The liquid sample collected in T_1 was analyzed on a Perkin Elmer 800 Gas Chromatograph equipped with a flame ionization detector. A 0.02 inch I.D. 150 foot open tubular column coated with polypropylene glycol (Perkin Elmer Column R) was used. Nitrogen was used as the carrier gas and the column was maintained at 60° C. Synthetic mixtures containing the components present in the liquid samples were used for calibration. These calibration mixtures contained the same relative amounts of the various components as the liquid samples so that a peak height comparison could be used to determine the composition of the liquid samples.

c) Results and Discussion

The pyrolysis of ethylbenzene was the subject of two investigations, one using the toluene carrier technique (23), and one using primarily aniline as carrier with toluene carrier runs interspersed (24). The weakest bond in the ethylbenzene molecule is the C-C bond in the side chain. Therefore, the appropriate reactions involved were

$$C_6H_5C_2H_5 \longrightarrow C_6H_5CH_2 + CH_3$$

and $CH_3 + C_6H_5CH_3 \longrightarrow CH_4 + C_6H_5CH_2$

or $CH_3 + C_6H_5NH_2 \longrightarrow CH_4 + C_6H_5NH.$

The aniline carrier technique was used to avoid corrections from the small amount of decomposition of the toluene. In both cases, benzyl radicals and its aniline anolog and methyl radicals were produced. The rate of formation of methane gave the rate of initial bond cleavage. However, the bond dissociation energies found were widely divergent, 63.0 (23) and 70.1 kcal (24) and thus subject to further investigation. Products from the ethylbenzene other than methane complicated the mechanism.

The present study of the pyrolysis of ethylbenzene was carried out in a toluene carrier system over the temperature range 910° K to 1089° K. The pressure in the system was varied between 20.4 and 37.9 mm. This extended the temperature range used in the previous publications (23,24) by 60 to 80 percent, and was done at pressures 2 to 3 times greater. An attempt was made to analyze for as many products as possible. The effects of surface were checked by using a reaction vessel packed with quartz tubes which increased the surface to volume ratio by a factor of 10. (Benzene, as well as toluene, was used as a carrier for the ethylbenzene.) Tables 1-3 list the results. A blank space indicates no analysis for the particular commodity.

The products from the toluene carrier runs included methane, ethylene, hydrogen, styrene and benzene. No ethane was observed. Dibenzyl was presumed formed but no analysis

TABLE I
PYROLYSIS OF ETHYLBENZENE
FUNDAMENTAL DATA AND THE FIRST ORDER RATE CONSTANT

Run	P (cm.)	Temp. (°K)	Time* (min.)	Toluene (gm.)	Ethylbenzene (moles x 10^4)	Tol/Alk (molar ratio)	% Decomp.	tc (sec)	$10^2 k$ (sec^{-1})	log k	$10^3/T$
P 63	2.23	1089	3,9,3	6.52	9.70	43	69.8	0.484	246.	0.392	0.918
P 62	2.11	1089	3,12,3	8.44	9.45	37	58.8	0.424	208.	0.318	0.918
45	2.90	1084	3,9,3	10.17	7.69	86	82.7	0.674	259.	0.414	0.922
77	2.39	1081	3,13,3	9.47	11.1	63	60.0	0.649	150.	0.177	0.925
43	2.36	1062	3,18,3	12.29	5.85	170	76.4	0.742	193.	0.287	0.941
P 58	2.27	1048	3,18,3	12.67	16.4	62	27.3	0.421	75.3	-0.122	0.954
46	2.19	1043	3,18,3	10.42	15.6	54	44.5	0.827	71.0	-0.148	0.958
P 61	3.49	1034	3,9,3	13.50	20.4	43	24.2	0.385	71.6	-0.144	0.967
P 60	2.33	1034	3,15,10	15.04	10.3	84	27.9	0.430	75.8	-0.120	0.967
P 59	2.32	1032	3,15,3	11.19	10.3	84	28.8	0.432	78.2	-0.106	0.968
47	2.32	1025	3,18,3	12.22	9.41	105	35.2	0.761	56.8	-0.245	0.975
41	1.97	1015	3,18,3	10.77	14.5	60	25.1	0.741	38.8	-0.410	0.985
P 29	2.26	1008	3,18,3	10.40	10.4	80	19.0	0.681	30.8	-0.510	0.992
P 28	2.24	1008	3,18,3	10.19	12.3	67	18.7	0.688	30.0	-0.522	0.992

TABLE I (cont'd)

Run	P (cm.)	Temp. (K^o)	Time (min.)	Toluene (gm.)	Ethylbenzene (moles x 10^4)	Tol/Alk (molar ratio)	% Decomp.	tc (sec)	$10^2 k$ (sec^{-1})	log k	$10^3/T$
40	2.07	998	3,18,3	11.48	11.8	78	16.3	0.743	23.8	-0.621	1.002
53	2.35	995	3,18,15	15.82	11.6	73	20.3	0.920	24.5	-0.609	1.005
52	2.29	995	3,18,10	15.68	12.6	77	16.9	0.778	23.6	-0.625	1.005
51	2.33	995	3,18,3	12.27	16.4	82	17.4	0.784	24.2	-0.615	1.005
B76	2.83	991	3,12,3	11.09	15.0	62	8.90	0.574	16.0	-0.794	1.009
B75	2.73	991	3,15,3	12.38	12.2	92	9.20	0.580	16.5	-0.781	1.009
P 27	2.30	977	3,18,3	10.71	7.93	109	7.80	0.693	11.6	-0.935	1.023
P 56	2.24	967	3,18,3	12.68	12.6	81	3.00	0.451	6.66	-1.176	1.034
P 57	2.26	966	3,18,10	16.59	14.4	72	2.90	0.449	6.39	-1.193	1.035
38	3.60	966	3,12,3	17.06	8.64	142	5.30	0.673	7.95	-1.099	1.035
37	2.24	966	3,18,3	12.43	11.2	90	6.20	0.765	8.33	-1.078	1.035
B74	2.94	960	3,18,3	15.24	9.96	146	3.70	0.597	6.22	-1.205	1.041
B73	2.75	960	3,12,3	10.71	7.89	115	4.50	0.597	7.68	-1.114	1.041
78	2.23	956	3,18,3	12.27	13.9	71	3.20	0.667	4.79	-1.318	1.046
36	2.32	951	3,18,3	11.58	11.5	86	4.10	0.864	4.80	-1.317	1.051

TABLE I (cont'd)

Run	P (cm.)	Temp. (K^o)	Time (min.)	Toluene (gm.)	Ethylbenzene (moles x 10^4)	Tol/Alk (molar ratio)	% Decomp.	tc (sec)	$10^2 k$ (sec^{-1})	log k	$10^3/T$
35	2.36	951	3,18,3	12.46	12.0	84	3.80	0.817	4.69	-1.327	1.051
79	2.24	943	3,18,3	12.38	16.5	60	2.20	0.673	3.22	-1.490	1.060
P 65	2.31	943	3,18,3	12.86	11.2	93	1.00	0.470	2.12	-1.671	1.060
PB69	2.62	942	4,14,3	11.59	16.0	71	0.90	0.439	1.90	-1.720	1.061
PB68	3.14	9.42	5,13,3	14.21	13.2	84	1.10	0.429	2.42	-1.614	1.061
80	2.22	927	3,18,3	12.30	16.4	60	1.20	0.684	1.63	-1.785	1.078
72	2.24	926	3,18,3	12.37	15.6	64	1.66	0.686	2.24	-1.648	1.079
71	2.26	926	3,18,3	12.55	11.6	87	2.00	0.683	2.90	-1.537	1.079
B70	2.56	926	5,15,3	12.53	10.3	101	1.10	0.629	1.72	-1.761	1.079
54	2.30	911	3,18,3	11.78	13.1	72	0.70	0.881	0.772	-2.111	1.097
P 67	2.28	910	3,18,3	12.48	11.8	85	0.40	0.495	0.604	-2.218	1.098
P 66	2.33	910	3,18,3	13.06	10.9	97	0.40	0.483	0.448	-2.348	1.098
55	2.56	910	3,18,15	12.19	12.0	54	1.20	1.423	0.792	-2.100	1.098

*The time is expressed as the length of the pre-run, ethylbenzene flow, and post run.

TABLE 2
PYROLYSIS OF ETHYLBENZENE
PRODUCTS OF THE REACTION

Run	Temp. (°K)	methane	hydrogen	benzene	methane	hydrogen	styrene	benzene	ethylene
		(total products, moles x 10^4)			(products from ethylbenzene, moles x 10^4)				
P 63	1089	7.34			6.77				0.246
P 62	1089	10.1		1.96	9.45		3.95	1.28	0.370
45	1084	7.40		2.54	6.36		1.72	1.50	0.168
77	1081	7.81	9.50	4.08	6.93	7.75	3.09	3.20	1.11
43	1062	5.11		2.24	4.46		0.845	1.59	0.376
P 58	1048	4.72		1.73	4.47		1.07	1.48	0.394
46	1043	7.24		2.37	6.93		2.22	2.06	0.188
P 61	1034	5.09		1.67	4.93		1.55	1.50	0.188
P 60	1034	3.12		1.30	2.89		0.618	1.07	.236
P 59	1032	3.11		1.28	2.96		.588	1.13	.244
47	1025	3.46		.624	3.31		.623	.495	.061
41	1015	3.75		.234	3.65		1.05	.131	.086
P 29	1008	2.15		.498	1.98		.439	.324	.106
P 28	1008	2.47		.555	2.30		.558	.383	.093
40	998	1.98		.091	1.92		,850	.034	.046

TABLE 2 (cont'd)

Run	Temp. (°K)	methane	hydrogen	benzene	methane	hydrogen	styrene	benzene	ethylene
		(total products, moles x 10^4)			(products from ethylbenzene, moles x 10^4)				
53	995	2.45		2.53	2.35		.525	2.43	.192
52	995	2.21		5.13	2.13		.414	5.05	.964
51	995	2.15		2.51	2.09		.341	2.45	.905
B76	991	1.32	15.5		1.32	9.78	2.51		1.63
B75	991	1.12	16.9		1.12	10.2	2.15		1.38
P 27	977	.737			.614		.118		.031
P 56	967	.459		.548	.374		.048	.463	.250
P 57	966	.520		.471	.409		.059	.359	.262
38	966	.480		.028	.450		.055		.013
37	966	.719		.021	.693		.104		.018
B74	960	.363	6.02		.363	4.16	1.22		.467
B73	960	.353	4.75		.353	3.50	.883		.471
78	956	.457	.235	0.00	.440	.200	.070	0.00	.615
36	951	.486		.019	.468		.056	.002	.014
35	951	.471		0.00	.453		.056	0.00	.016
79	943	.368	.171	0.00	.356	.146	.093	0.00	.398

TABLE 2 (cont'd)

Run	Temp. (°K)	methane	hydrogen	benzene	methane	hydrogen	styrene	benzene	ethylene
		(total products, moles x 10^4)			(products from ethylbenzene, moles x 10^4)				
P 65	943	.175			.111				.074
PB69	942	.133	.517		.133	.144	.216		.057
PB68	942	.137	.551		.137	.130	.146		.053
80	927	.191	.104		.182	.086			
72	926	.248	.112		.239	.095			.642
71	926	.237	.338		.229	.321			.858
B70	926	.111	1.82		.111	1.50	.561		.207
54	911	.098			.090				.079
P 67	910	.052		0.00	.035		0.00	0.00	.007
P 66	910	.040			.024				.013
55	910	.150			.135				.144

TABLE 3
PYROLYSIS OF ETHYLBENZENE
PRODUCT RATIOS WITH RESPECT TO ETHYLBENZENE AND METHANE

Run	hydrogen	methane	ethylene	styrene	benzene	hydrogen	ethylene	styrene	benzene
	(molar ratio to ethylbenzene x 10)					(molar ratio to methane x 10)			
P 63		6.97	.254				.364		
P 62		5.87	.227	2.23	.797		.387	3.79	1.35
45		8.26	.218	2.24	1.95		.264	2.71	2.36
77	6.97	6.24	1.00	2.77	2.88	11.1	1.60	4.45	4.61
43		7.63	.642	1.44	2.71		.842	1.89	3.56
P 58		2.72	.240	.651	.904		.882	2.39	3.32
46		4.44	.121	1.42	1.32		.272	3.20	2.97
P 61		2.41	.092	.762	.737		.381	3.15	3.05
P 60		2.78	.227	.595	1.03		.817	2.13	3.72
P 59		2.87	.237	.570	1.09		.826	1.98	3.82
47		3.51	.065	.661	.498		.184	1.88	1.41
41		2.50	.059	.723	.090		.234	2.89	.359
P 29		1.89	.101	.420	.310		.536	2.21	1.63
P 28		1.86	.075	.452	.310		.402	2.42	1.66
40		1.62	.039	.717	.028		.237	4.40	.175

TABLE 3 (cont'd)

Run	hydrogen (molar ratio to ethylbenzene x 10)	methane (molar ratio to ethylbenzene x 10)	ethylene (molar ratio to ethylbenzene x 10)	styrene (molar ratio to ethylbenzene x 10)	benzene (molar ratio to ethylbenzene x 10)	hydrogen (molar ratio to methane x 10)	ethylene (molar ratio to methane x 10)	styrene (molar ratio to methane x 10)	benzene (molar ratio to methane x 10)
53		2.02	.783	.451	2.09		3.87	2.23	10.3
52		1.68	.760	.326	3.99		4.51	1.94	23.7
51		1.73	.748	.282	2.03		4.31	1.62	11.7
B76	6.51	.880	1.08	1.67		73.9	12.3	19.0	
B75	8.35	.915	1.12	1.76		91.2	12.3	19.2	
P 27		.773	.039				.507		
P 56		.296	.198	.039	.366		6.69	1.27	12.3
P 57		.283	.181	.041	.249		6.41	1.44	8.78
38		.521	.014	.064			.277	1.22	
37		.618	.016	.093			.257	1.50	
B74	4.18	.362	.469	1.22		114.	12.8	33.5	
B73	4.44	.448	.598	1.11		99.1	13.3	24.9	
78	.143	.315	.440	.050		4.56	13.9	1.59	
36		.407	.012	.049	.001		.298	1.19	.040
35		.376	.013	.047			.347	1.24	
79	.088	.215	.240	.056		4.10	11.1	2.61	

TABLE 3 (cont'd)

Run	hydrogen	methane	ethylene	styrene	benzene	hydrogen	ethylene	styrene	benzene
	(molar ratio to ethylbenzene x 10)					(molar ratio to methane x 10)			
P 65		.099	.066				6.58		
PB69	.090	.083	.036	.135		10.8	4.28	16.2	
PB68	.098	.103	.040	.109		9.48	3.83	10.5	
80	.052	.111				4.70			
72	.061	.152	.410			3.98	26.8		
71	.275	.196	.736			14.0	37.4		
B70	1.46	.108	.200	.543		135.	18.5	50.2	
54		.068	.060				8.77		
P 67		.030	.006				2.10		
P 66		.022	.012				5.54		
55		.112	.119				10.6		

was performed. Hydrogen analyses were done only on thirteen of the runs listed.

As was done in the two previous publications (23,24), the first order rate constants for ethylbenzene were calculated from the methane formed. Corrections for methane from toluene were applied using the data of Price (10) in order to get the correct value for the methane from ethylbenzene. In the runs using benzene as carrier, no correction for methane was necessary. A calculation (see appendix) was done to determine the possibility of ethylbenzene formation from the recombination of methyl and benzyl radicals. The minimum detectable concentration of ethane was calculated and used to get an upper limit to the methyl radical concentration. With the values for the recombination process from Kominar, Jacko, and Price (33), the maximum amount of ethylbenzene by recombination at 1000°K was found. The value, 8.23×10^{-7} moles, is negligible as about 10^{-3} moles of ethylbenzene was used in each run. A similar calculation at 1089°K with a higher methyl radical concentration gives the value 4.16×10^{-6} moles which is still too small to affect the value of the first-order rate constant significantly. Therefore, for all practical purposes, all methyl radicals generated by ethylbenzene react with the carriers.

The rate constants calculated were independent of pressure, contact time, and surface effects in agreement with the observations of the previous workers (23,24). The fall-off of the values of the rate constants at the highest

temperatures cannot be attributed to the formation of ethylbenzene from the recombination of methyl and benzyl radicals as already noted and will be discussed later. Rate constants at temperatures above 1065°K were omitted from the calculation of the Arrhenius parameters. Table 1 lists the data and figure 7 shows the Arrhenius plot of the rate constants as well as the lines of best fit for the previous two publications (23,24). The percent decomposition column (% Decomp.) in Table 1 is based on methane formation only. The least squares treatment for the present data yields the following equation:

$$\log_{10}k(\text{sec}^{-1}) = 14.7 - (70{,}300/2.303RT):$$

This equation agrees quite well with that found by Esteban, Kerr, and Trotman-Dickenson (24):

$$\log_{10}k(\text{sec}^{-1}) = 14.6 - (70{,}100/2.303RT).$$

These findings disagree with the equation of Szwarc (23):

$$\log_{10}k(\text{sec}^{-1}) = 13.0 - (63{,}200/2.303RT).$$

Using the average of the values obtained by Esteban, Kerr, and Trotman-Dickenson and this report, the C-C bond strength in the side chain of ethylbenzene can be put at 70.2 kcal/mole. This value, also substantiates the calculated value of 70.5 kcal/mole of Kominar, Jacko, and Price (25).

Previously, (23,24), no attempt had been made to analyze quantitatively all the remaining products of the reaction. Table 2 lists the data for the products of each run. Table 3 lists the molar ratios of each of the products to ethylbenzene, and the main product methane. The following reaction

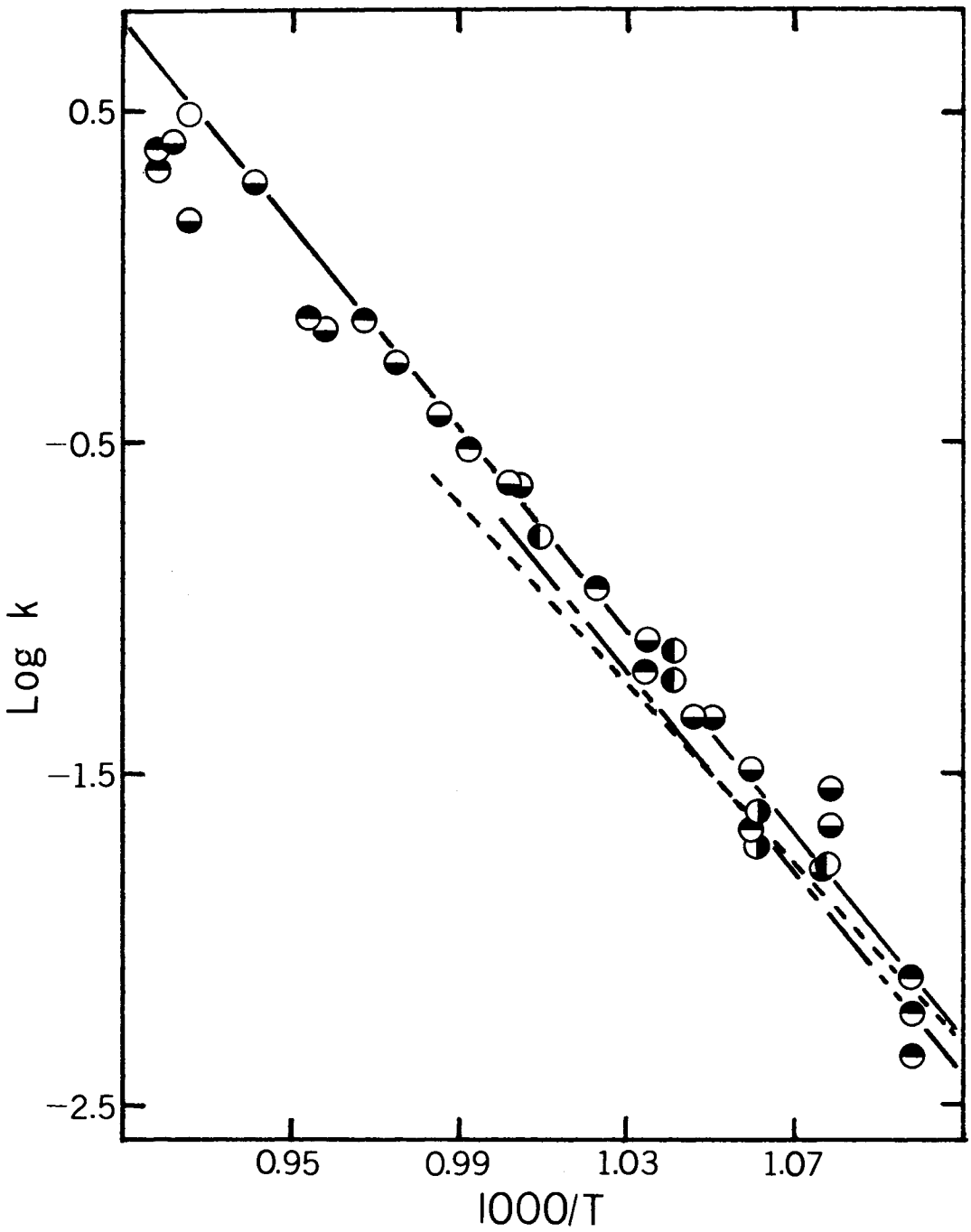

FIGURE 7: Arrhenius plot of the first-order rate constants for the pyrolysis of ethylbenzene

Toluene carrier runs; ◒ unpacked, ◓ packed vessel.

Benzene carrier runs; ◐ unpacked, ◑ packed vessel.

○ Point calculated from the parallel reaction scheme at 1081°K.

Line of best fit: —— present work; —·— Esteban et al.;

--- Szwarc.

scheme will be used to discuss the products and their distribution:

$$C_6H_5C_2H_5 \longrightarrow C_6H_5CH_2 + CH_3 \qquad [1]$$

$$C_6H_5CH_3 \longrightarrow C_6H_5CH_2 + H \qquad [2]$$

$$C_6H_6 \longrightarrow C_6H_5 + H \qquad [2b]$$

$$CH_3 + C_6H_5CH_3 \longrightarrow CH_4 + C_6H_5CH_2 \qquad [3]$$

$$CH_3 + C_6H_6 \longrightarrow CH_4 + C_6H_5 \qquad [3b]$$

$$H + C_6H_5CH_3 \longrightarrow H_2 + C_6H_5CH_2 \qquad [4]$$

$$H + C_6H_5CH_3 \longrightarrow C_6H_6 + CH_3 \qquad [5]$$

$$H + C_6H_6 \longrightarrow C_6H_5 + H_2 \qquad [4b]$$

$$CH_3 + C_6H_5C_2H_5 \longrightarrow CH_4 + C_6H_5C_2H_4 \qquad [6]$$

$$H + C_6H_5C_2H_5 \longrightarrow H_2 + C_6H_5C_2H_4 \qquad [7]$$

$$H + C_6H_5C_2H_5 \longrightarrow C_6H_6 + C_2H_5 \qquad [8]$$

$$C_6H_5C_2H_4 \longrightarrow C_6H_5C_2H_3 + H \qquad [9]$$

$$C_2H_5 \longrightarrow C_2H_4 + H \qquad [10]$$

$$C_6H_5C_2H_5 \longrightarrow C_6H_6 + C_2H_4 \qquad [11]$$

$$C_6H_5C_2H_5 \longrightarrow C_6H_5C_2H_3 + H_2 \qquad [12]$$

Reactions 2, 3, 4, and 5 belong exclusively to runs using toluene as carrier. Reactions [2b], [3b], [4b] belong exclusively to runs using benzene as carrier. All other reactions are considered common to both cases. The reaction

$$H + C_6H_6 \longrightarrow H + C_6H_6 \qquad [5b]$$

is omitted as no net change results. In general, for all products, the ratios with respect to ethylbenzene increase

with an increase in temperature. No trends can be seen due to changes in pressure, contact time, or surface area. The product ratios with respect to methane show the same result for the last three variables, and no trend for the variation of temperature. Although the change in the ratio of carrier to ethylbenzene is relatively large (40 - 149), the lowest value is sufficiently high to prevent any extensive radical attack on the ethylbenzene as no effect of the carrier to ethylbenzene ratio on the products is observed.

As a result of these observations, reactions [1], [11], and [12] are considered to be the main processes involved in ethylbenzene consumption. The non-effect of the variation of the ratio of carrier to ethylbenzene on the product amounts indicates reactions [6] through [10] are of minor importance.

Recalculation of the first-order rate constants based on the parallel reaction scheme, [1], [11], [12] shows that the difference from calculating the rate constants based on methane formation only is insignificant below 1040°K. However, once the total percent decomposition of ethylbenzene reaches the 90% value, if it is assumed that $k_1 = k_{11} + k_{12}$, the value of $\log k_1$ calculated from the parallel scheme is about 0.3 log units greater than $\log k_1$ based on methane alone. For the runs done at 1081°K or greater, these assumptions hold true and the values of $\log k_1$ based on methane only are about 0.3 log units lower than the line of best fit for the rest of the data. Since this calculation accounts

for the fall-off of the Arrhenius plot at the highest temperatures, no undetected forms of ethylbenzene decomposition should exist.

The unusual amount of hydrogen production in the benzene carrier runs as compared to the toluene carrier runs, indicates another source of hydrogen. Only the benzene could be such a source, but the strength of the carbon-hydrogen bond determined by various methods lies in the range 103-112 kcal/mole (26) and would seemingly belie this possibility. However, pyrolysis of pure benzene in the flow system results in the formation of hydrogen gas and biphenyl (Table 4). The analysis of the condensable liquid showed no other coupled product than biphenyl which proved to be in about equal portions with the hydrogen formed.

First order rate constants based on the sequence of reactions [2b], [4b], and

$$2C_6H_5 \longrightarrow C_{12}H_{10} \qquad [13]$$

were calculated. The resulting Arrhenius plot (figure 8) showed a slight curvature which would indicate some possible surface effect. No packed vessel runs with pure benzene were carried out. However, in the packed vessel runs with benzene carrier, the total amount of hydrogen formed is much less than in the other benzene carrier runs. After the packed vessel runs, the reaction vessel had been taken out of the furnace, the packing removed, and the vessel reinserted. The packing had not been previously conditioned.

The vessel was not treated in the proper manner as was

TABLE 4

PYROLYSIS OF BENZENE

FUNDAMENTAL DATA, PRODUCTS, AND FIRST-ORDER RATE CONSTANTS

Run	P (cm.)	Temp. (^{o}K)	Time (min.)	Benzene (moles x 10^{2})	% Decomp.	tc (sec)	$10^{3}k$ (sec^{-1})	diphenyl (moles x 10^{5})	hydrogen (moles x 10^{5})
75A	2.73	993	3,12	9.13	.612	.677	9.06	46.6	35.0
78A	2.76	956	3,18	15.6	.098	.622	1.57	5.73	8.96
79A	2.57	943	3,15	10.4	.058	.729	.788	2.18	3.98
80A	2.46	927	3,15	10.0	.032	.744	.431	.693	1.93

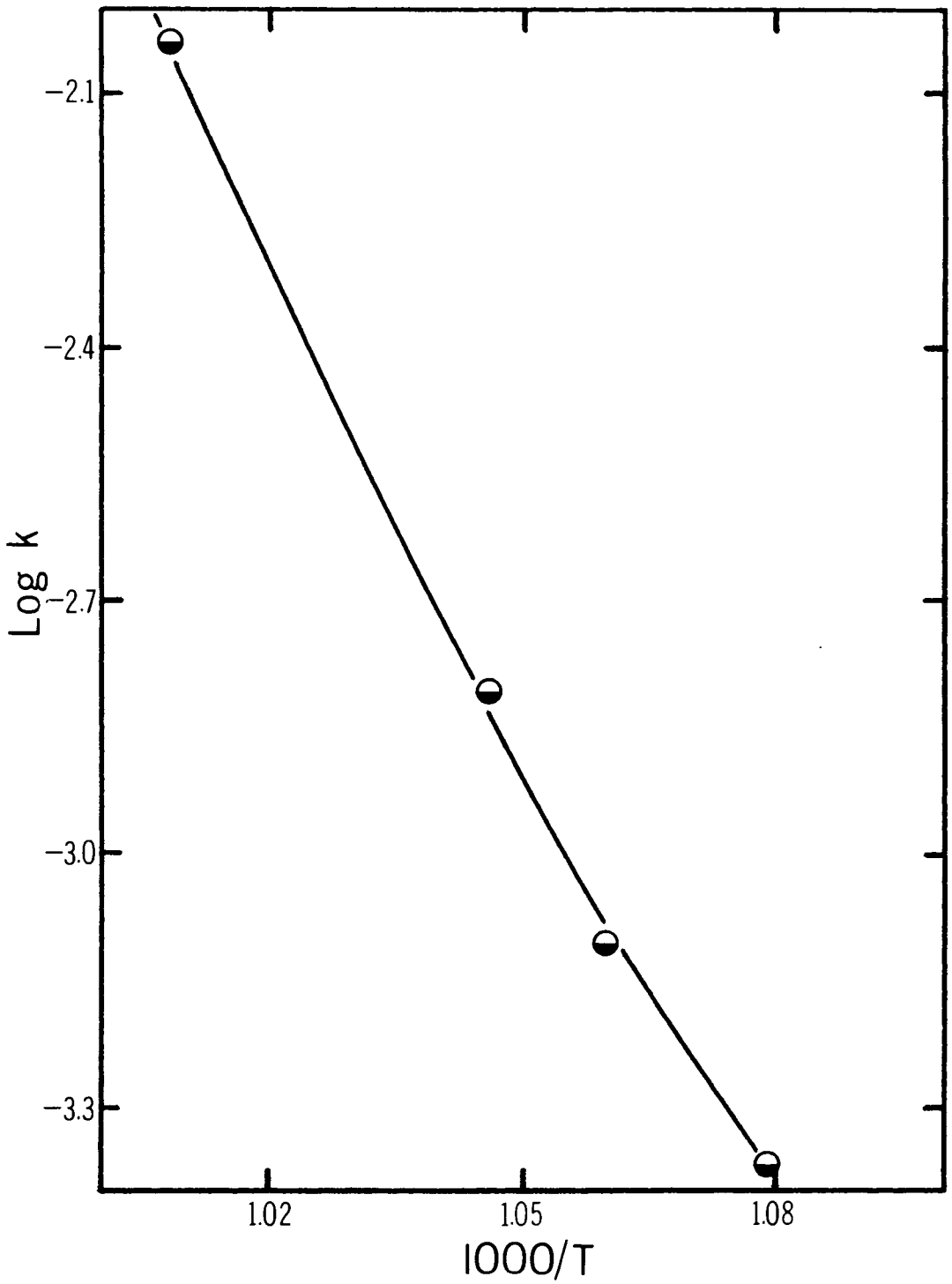

FIGURE 8: Arrhenius plot of the first-order rate constants for the pyrolysis of benzene.

later discovered. As a result, some form of catalytic surface was produced and affected all subsequent work (runs 70-80, and runs with pure benzene). It should also be noted that ethylene production using this treated vessel was enhanced in both benzene and toluene carrier runs. However, styrene production remained as expected in the toluene carrier runs but was slightly enhanced in the benzene carrier runs. The methane production remained unaffected throughout.

It would then seem in the benzene carrier runs, that reactions involving hydrogen atoms play a greater role in the mechanism, which accounts for the increased hydrogen, styrene, and ethylene production. The fact that ethylene maintains its high level with toluene carrier in this treated vessel indicates some other source than the proposed reactions for this case.

A steady-state treatment was done on the reactions given for both the toluene carrier and benzene carrier runs. For the toluene carrier runs, the assumption $k_4 = 2k_5$ was made based on the observations of Price (10) that twice as much hydrogen as methane was produced in the pyrolysis of toluene. Due to similarities in some of the reactions, it is also assumed that $k_7 = 2k_8$, $k_3 = k_6$, and $k_5 = k_8$. On this basis, the following expressions for radical steady-state concentration were derived:

$$[H] = \frac{k_2 R^2 + k_1}{3k_5 + R^2},$$

$$[C_2H_5] = \frac{k_2R^2 + k_1}{3k_{10}R^2} [C_6H_5C_2H_5] ,$$

$$[CH_3] = \frac{k_2R + 3k_1}{3Rk_3} ,$$

$$[C_6H_5C_2H_4] = \frac{k_2}{k_9} + \frac{k_1}{Rk_9} + \frac{2k_1}{3R^2k_9} [C_6H_5C_2H_5]$$

where R is the molar ratio of toluene to ethylbenzene. Using these quantities, expressions for the rate of formation of each of the products, methane, hydrogen, styrene, benzene, and ethylene can be derived:

$$\frac{d[CH_4]}{dt} = \frac{Rk_2}{3} + k_1 [C_6H_5C_2H_5] \quad [14]$$

$$\frac{d[C_2H_4]}{dt} = \frac{k_2}{3} + \frac{k_1}{3R^2} + k_{11} [C_6H_5C_2H_5] \quad [15]$$

$$\frac{d[H_2]}{dt} = \frac{2k_2R}{3} + \frac{2k_1}{3R} + k_{12} [C_6H_5C_2H_5] \quad [16]$$

$$\frac{d[C_6H_6]}{dt} = \frac{k_2R}{3} + \frac{k_1}{3R} + k_{11} [C_6H_5C_2H_5] \quad [17]$$

$$\frac{d[C_6H_5C_2H_3]}{dt} = k_2 + \frac{k_1}{R} + k_{12} [C_6H_5C_2H_5]. \quad [18]$$

Therefore, k_{11} and k_{12} may be calculated in terms of known product rates of formation, k_1, k_2, and the toluene to ethylbenzene ratio.

Similarly for the benzene carrier runs, the radical steady state concentrations are:

$$[H] = \frac{R^2k_2 + k_1}{R^2k_4},$$

$$[CH_3] = \frac{k_1}{Rk_3}$$

$$[C_2H_5] = \frac{R^2k_2 + k_1}{2k_{10}R^2} [C_6H_5C_2H_5],$$

$$[C_6H_5C_2H_4] = \frac{k_1}{Rk_9} + \frac{k_2}{k_9} [C_6H_5C_2H_5].$$

The rates of formation of the various products are:

$$\frac{d[CH_4]}{dt} = k_1[C_6H_5C_2H_5],$$

$$\frac{d[C_2H_4]}{dt} = \frac{k_2}{2} + \frac{k_1}{2R^2} + k_{11} [C_6H_5C_2H_5],$$

$$\frac{d[H_2]}{dt} = \frac{k_1}{R} + Rk_2 + k_{12} [C_6H_5C_2H_5],$$

$$\frac{d[C_6H_5C_2H_3]}{dt} = \frac{k_1}{R} + k_2 + k_{12} [C_6H_5C_2H_5].$$

Any terms in the derivations which seemed to contribute negligibly to the numerical value of the expression in comparison with the other terms, were left out.

Using the expressions involving k_{11} and k_{12}, values were calculated for these two rate constants at various temperatures. The results appear in Table 5, and the Arrhenius plots are in figures 9 and 10.

The Arrhenius plots for k_{11} and k_{12} point up the various aspects of the mechanism: namely the joint action of

TABLE 5

RATE CONSTANTS FOR THE MOLECULAR BREAKDOWN OF ETHYLBENZENE

Run	Temp. (°K)	C_2H_4 k_{11}	C_6H_6 k_{11}	H_2 k_{12}	C_8H_8 k_{12}
			(x 10^2 sec^{-1})		
45	1084	3.22	33.0		29.6
77	1081	25.7	83.7	199.	68.7
43	1062	9.42	37.6		18.2
P 58	1048	5.67	21.6		14.1
P 60	1034	5.26	25.4		12.9
P 61	1034	2.35	18.0		18.0
40	998	.511	.183		6.99
51	995	9.63	25.8		3.32
B76	991	17.9		28.3	26.9
P 56	967	4.41	8.34		.712
38	966	.216	.028		
B74	960	7.61		19.8	20.0
78	956	6.77		2.24	.697
79	943	3.60		1.31	.779
PB68	942	.892		2.57	2.47
B70	926	3.10		8.66	8.47
54	911	.682			

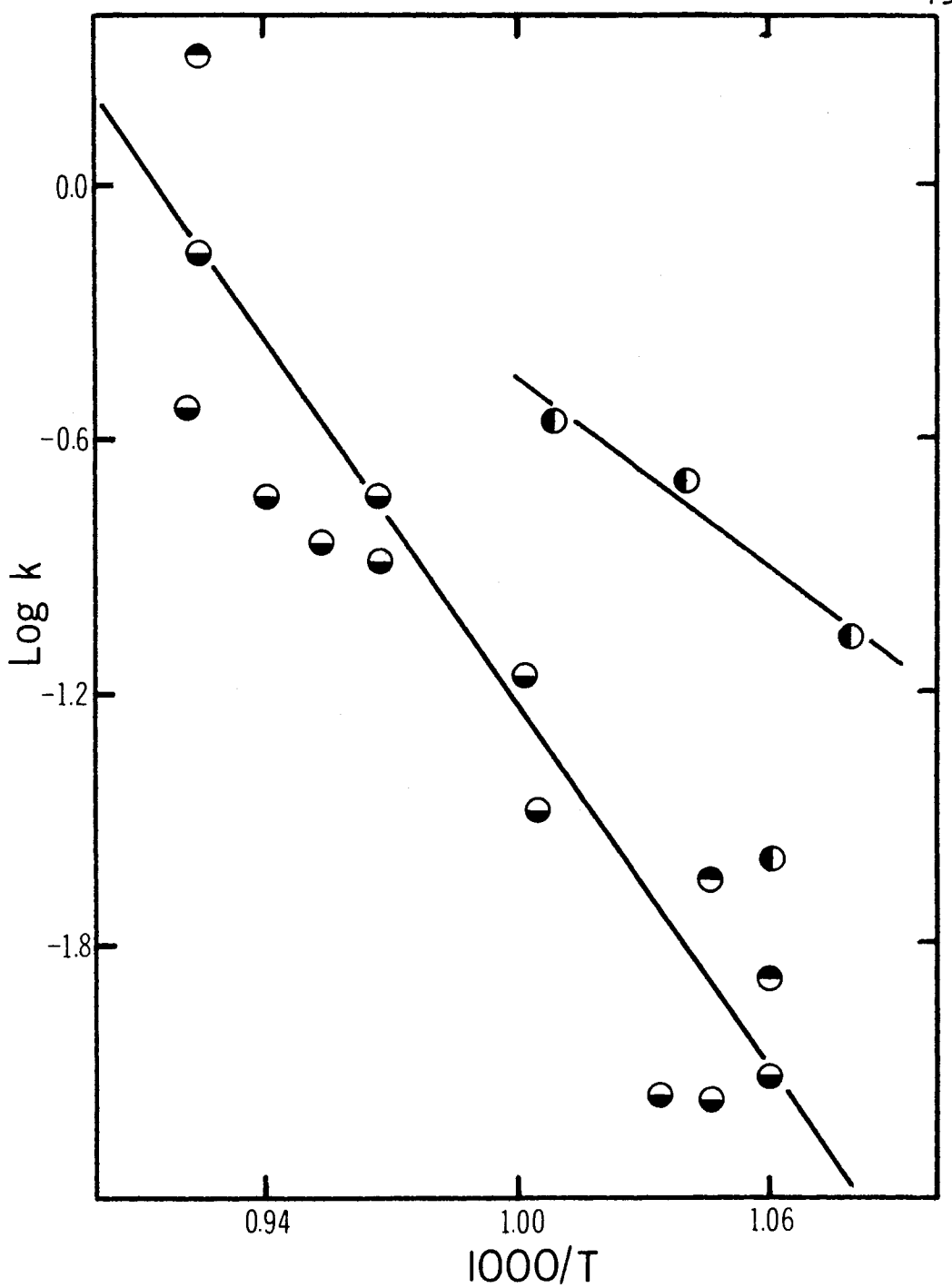

FIGURE 9: Arrhenius plot of the first-order rate constant for reaction 12

Toluene carrier: k_{12} calculated from the rate of formation of styrene ◒ ; hydrogen ◒ .

Benzene carrier: k_{12} is the average value from styrene and hydrogen ◐ .

—— Line of best fit for toluene, and benzene carrier runs.

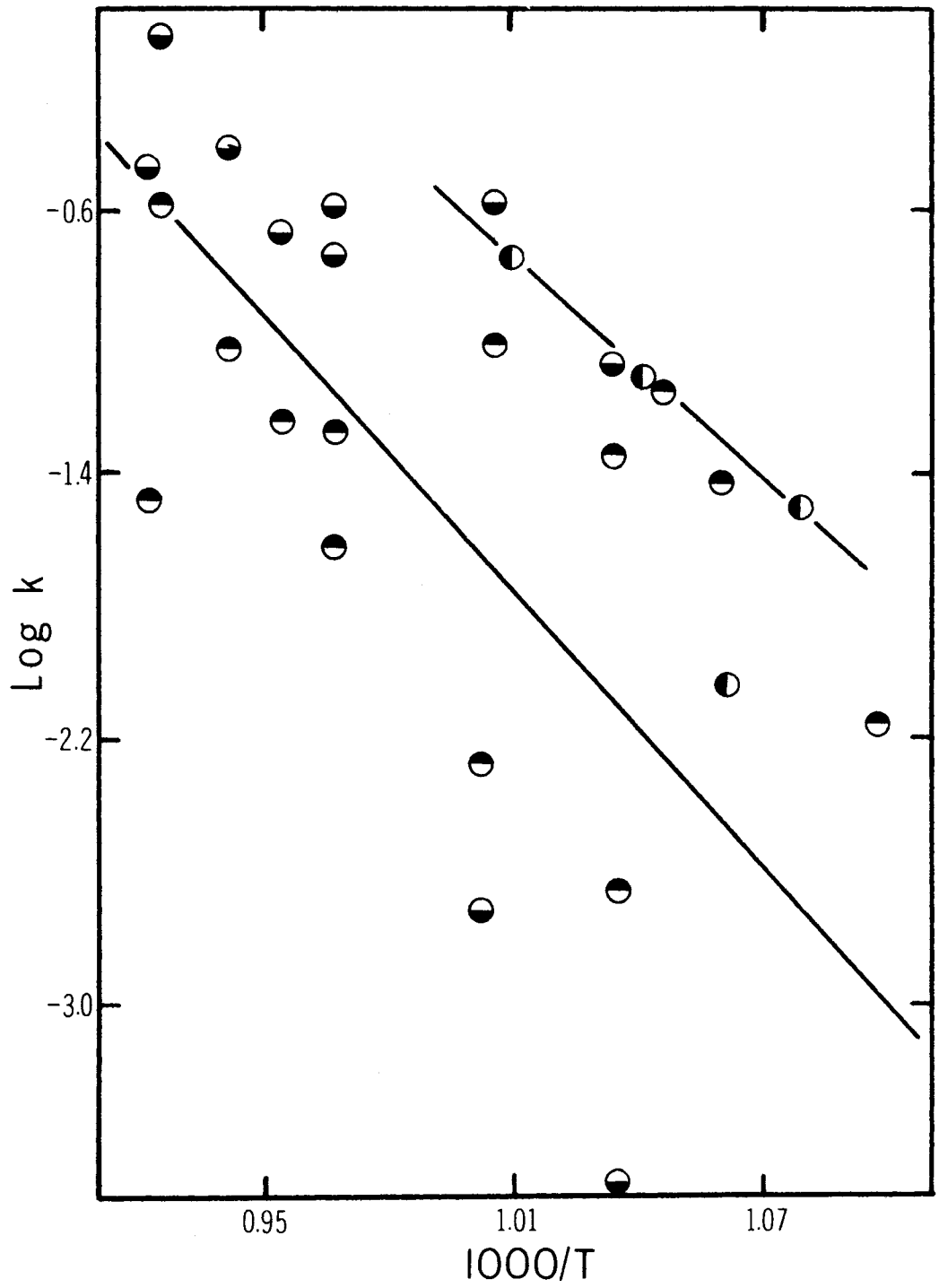

FIGURE 10: Arrhenius plot of the first-order rate constant for reaction 11

Toluene carrier: k_{11} calculated from the rate of formation of benzene ◒ ; ethylene◒.

Benzene carrier: k_{11} calculated from ethylene only◐.

—— Line of best fit for toluene, and benzene carrier runs.

radical and molecular reactions, heterogeneous (surface) and homogeneous processes, and the effectiveness of toluene and benzene as radical scavengers.

The calculation of k_{11} and k_{12} by two different sets of equations (equations [15] and [17], and [16] and [18] respectively) should produce the same result. For the toluene carrier runs, the differences in rate constants was a factor of 2 to 4 which is within an order of magnitude and probably quite good for the approximate treatment used. The scatter on the Arrhenius plot (figure 9) for the case of k_{12} in the toluene carrier runs is relatively small and gives the following two equations based on equations [18] and [16] respectively:

$$\log k_{12} = 15.2 - 73{,}600/2.3RT$$

and $$\log k_{12} = 12.5 - 63{,}500/2.3RT.$$

The relatively small scatter for the values of $\log k_{12}$ for runs carried out over a variety of treated surfaces would indicate reaction [12] is largely homogeneous. Inclusion of all points for k_{12} for the toluene carrier runs gives

$$\log k_{12} = 13.1 - 65{,}600/2.3RT.$$

This would indicate reaction [12] proceeds with an activation energy of comparable magnitude to the C-C bond fission in the side chain but due to the size of the A factor, the products, hydrogen and styrene, will be about 5-10 times less than the methane which is what is generally observed.

The values of k_{12} derived from the benzene carrier runs

agree within about 4% of each other which is amazingly good for this type of treatment. As a result, just average values of k_{12} are plotted. With such close agreement of the calculated values, it would seem, that the proposed mechanism for the benzene carrier runs fits better than its counterpart for the toluene carrier runs. Moreover, the peculiarities of the benzene carrier system seems to be exemplified in the Arrhenius plot. The three unpacked runs fit the Arrhenius expression:

$$\log k_{12} = 6.87 - 33{,}500/2.3RT$$

while the value for the packed vessel run used is in better agreement with the toluene carrier runs. The unusually low A factor indicates something other than a simple homogeneous gas phase reaction. The agreement of runs 77-79 which were done in the same vessel as 70, 74, 76, with the other toluene carrier runs done in different vessels would indicate the occurrence of a possible short chain process rather than a surface catalyzed reaction. The fact that benzene is a poorer radical scavenger (27) than toluene would also support the possibility of short chain processes.

In the Arrhenius plot for the values of k_{11} (figure 10), the most immediate observation in comparison with the plot for k_{12} is the greater scatter of the results. While the values of k_{11} for the benzene runs are only based on calculation by one means (rate of formation of ethylene), they show the same variation as k_{12}, namely a linear relationship between the three unpacked runs, and large deviation of the

packed run from these three. However, in this case, the unpacked benzene carrier runs agree with some of the toluene carrier runs. These particular toluene carrier runs were ones which were the first of a group done after a long inactive period of the apparatus, or after the reaction vessel was removed and reinserted. Therefore it would seem that the process for ethylene generation is a heterogeneous rather than homogeneous process. The Arrhenius equations for these respective sets of data are:

$$\log k_{11} = 10.4 - 50{,}300/2.3RT$$

for the unpacked benzene carrier runs, and

$$\log k_{11} = 13.4 - 64{,}200/2.3RT$$

for the toluene carrier runs. The equation considering all points for this set is

$$\log k_{11} = 12.4 - 58{,}400/2.3RT.$$

In summary, it can be said that the pyrolysis of ethylbenzene in a toluene carrier system is a complex process involving both radical and molecular breakdown of the ethylbenzene. The three paths of decomposition in the toluene carrier runs include the major C-C bond scission in the side chain, and two less important molecular decompositions. The formation of hydrogen and styrene occurs by a homogeneous gas phase molecular decomposition while ethylene formation can be attributed to a surface sensitive process. The benzene carrier runs add a fourth path of decomposition, namely the hydrogen atom attack on the ethylbenzene due to the relatively large concentration of hydrogen atoms generated by the

surface catalyzed fission of the C-H bond in benzene, and maintained by the poorer radical scavenger properties of benzene as compared to toluene.

CHAPTER IV

REACTION CALORIMETRY OF TRIMETHYLINDIUM

a) Preparation of Materials

i) Trimethylindium

Trimethylindium was prepared in the apparatus shown in figure 11. Dimethylmercury was refluxed over finely cut indium metal in pot B under a dry nitrogen atmosphere (28). Indium metal in 99.9% purity was purchased from Fisher Scientific Co. Dimethylmercury was originally produced by adding methylmagnesium iodide to mercuric chloride in ether solution over a period of 1 hr. and refluxing for an additional 3 hrs. (27). Later it was supplied as a reagent grade chemical by Alfa Inorganics. Product could be removed after 4-8 days. The reaction flask B was cooled to 0° C (vapour pressure of trimethylindium, 0.2 mm) and the unreacted dimethylmercury vacuum distilled into flask A. The crude trimethylindium was transferred to flask C and from there transferred to a main alkyl storage area where the remaining dimethylmercury was removed by repeated outgassing at 0° C. The final product melted at 89.5° C and gave vapour pressure measurements consistent with literature values (28). It was stored under its own vapour pressure at dry ice temperature. Weighed thin glass bulbs blown from 4 mm Pyrex

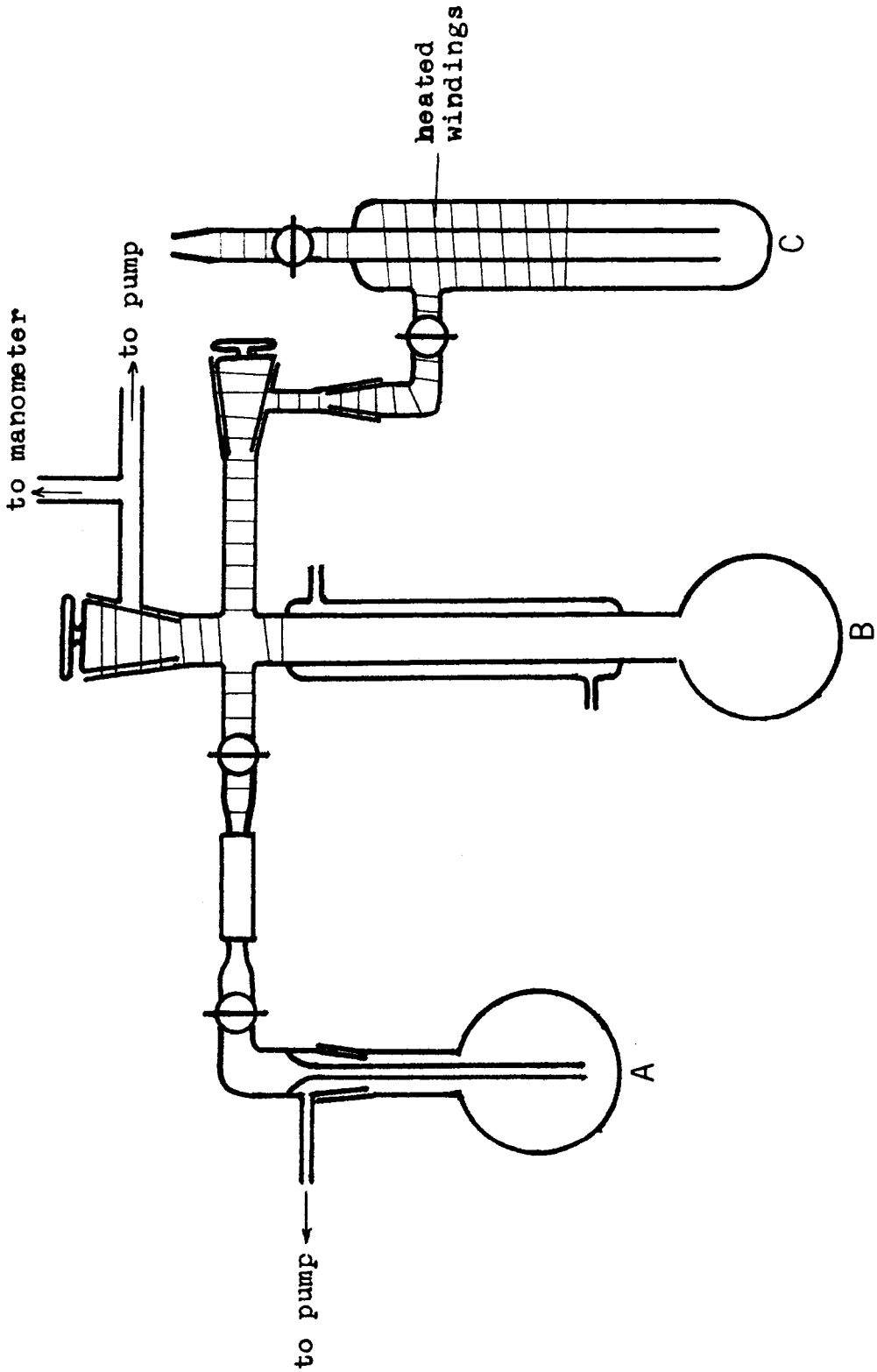

FIGURE 11: Apparatus for the production of trimethylindium.

tubing were filled with $In(CH_3)_3$ from the storage area, sealed, reweighed, and stored over dry ice.

ii) Bromine solution

Bromine and chloroform purchased from Fisher Scientific Co. were fractionally distilled and then degassed by bulb to bulb distillation. Bromine distilled at 57-58° C, and chloroform distilled at 60-61° C. Sufficient bromine was vacuum distilled into chloroform to give an approximately 1N solution. The resulting solution was stored in the vessel in figure 12, under a nitrogen atmosphere.

iii) Indium tribromide

Indium tribromide, reagent grade, was purchased from Alfa Inorganics, and dried in a nitrogen atmosphere using phosphorus pentoxide as dessicant.

b) Apparatus and Procedure

The apparatus used was similar to that of Fowell and Mortimer (19) and is depicted in figure 12. It consisted of a 30 cc. Pyrex reaction vessel (figure 12), 14 cm long with an outer 14/30 ground tapered joint at one end. The inner portion of the 14/30 joint was attached to a piece of 14 mm O.D. tubing 10 cm long at the top, and a 5 mm O.D. tube, 3 cm long, at the bottom. The smaller tubing allowed a 3 mm O.D., 20 cm long piece of glass rod to slide smoothly yet snugly through it with the aid of Dow Corning Silicon grease as lubricant and sealing agent. To the end of the rod was attached 2 cm of 4 mm I.D. tubing when held the glass ampoules blown from 4 mm O.D. tubing. Glass hooks welded just

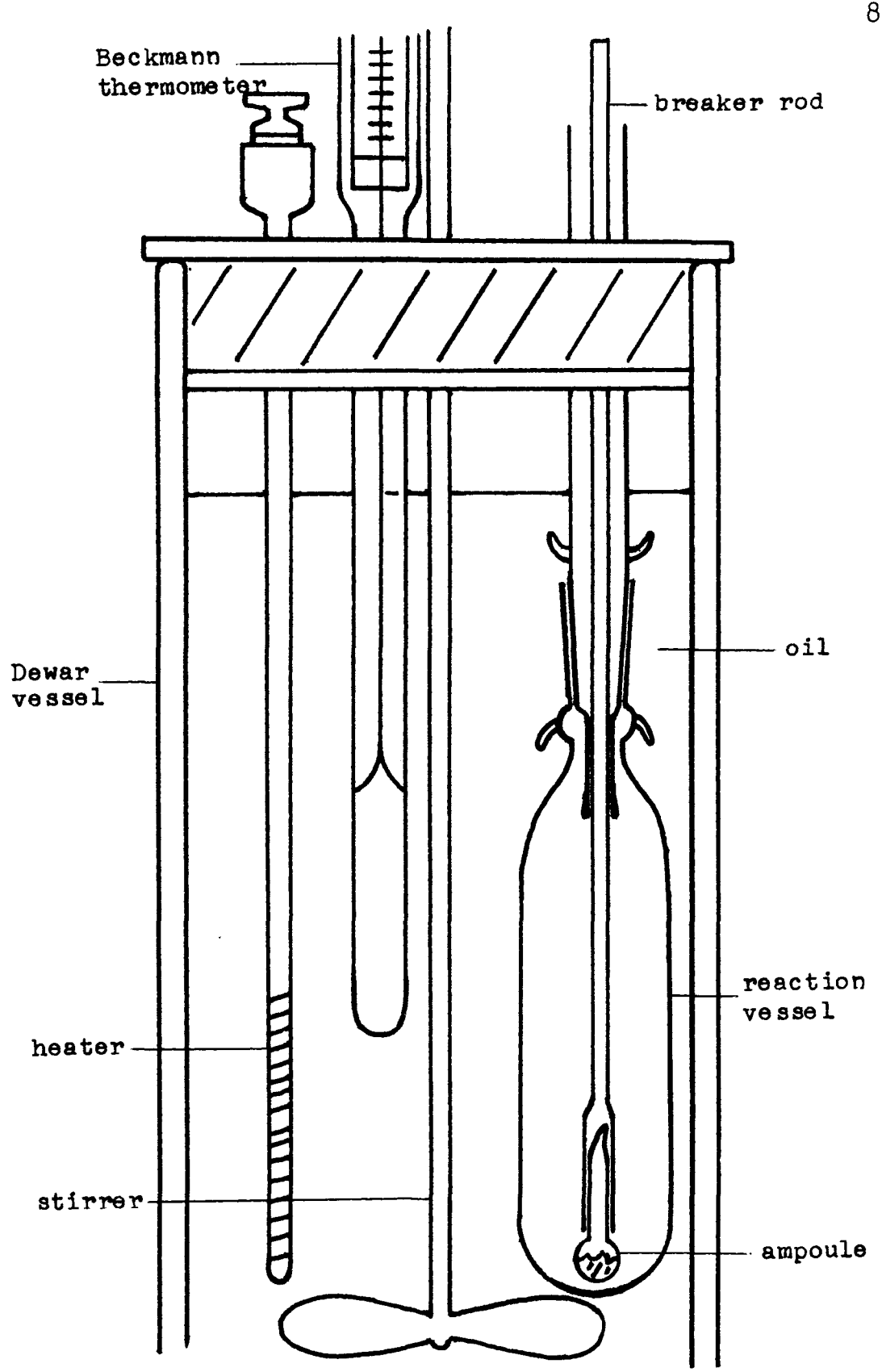

FIGURE 12: Reaction calorimeter for trimethylindium study

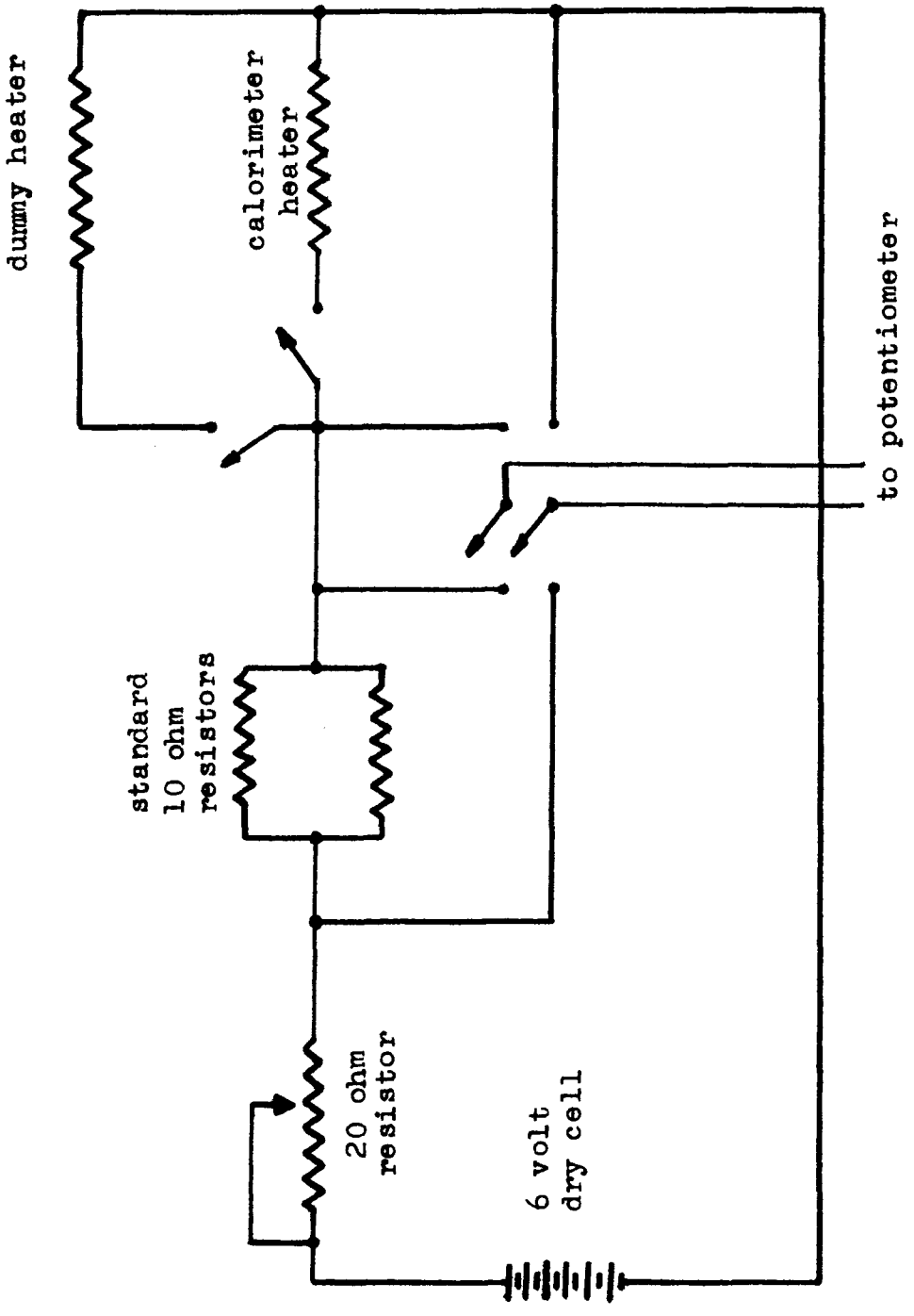

FIGURE 13: Circuit diagram for the electrical calibration of the reaction calorimeter used in the trimethylindium study.

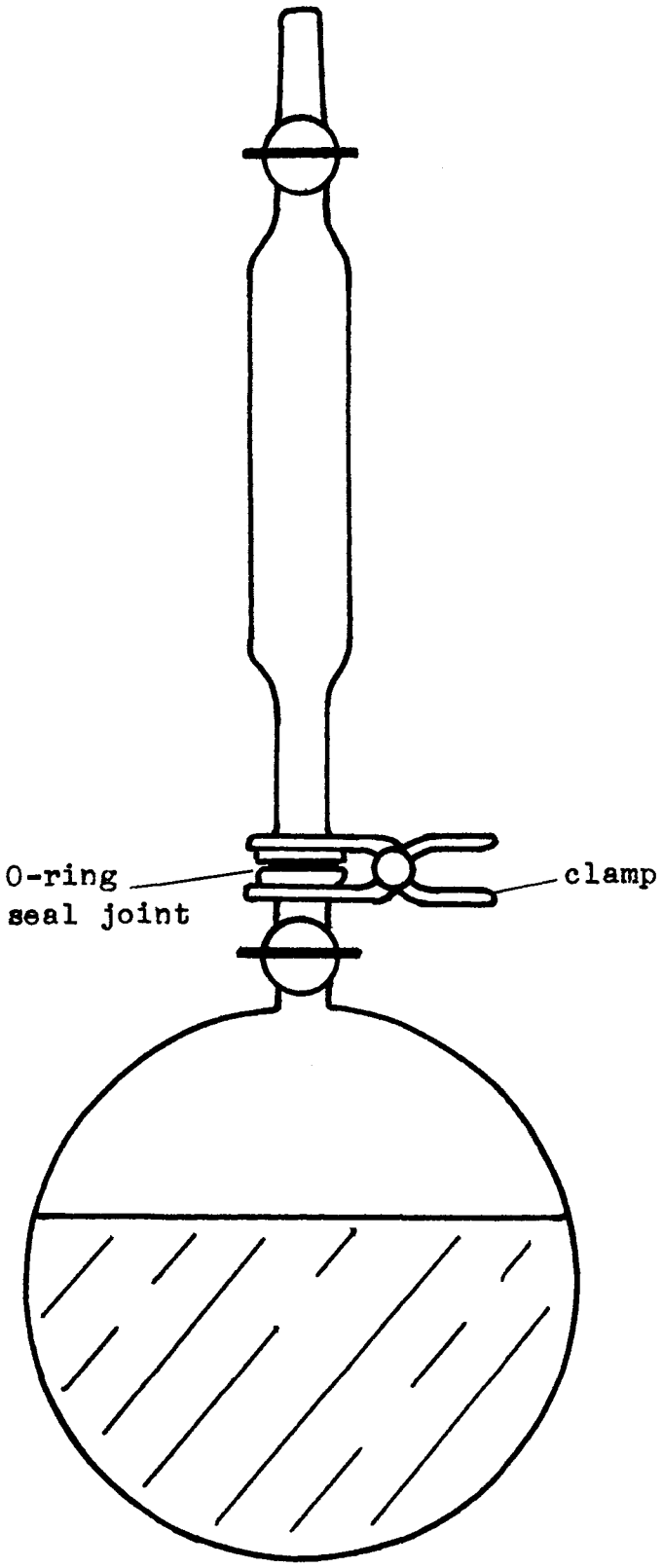

FIGURE 14: Storage vessel for the 1N bromine in chloroform solution.

below the ground joint on the reaction vessel, and just above the joint on the 14 mm tubing allowed the reaction vessel to be secured to the upper portion with a stopper tie and thus prevent the joint from coming apart during the experiment.

The reaction vessel was totally submerged in 500 cc. of Balzer's Duo 5 oil which was stirred with a 3 blade propellor-type plastic coated stirrer. The power to the stirrer was supplied through a 120 volt Variac to a 1525 R.P.M., 120 volt electric motor supplied by Precision Scientific Co. The motor was connected to the stirrer by a flexible shaft manufactured by E.H. Sargent Co.

The temperature of the calorimeter fluid was measured by means of a Beckmann thermometer equipped with a magnifying lens. Temperatures could be read to 0.001° C. Time was recorded with a Heuer stopwatch capable of being read to 0.1 seconds.

A 0.20 W immersion heater constructed of 0.1 mm Chromel wire wound on a glass support was used to supply the heat for calibration purposes. The glass support, 7.5 mm O.D. tapering to 3.5 mm O.D. was 25 cm long and had two inner channels housing the leads of the heating windings which were wound on the last 6 cm of the rod. The leads were attached to two metal screw type binding posts mounted on a triangular piece of plexiglass to which the heater support was cemented.

The heater was part of an external circuit (figure 13)

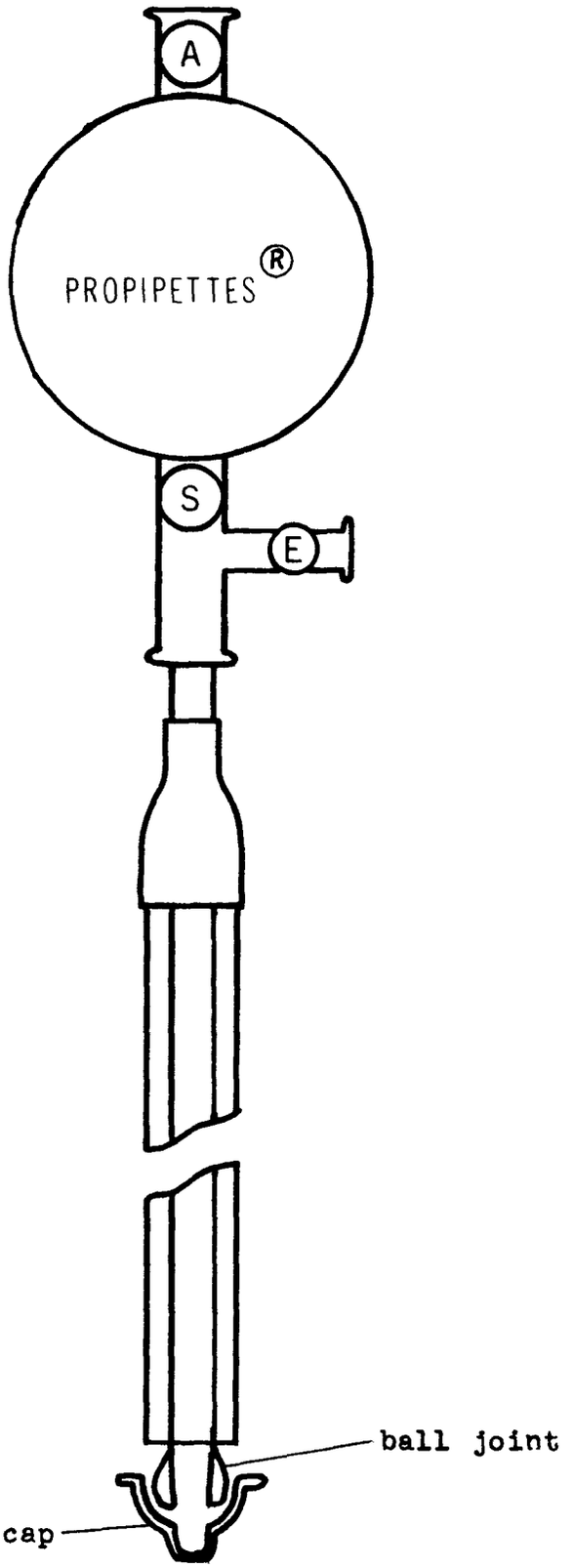

FIGURE 15: Vessel for release of indium tribromide into chloroform.

containing two standard 10 ohm resistors and a 0.20 W dummy heater. Power to the circuit was supplied from a 6 volt car battery through a Leeds and Northrup plug type resistance box set at 20 ohms. A two-pole double-throw switch allowed the power to be diverted from the dummy heater to the calorimeter heater.

The stirrer, heater, thermometer and reaction vessel were suspended through appropriate size, close fitting holes in a styrofoam-plexiglass top. The 1 inch thick styrofoam was sandwiched between two ¼ in. circular pieces of plexiglass held together by long screws. The styrofoam pressed firmly against the top inside edge of a J. C. Martin Co. Dewar flask 6.8 cm I.D. and 30 cm deep.

A typical determination included the following steps. An approximately 40 ml. aliquot of bromine solution was removed from the storage vessel (figure 14) by evacuating the upper cylindrical portion, inverting the vessel, and opening the connecting top to allow the nitrogen atmosphere above the solution to push the required amount of solution into the now lower area. Ten ml. and 25 ml. aliquots were pipetted from this lower region for use in standardization of the bromine solution, and reaction respectively. A previously weighed ampoule containing trimethylindium was placed in the holder on the end of the breaking rod and the reaction vessel assembled. The reaction vessel and all other components were placed in the Dewar flask and allowed to equilibrate for at least ½ hr. The dummy heater was also turned on at this

time.

After an initial period of time-temperature readings the ampoule was broken against the bottom of the reaction flask by depressing the rod. Readings were continued for a period equal to the initial one after the temperature assumed a linear relationship with time. An electrical calibration was then performed to determine the energy equivalent of the system. Calibration prior to the reaction produced the same value. The unreacted bromine in the reaction flask was treated with an excess of potassium iodide and the liberated iodine was titrated with standardized potassium thiosulphate. Similar treatment of the 10 ml aliquot was used to determine the normality of the bromine solution prior to the run. Titrations before and after runs without trimethylindium showed no loss of bromine occurs. Runs were also done by breaking empty ampoules to show that no heat was generated (29) from this source.

The heat of solution of indium tribromide in chloroform was done in a modified apparatus. A Pyrex tube, 8 mm O.D. and 28 mm long ended in an inner ground ball joint (figure 15). A small cap made from the outer ball joint fit over the end. This tube was placed inside a 16 mm O.D. tube, 21 mm long which fit through the cork lid of the 7 cm I.D. by 19 cm deep Dewar flask. A piece of rubber tubing which fit snugly over the inner tube also was fastened over the outer tube to seal the system. This piece of apparatus took the place of the reaction vessel in the calorimeter system. A

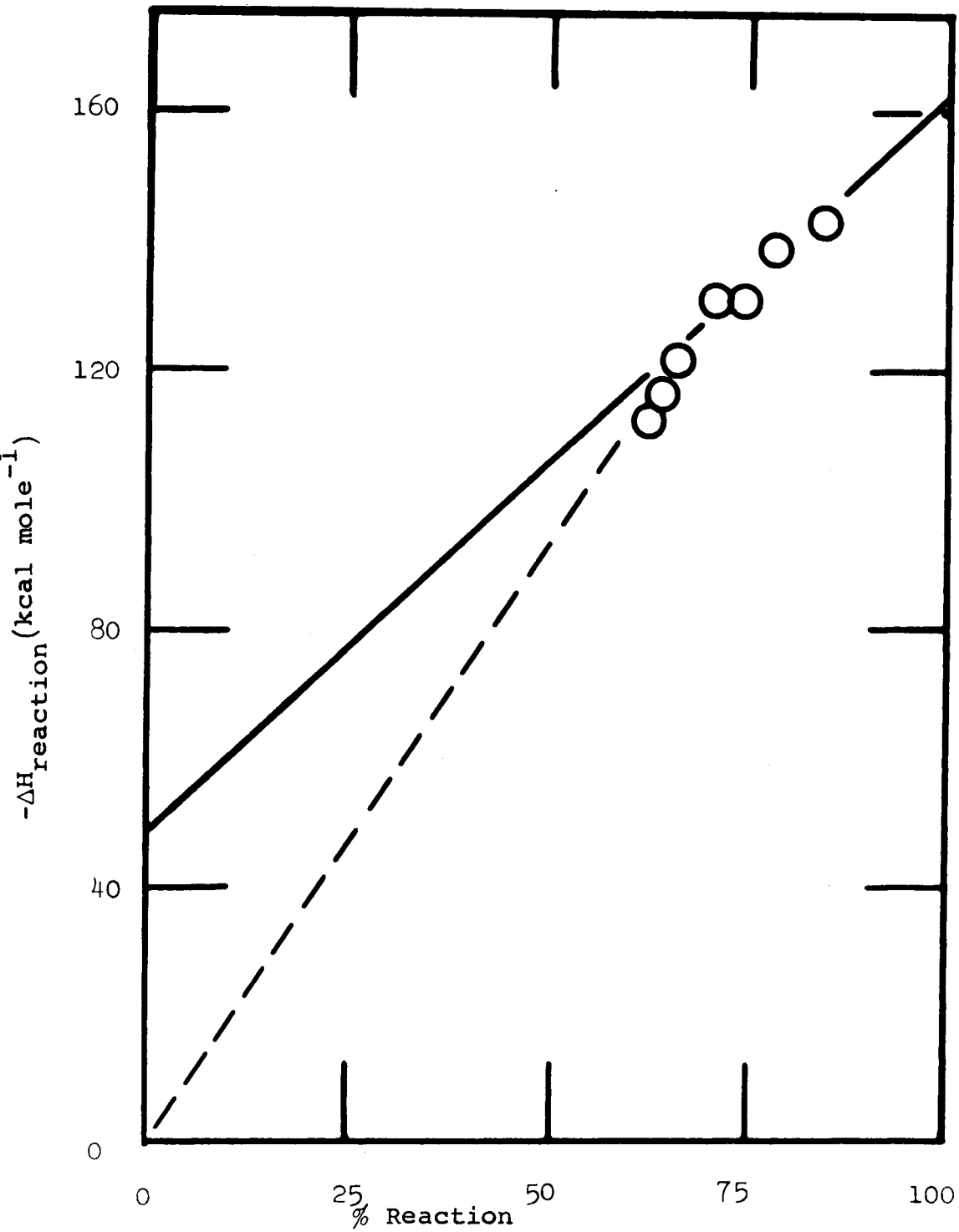

FIGURE 16: Variation of the heat of reaction of trimethylindium with bromine in chloroform solution at 25°C.

———, linear least mean squares line obtained using the points above 66% reaction; ---, plot obtained if the first two methyl groups are readily replaced by bromine so that a linear relationship holds from 0-66.7% conversion.

magnetic stirring bar in the bottom of the Dewar vessel provided for the stirring of the A.C.S. grade chloroform which was placed in the Dewar.

The previously weighed solution tube was filled with $InBr_3$ in a dry nitrogen filled glove box, and reweighed. The open end of the inner 8 mm tube had been sealed with a cork which was now replaced with a propipette (purchased from Fisher Scientific Co.) when the apparatus was assembled.

After an initial period the cap was knocked from the tube by pulling the inner tube up through the sealing rubber tubing and dislodging the cap on the outer tube. The propipette was used to flush the inner tube with chloroform. Blank runs with no $InBr_3$ showed that no heat was generated by this process.

c) Results and Discussion

Very few calorimetric studies of the group IIIB metal alkyls have been done. Until the publication of this work (30), only two articles had appeared, both concerning trimethylgallium. In a study done in a static bomb calorimeter by Long and Sackman (31) $\Delta H_f^{\circ}(Ga(CH_3)_3,l) = 17.6$ kcal/mole. The mean gallium-carbon bond energy was 57.7 ± 2 kcal/mole.

Powell and Mortimer (19) used the reaction of trimethylgallium with excess iodine to determine the heat of formation of the alkyl. Because of the high strength of the gallium-carbon bond in methylgallium (32), only two methyl groups were readily displaced. Concentrated iodine solution at an

elevated temperature was required to obtain a sufficient extent of reaction to allow the heat of formation of the alkyl to be determined. The mean gallium-carbon bond energy was 56.7 ± 4 kcal/mole and $\Delta H_f^\circ(Ga(CH_3)_3,l) = 14.5 \pm 8$ kcal/mole.

The pyrolysis of trimethylindium has been studied in a toluene carrier system (33). From the break in the Arrhenius plot of the kinetic data at 67% theoretical yield of methyl radicals, it was concluded that reaction [2] rapidly follows reaction [1], but reaction [3] does not occur to any appreciable extent under the conditions used.

$$In(CH_3)_3 \longrightarrow In(CH_3)_2 + CH_3 \qquad [1]$$

$$In(CH_3)_2 \longrightarrow InCH_3 + CH_3 \qquad [2]$$

$$InCH_3 \longrightarrow In + CH_3 \qquad [3]$$

From the Arrhenius plot, the following values were estimated: $D[(CH_3)_2In\text{-}CH_3] = 47.2$ kcal/mole, and $D[In\text{-}CH_3] = 40.7$ kcal/mole. The present study was undertaken to determine the mean metal-carbon bond energy in trimethylindium and hence $D(CH_3In\text{-}CH_3)$.

Initial trials were carried out with various solutions to determine if 100% reaction could be achieved. Only solutions whose products had readily available thermodynamic data were used. The results are shown in Table 6.

The percent conversion was based on how much of the reactant in the solution was consumed as compared with the amount of metal alkyl used. No solution tested provided 100% reaction of the alkyl. The result with aequeous hydrochloric

TABLE 6

REACTION OF TRIMETHYLINDIUM WITH VARIOUS SUBSTANCES

Weight $In(CH_3)_3$ (gm.)	Solution used	Normality of solution	Conversion %
0.1113	I_2 in benzene	0.852	85.4
0.0824	"	0.846	85.8
0.4446	"	0.852	67.1
0.0670	"	0.846	78.9
0.0247	HCl aequeous	1.202	84.9
0.1080	Br_2 in chloroform	0.979	92.1
0.0503	"	0.979	89.9

TABLE 7

ENTHALPY OF REACTION OF TRIMETHYLINDIUM WITH BROMINE IN CHLOROFORM SOLUTION

Sample Weight (g)	Normality of Br_2 solution*	Conversion (%)	ΔH_{rx} (kcal $mole^{-1}$)
0.0897	1.085	84	143
0.1043	0.972	78	139
0.0657	0.053	75	131
0.0907	0.656	71	132
0.1461	0.827	66	121
0.0805	0.658	65	116
0.1422	1.055	63	112

*25.0 ml bromine solution used in each run.

acid represented only one successful attempt in a half a dozen. Most often a white gelatinous solid was formed and very low percent conversions found. Attempts were also made with aequeous sulfuric acid solutions, but even less success was achieved.

The tests with bromine and iodine solutions produced comparable results. However, it was decided to work with bromine due to slightly higher percent reactions and the easier handling of the bromine solutions. Iodine tended to come out of solution on standing in the volumetric flask.

The calorimetric results are shown in Table 7. All experiments were carried out at approximately 25° C. The time temperature curves follow the pattern depicted in figure 1, and the data was treated according to the method of Dickenson (16). Within the experimental scatter the observed heats of reaction are consistent with the percentage of the alkyl undergoing reaction. The data are limited, but inspection of figure 16 indicates a pattern of reaction similar to that previously observed by Fowell and Mortimer for the reaction of trimethylgallium with iodine (19). In this case, immediate quantitative replacement of two methyl groups by halogen was observed, followed by slow replacement of the third methyl group. The linear least mean squares extrapolation to 100% based on this mechanism gives $\Delta H = -162.5$ kcal/mole for reaction [4].

$$In(CH_3)_3(c) + 3Br_2(soln.) \longrightarrow InBr_3(soln.) + 3CH_3Br(g). \qquad [4]$$

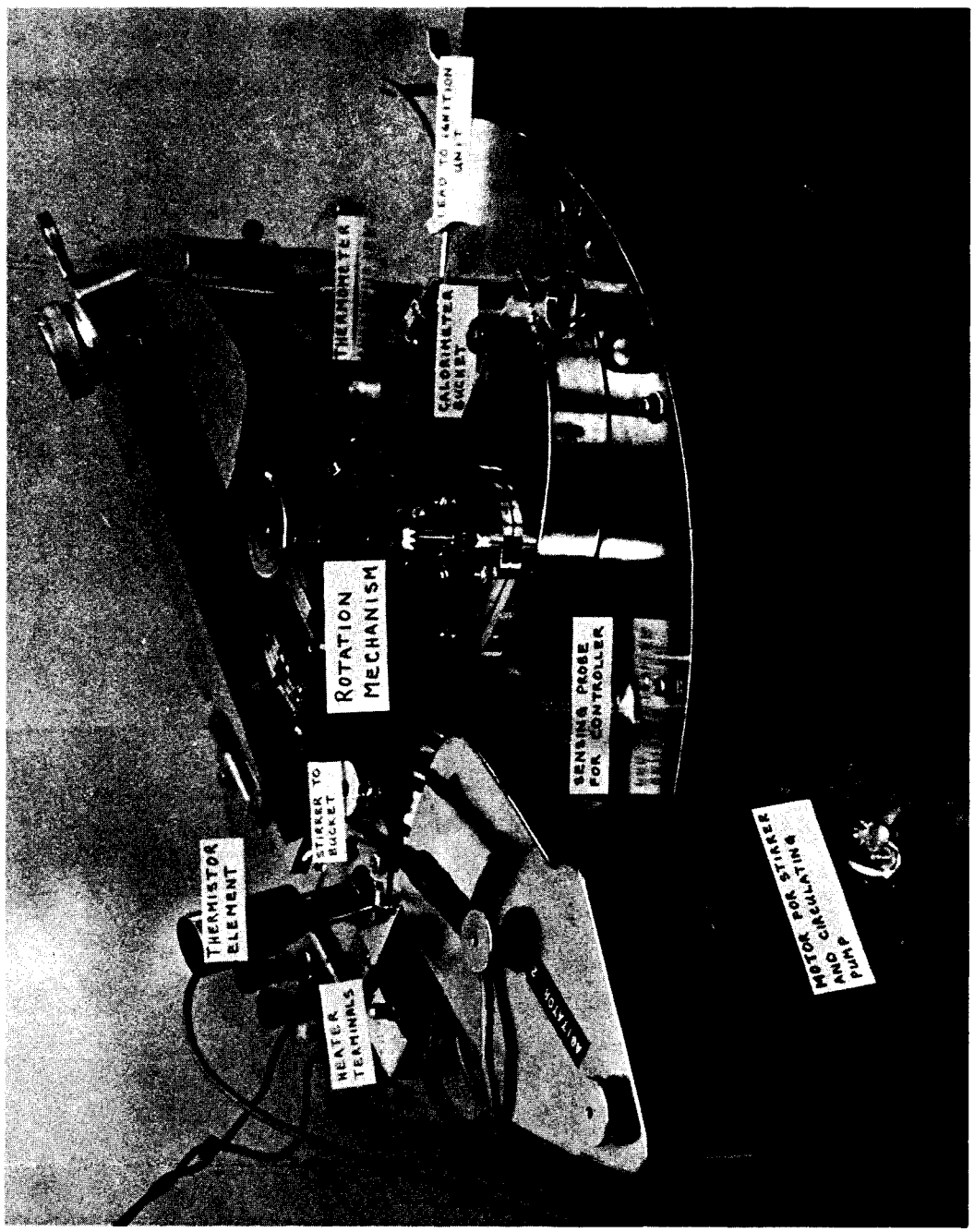

FIGURE 17: Figure of the rotating bomb calorimeter.

Extrapolation to 66.7% gives ΔH = -124.7 kcal/mole for reaction [5].

$$In(CH_3)_3(c) + 2Br_2(soln.) \longrightarrow CH_3InBr_2(soln.) + 3CH_3Br(g). \quad [5]$$

No correction has been made for the heat of solution of any CH_3Br which remains in solution. The heat of solution of $InBr_3$, c in chloroform was determined in separate experiments as ΔH_{soln} = -1.4 $\pm$ 0.3 kcal/mole. The heat of solution of CH_3InBr_2, c in chloroform is assumed to be the same as $InBr_3$, c. The enthalpy of solution of bromine in chloroform is 0.7 kcal/mole (4).

With $\Delta H_f^\circ{}_{298}(InBr_3,c)$ = -102.5 kcal/mole (4) and $\Delta H_f^\circ{}_{298}(CH_3Br,g)$ = -9.0 kcal/mole (34), $\Delta H_f^\circ{}_{298}(In(CH_3)_3,c)$ = 29.5 kcal/mole. Using this value along with the heat of reaction for equation [5], $\Delta H_f^\circ{}_{298}(CH_3InBr_2,c)$ = -85.5.

Combining the value for $In(CH_3)_3$,c with $\Delta H_{sublimation}$ $(In(CH_3)_3,c)$ = 11.6 kcal/mole (28) gives $\Delta H_f^\circ{}_{298}(In(CH_3)_3,g)$ = 41.4 kcal/mole. With $\Delta H_f(CH_3,g)$ = 33.2 (4) and $\Delta H_f(In,g)$ = 58.2 (4), the mean metal-methyl bond dissociation energy in trimethylindium, $\overline{E}(In\text{-}CH_3)$, is 38.9 kcal/mole. This gives $D[CH_3In\text{-}CH_3]$ = 28.8 kcal/mole, a value consistent with the previously proposed kinetic mechanism for the decomposition of trimethylindium in a toluene carrier system (33).

CHAPTER V

ROTATING BOMB CALORIMETRY OF TRIMETHYLINDIUM

a) Preparation of Materials

i) Trimethylindium was prepared as described in the materials section of Reaction Calorimetry (Chapter IV).

ii) Benzoic acid was purchased from the Parr Instrument Company in the form of one gram pellets. The pellets had a certified heat of combustion of 6318 cal. per gm.

iii) The auxiliary materials included Paraffin Oil, N.F. supplied by Fisher Scientific, Mylar and polyethylene plastic sheeting supplied by Handee Plastic Company, and unmercerized cotton thread purchased from the S.S. Kresge Co.

iv) Oxygen listed as 99.999% pure was purchased from Matheson Co. Argon at 99.998% purity was supplied by Union Carbide.

b) Apparatus and Procedure

The calorimeter used (figure 17) was a modified U.S. Bureau of Mines design rotating bomb calorimeter made from plated brass. The major modification was the rotating mechanism which involved the use of a low R.P.M., high torque motor coupled to the rotating mechanism on the bomb by a series of gears and shafts. The shaft going through the lid was of two portions, one fixed, and one capable of being

raised and lowered which allowed the coupling to the gear on the motor when desired. The high torque motor was a 115V. Bodine motor, type KYC-22RC, with an R.P.M. of 10, and torque of 32 in.oz. The stirring and circulation of the water in the calorimeter jacket and lid was done by blade stirrer and a circulating pump driven by two Electrohome 115V, 1.25 amp motors, R.P.M. 1550. One of these motors as well as driving the circulating pump, also supplied power to the stirrer for the water in the calorimeter bucket.

The calorimeter jacket housed two circular heaters, one 500 watt heater, and one 125 watt heater, and a set of cooling coils. Cool, thermostated water from an external bath was circulated through the coils and worked against the heaters in keeping the calorimeter jacket at 25.000°C. The temperature of the external bath was controlled by a Haake stirrer-temperature controller working against a cooling coil from a Portable Cooler Unit made by Precision Scientific Company. Power to the circular heaters was supplied by a Thermotrol proportional temperature controller, Shell Development Design, Hallikainen Instruments. Temperature of the jacket could be controlled to $\pm$0.001°C.

Besides a 3-blade stirrer, and part of the rotating mechanism, the calorimeter bucket (figure 18) housed a 15 watt rod heater and the mechanism for coupling the bomb to the ignition unit. The rod heater was used to adjust the temperature of the water in the bucket if it was lower than desired. The coupling mechanism involved a spring clip

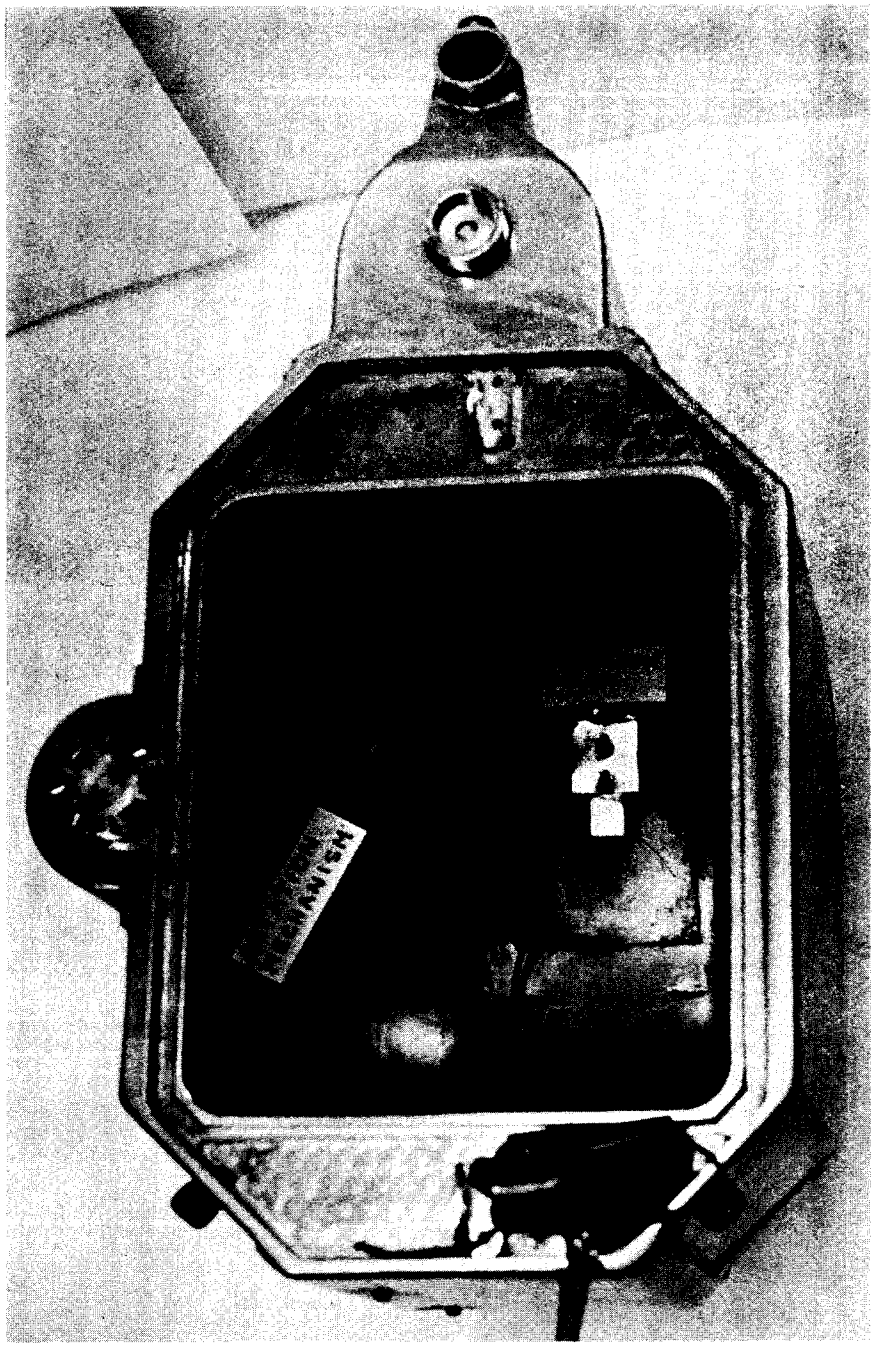

FIGURE 18: Photograph of the calorimeter bucket.

which released when the rotation of the bomb was begun.

The temperature of the water in the calorimeter bucket was monitored by a 2000 ohm thermistor in conjunction with a Honeywell Wheatstone Bridge, Model 1081, and a Leeds and Northrup D-C Null Detector with variable sensitivity. The thermistor was calibrated against a Parr certified thermometer capable of being read to 0.001°C. The resistance of the thermistor could be estimated at better than 0.01 ohms (about 0.0001°C) with the null detector set for low to moderate sensitivity. Time was measured and recorded on a Simplex Punch Timer capable of recording intervals of 0.01 minutes.

The ignition unit consisted of two 250 mfd. capacitors, a 2K ohm resistor, and a 250V diode. The diode rectified the current from a 115V A.C. Powerstat. A charge of 120V across the two parallel capacitors was sufficient for the ignitions.

The bomb used was a platinum-lined, high pressure Parr Bomb, Model No. 1004 made according to a U.S. Bureau of Mines Design. To the exterior of the bomb was attached a collar and gear to give a twisting end over end motion to the bomb when it was rotated. A special clamping handle which fitted into two small holes near the bottom of the bomb was used to lower the bomb in an inverted position into the bucket. The inverted position directs the flame of the combustion towards the bottom of the bomb and therefore, protects the inner fittings from damage. Platinum crucibles used in the combustions were purchased from the Fisher Scientific Company.

The handling of moisture and oxygen sensitive materials was done in a Labconco fiberglass glove box measuring approximately 3' x 2' x 2'. An evacuable side port approximately 1' x 8" x 8" allowed the passage of materials to and from the box without the disturbance of the box atmosphere. The box was also equipped with five inlet-outlet ports for the introduction of gases and three internal electrical outlets. A small manometer measured pressure in the box in inches of water.

An inert atmosphere was achieved in the box by inflating a ten foot diameter neoprene balloon in the box using high purity argon. Once the balloon was firmly pressed against all sides of the box, any ports which were open to allow the escape of air were now closed, and the balloon was deflated in the box. Two or three inflations and deflations of the balloon produced an atmosphere of less than 0.1% oxygen.

A Neptune Dyna-Pump supplied by Fisher Scientific Co. was used to circulate the box atmosphere through external Tygon tubing. A T-piece in the tubing with a Silicone-gum rubber septum allowed sampling of the box contents with a 1 cc gas syringe. An argon-oxygen separation (35) and oxygen analysis was achieved using an eight foot by 1/8 inch I.D. column filled with 40/60 mesh 5A molecular sieve at -70°C in conjunction with a Perkin Elmer 154D gas chromatograph with a thermal conductivity detector. The helium carrier gas flow rate was about 50 cc per min. The areas of the oxygen

peaks from air injections were compared with the oxygen areas from the sample. Oxygen could be measured quantitatively to 0.01% of a sample and observed in portions as small as 0.001%. The purified argon listed at 99.998% purity showed no traces of oxygen.

Traces of moisture in the box were eliminated by the use of a dish of P_2O_5 in the box or a drying tube of P_2O_5 coupled to the external tubing through which the box atmosphere was circulated.

Tests on the rate of diffusion of oxygen into the box showed that the oxygen content of the box increased at the rate of 0.01% to 0.02% per hour. This rate is well below the limit set by White and Smith (36) to indicate the glove box is functioning properly. Attempts to get rid of the oxygen diffusing into the box by circulating the box atmosphere through a U-tube containing a 80% potassium, 20% sodium alloy (37) which is liquid at room temperature proved fruitless. However, this did not affect operations in the box, but necessitated the inconvenience of flushing the box each time it was to be used.

Thermoplastic bags made by the use of an impulse heat scaler purchased from Vertrod Corporation were used to house the metal-alkyl samples for combustion. The bags of the best design (38) were made as follows: a piece of plastic 8-10 cm long and 2-3 cm wide was folded lengthwise and sealed along its length; the plastic was creased flat so that the seal was centered along the length, and one end was sealed.

Once the sample was placed in the bag, the last seal was done with the first seal at the edge rather than in the center. The resulting bag had a triangular, box-like appearance. This type of bag sat more firmly in the crucible and allowed better combustion of the sample (38).

The bags were filled in the glove box by placing the bag over the end of a long stem funnel and spooning $In(CH_3)_3$ crystals into the funnel. In the case of a liquid substance, a syringe could be used. The material was confined to the bottom 10 mm of the bag. As much of the gas in the bag was removed as possible by pressing with the fingers. Several folds were made in the top of the bag which was then temporarily sealed with a pinch clamp or paper clip. The bag was removed from the box and sealed as close to the sample as possible with the heat sealer. The weight of metal alkyl in the bag was determined by difference. In the case of $In(CH_3)_3$ the filled bags were stored in the dark.

Both polyethylene and Mylar (polyester) were used as containers. While Mylar (2 ml thickness) was acceptable for $Pb(CH_3)_4$ (39), it was attacked by $In(CH_3)_3$ and would crack and allow sample decomposition within an hour of being filled. Polyethylene bags (6 ml thickness) showed no signs of attack and maintained samples 2-3 days without signs of decomposition. Both plastics were supplied by the Handee Plastic Company, Windsor, Ontario, Canada.

The amount of carbon dioxide produced in a combustion was measured by absorption on Indicarb supplied by Fisher

Scientific Company. The absorption tube used was an improved design of Prosen and Rossini (8). The tube was filled with absorbent, evacuated and weighed. A magnesium perchlorate drying tube was placed between the absorption tube and the bomb to absorb any water vapour. The bomb gases were passed through the absorption train and the bomb flushed 3 to 4 times with oxygen. The absorption tube was reevacuated and weighed. Subsequent evacuations and reweighings showed no weight loss for the tube, as was the case in the initial weighing. Absorption of CO_2 from benzoic acid samples showed absorption of CO_2 within 0.001 gm of the amount expected. Approximately 2.5 gm of CO_2 were absorbed in these cases.

Analysis for carbon monoxide in the bomb gases was carried out by placing a sampling tube after the absorption tube. The sample was analyzed on a Perkin Elmer 154D gas chromatograph with a thermal conductivity detector. A silica-gel column at 80°C and a helium carrier gas flow rate of about 20 cc per minute were used.

Indium metal was analyzed by the method of Flaschka and Abdine (40) using an EDTA titration with a copper-PAN complex as indicator.

In a typical combustion of a metal-alkyl, the following procedure was used. Twenty-five to fifty milliliters of solution which would dissolve the products of combustion were pipetted into the bomb. A previously weighed bag of metal-alkyl along with enough hydrocarbon oil to give a total liberation of 7-8 thousand calories was put into the platinum

crucible. A fuse of unmercerized cotton thread 10 cm long connected the oil with a coiled platinum wire attached to the terminals on the bomb head. The platinum wire, about 10-12 cm in length, was coiled about an Allen wrench 1 mm O.D. The coil in the centre portion of the wire was 1 cm long. The cotton thread was doubled through the coil to prevent it from springing loose. The head (figure 19) which has previously been in an inverted position, was turned right side up and the experimenter makes sure the thread doesn't catch on any of the crucible support fittings. The head was placed on the bomb and the cap screwed on. The set screws in the cap were alternatively tightened from side to side until all set screws were tight. The bomb was allowed to set 10 minutes to allow the Teflon gaskets in the head to flow. After this period, the set screws were given a final tightening.

The calorimeter bucket was weighed, and a known amount of water weighed into the bucket (approximately 3800 gm). This amount of water is sufficient to cover all parts of the bomb even when it is rotating. The bucket was covered after weighing to prevent any undue losses due to evaporation.

The bomb was flushed 3 to 4 times and then pressurized to 30 atmospheres with ultra high purity oxygen supplied by Matheson Co. The bucket was placed in the calorimeter, and the bomb was placed in the bucket. The firing mechanism for the bomb was engaged and the calorimeter closed. Power was supplied to the heater in the bucket if necessary, to bring

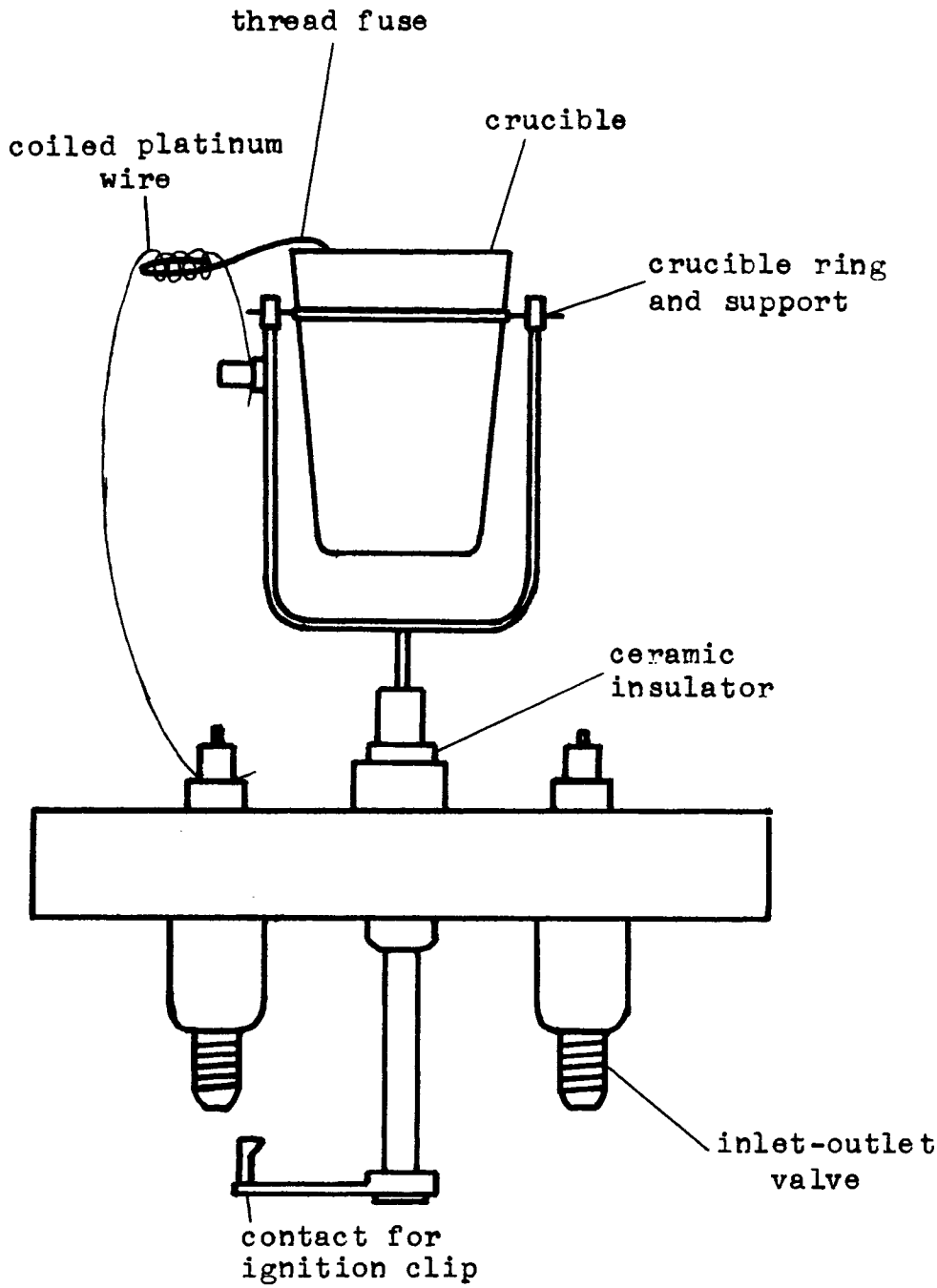

FIGURE 19: Diagram of the bomb head.

the temperature of the bucket within a reasonable value of the desired starting temperature. The system was allowed 20 to 30 minutes to equilibrate.

Time, thermistor resistance readings were recorded for a period of about 10 minutes (at intervals of not more than half a minute). Just before firing, the condensors of the ignition unit were charged, and the voltage across them measured. The condensors were discharged for at least 1 minute, and after 1-2 minutes the bomb rotation was begun. During this period of rapid temperature rise, readings were taken less than every 15 seconds (14). Once the time-temperature readings assumed a steady progression, recordings were continued for another 10 minutes, or as long as was necessary for the products of combustion to dissolve.

After the readings were stopped, the bomb was removed from the calorimeter, dried, and connected to the absorption train. The carbon dioxide was absorbed, and a sample for gas chromatographic analysis taken. The bomb solution was analyzed for the metal present, and also for the reaction of any oxidizing or reducing agent which had been used.

In the case of a calibration with benzoic acid, or the combustion of the auxiliary materials such as the oil, thread, or plastic film, the 50 ml of solution is replaced by 1 ml of water. Also, no initial flushings of the bomb are needed, as the nitric acid formed from the reaction of nitrogen in the air in the bomb, can be analyzed.

c) Results and Discussion

At least six studies have been done using the rotating bomb calorimeter for the combustion of organometallic compounds (41). Included in these studies are tetraethyllead (15), lead oxalate (15), tetramethyllead (39), magnesium decacarbonyl (41), hexamethyldisiloxane (41), and triphenylarsine (42). Each piece of work involved the use of bomb solutions of various complexities in order to obtain well defined products and ranged from an approximately 4N sodium hydroxide solution in the triphenylarsine investigation to a 10% by weight nitric acid solution with 0.1 wt. % arsenious acid in the study of tetraethyllead. Also, in all cases, simple to complex comparison experiments were necessary as sufficient auxiliary data for the products of the combustion was unavailable.

In the cases where previous combustion studies were carried out in static bombs, marked and often surprising differences in the resultant heats of combustion were found. As an example, in the combustion of tetramethyllead, a static bomb study (43) gave $\Delta H^{o}_{f298}(g)$ for tetramethyllead as 3.2 $\pm$3 kcal/mole, whereas the rotating bomb study (39) gave the value 32.6 kcal/mole. The laboratory reporting the rotating bomb work on tetramethyllead also did tetraethyllead (15) by the above static bomb method as well as the rotating bomb method. The value for tetraethyllead done by the static bomb method differed from the rotating bomb value by 39 kcal/mole but in the opposite direction from the difference found

for tetramethyllead (39). Therefore, the superiority of the rotating bomb method over the static bomb procedure for organometallic compounds can be quite striking. Even though this superiority exists, the rotating bomb method still requires painstaking effort as does the static bomb method to achieve a high degree of accuracy. The first prerequisite to high accuracy is detailed characterization of the calorimeter.

In bomb calorimetric work, one of the important aspects of the calorimetric part of the investigation as opposed to the chemical portion of the investigation, is the measurement of the temperature increase with time and the subsequent calculation of the corrected temperature rise. The use of a thermistor as the temperature sensing device requires calibration over the temperature ranges to be studied (Table 8).

Thermistors have been used in a number of calorimetric investigations and several relationships between resistance, R, and absolute temperature, T, have been put forward. The following three formulas were tested as well as the polynomial curve fits for the variables used in each case:

$$\ln R = \frac{A}{T} + B \quad (18), \qquad [1]$$

$$\ln R = \frac{C}{T+\theta} + D \quad (44), \qquad [2]$$

and

$$T = A^1 \ln R \quad (45), \qquad [3]$$

where A, B, C, D, , and A^1 are constants. Of these

TABLE 8

CALIBRATION OF THERMISTORS AGAINST CALIBRATED THERMOMETERS

Thermistor 1 (resistance in ohms)	Thermistor 2	Temperature (°K)
2539.2	2568.3	295.700
2529.9	2558.6	295.783
2518.8	2547.6	295.879
2508.0	2536.4	295.977
2496.7	2525.1	296.077
2485.7	2513.8	296.177
2474.8	2502.9	296.275
2464.0	2491.9	296.373
2453.0	2480.7	296.473
2442.1	2469.5	296.575
2431.5	2458.9	296.672
2420.6	2448.1	296.775
2409.9	2437.1	296.874
2399.2	2426.3	296.973
2388.8	2415.7	297.071
2375.9	2402.6	297.191
2365.4	2391.9	297.291
2355.5	2381.7	297.385
2345.4	2371.7	297.482
2335.3	2361.4	297.580
2324.9	2341.0	297.780
2314.9	2341.0	297.780
2304.6	2330.4	297.881
2294.8	2320.4	297.980
2285.0	2310.5	298.075
2277.7	2303.2	298.147

relationships, equation [2] is mentioned as the most accurate (17), while equation [3] is quoted as only accurate for small temperature changes (about 0.75°C) (17). All data in this and subsequent sections was processed in Fortran II D programs written for the IBM 1620 II digital computor.

The curve fit program (see subroutine G05CSP in appendix) was tested against data generated from the quadratic expression $y = 2 + 4x + x^2$ for polynomials ranging in degree from one to five. Table 9 lists the data used and the coefficients of the various polynomials in ascending powers of x. The standard deviation, σ, was calculated according to the formula (18),

$$\sigma = \left(\frac{\sum_{i=1}^{n} r_i^2}{n - 1} \right)^{1/2}$$

and is the least for the polynomial of degree 2.

The results of the curve fits for the variables in equations [1], [2], and [3] are listed in Table 10. A plot of 1/lnR vs T was necessary to determine θ (see appendix) which was then used in equation [2]. The value of θ for thermistor 1 and thermistor 2 was 121.6 and 121.8 respectively.

Examination of the standard deviations for the various polynomial curve fits of the different variables reveals that a linear relationship satisfies all cases except for the instance of T vs lnR. However, even in this case, the variation of T with lnR is essentially linear over portions of about one-third of the range of the data. The plots of

TABLE 9

TEST FOR THE POLYNOMIAL CURVE-FITTING PROGRAM

Data	
X	Y
.10000000E+01	.70000000E+01
.20000010E+01	.14000010E+02
.30000010E+01	.23000010E+02
.40000010E+01	.34000010E+02
.50000010E+01	.47000010E+02
.60000010E+01	.62000010E+02
.70000010E+01	.79000010E+02
.80000010E+01	.98000010E+02
.90000010E+01	.11900001E+03
.10000001E+02	.14200001E+03
.11000001E+02	.16700001E+03
.12000001E+02	.19400001E+03
.13000001E+02	.22300001E+03
.14000001E+02	.25400001E+03
.15000001E+02	.28700001E+03
.15999999E+02	.32200001E+03
.16999999E+02	.35900001E+03
.17999999E+02	.39800001E+03
.18999999E+02	.43900001E+03
.19999999E+02	.48200001E+03
.20999999E+02	.52699999E+03
.21999999E+02	.57399999E+03
.22999999E+02	.62299999E+03
.23999999E+02	.67399999E+03
.24999999E+02	.72699999E+03
.25999999E+02	.78199999E+03
.26999999E+02	.83899999E+03
.27999999E+02	.89799999E+03
.28999999E+02	.95899999E+03
.30000000E+02	.10220000E+04

Results

COEFFICIENTS OF THE POLYNOMIAL OF DEGREE 1 ARE

-1.6333329E+02 3.5000000E+01

STANDARD DEVIATION = .68039184E+02

COEFFICIENTS OF THE POLYNOMIAL OF DEGREE 2 ARE

1.9999000E+00 4.0000280E+00 9.9999923E-01

STANDARD DEVIATION = .84305855E-04

COEFFICIENTS OF THE POLYNOMIAL OF DEGREE 3 ARE

1.9998800E+00 4.0000450E+00 9.9999700E-01 6.0360529E-08

STANDARD DEVIATION = .91808458E-04

COEFFICIENTS OF THE POLYNOMIAL OF DEGREE 4 ARE

2.0004800E+00 3.9997680E+00 1.0000205E+00-1.6314673E-06
2.5989473E-08

STANDARD DEVIATION = .53717878E-02

COEFFICIENTS OF THE POLYNOMIAL OF DEGREE 5 ARE

2.0008600E+00 4.0004700E+00 9.9997387E-01 4.7681243E-06
-4.7823600E-07 6.4390651E-09

STANDARD DEVIATION = .40202743E-01

TABLE 10

POLYNOMIAL CURVE FITS TO THE THERMISTOR CALIBRATION DATA

Example	Degree	Coefficient (in increasing powers of x)	Standard Deviation	Sum of Residuals Squared
T vs lnR	1	4.722E+02-2.25E+01	.1922E-02	.992E-04
Th_1*	2	5.694E+02-4.749E+01 1.604E+00	.1213E-02	.3681E-04
	3	7.644E+03-2.773E+02 3.518E+02-1.499E+01	.1202E-02	.3615E-04
	1	4.720E+02-2.246E+01	.2501E-02	.1569E-03
Th_2	2	5.868E+02-5.190E+01 1.887E+00	.1666E-02	.6939E-04
	3	8.274E+02-3.010E+03 3.813E+02-1.622E+01	.1887E-02	.8906E-04
lnR vs 1/T	1	-5.402E+00 3.915E+03	.5381E-04	.7239E-07
Th_1	2	-6.205E+00 4.392E+03 -7.077E+04	.5386E-04	.7253E-07
	3	1.501E+03-1.338E+06 3.987E+08-3.947E+10	.5091E-03	.6481E-05
	1	-5.420E+00 3.924E+03	.7438E-04	.1383E-06
Th_2	2	-3.957E+00 3.055E+03 1.289E+05	.7399E-04	.1368E-06
	3	1.625E+03 -1.448E+06 4.311E+08 -4.265E+10	.4323E-03	.4672E-05

TABLE 10 (Cont'd)

Example	Degree	Coefficient (in increasing powers of x)	Standard Deviation	Sum of Residuals Squared
1/lnR vs T	1	-8.914E-02 7.328E-04	.1282E-05	.4110E-10
Th_1	2	7.438E-02 -3.686E-04 1.854E-06	.8838E-06	.1952E-10
	3	2.454E+01 -2.476E-01 8.345E-04 -9.347E-07	.3552E-05	.3155E-09
	1	-8.918E-02 7.323E-04	.1411E-05	.4980E-10
Th_2	2	3.713E-02 -1.184E-04 1.432E-06	.1215E-05	.3693E-10
	3	2.662E+01 -2.687E-01 9.061E-04 -1.015E-06	.1749E-05	.7651E-10
lnR vs 1/T+θ	1	1.328E-04 1.364E+03	.7786E-04	.1515E-06
Th_1	2	-3.470E+00 2.581E+03 -1.066E+05	.5359E-04	.7180E-07
	3	3.008+02 -1.574E+05 2.794E+07 -1.638E+09	.5711E-04	.8154E-07
	1	1.198E-04 1.365E+03	.8584E-04	.1842E-06
Th_2	2	-2.690E+00 2.308E+03 -8.254E+04	.7376E-04	.1300E-06
	3	3.250E+02 -1.699E+05 3.007E+07 -1.760+09	.7562E-04	.1429E-06

*Th_1 - Thermistor 1, Th_2 - Thermistor 2.

the respective variables exemplifies the results even more (figures 20 through 22).

In an attempt to make the plots more sensitive, and to obtain T as the dependent variable, the data of lnR vs 1/T was treated to minimize roundoff error by subtracting the first temperature from all temperature readings, and the curve fitting program applied to 1/T vs lnR. However, the net result was still the same, but arbitrarily the quadratic expression was used as the formula for the conversion of resistance to temperature and appears in the subroutine G05CON in the appendix. From the magnitude of the standard deviations, and the ability to estimate the resistance of the thermistor to 0.01 ohm, the temperature can be measured to $\pm 0.0001^{\circ}C$.

In order to use the equations presented in Chapter II to evaluate the corrected temperature rise, the effects of stirring and heat exchange for the calorimeter had to be investigated. Equation [33] in Chapter II can be rearranged to the form

$$\frac{dT}{dt} = (u + gT_j) - gT. \qquad [4]$$

Therefore, time-temperature readings were taken for the calorimeter system with an empty bomb over a range of temperature with and without the bomb rotating. The slopes of the readings were plotted against the mid-temperature of each interval done. The data is listed in Table 11 and shown in Figure 23. The three sets of data were compiled on three separate occasions.

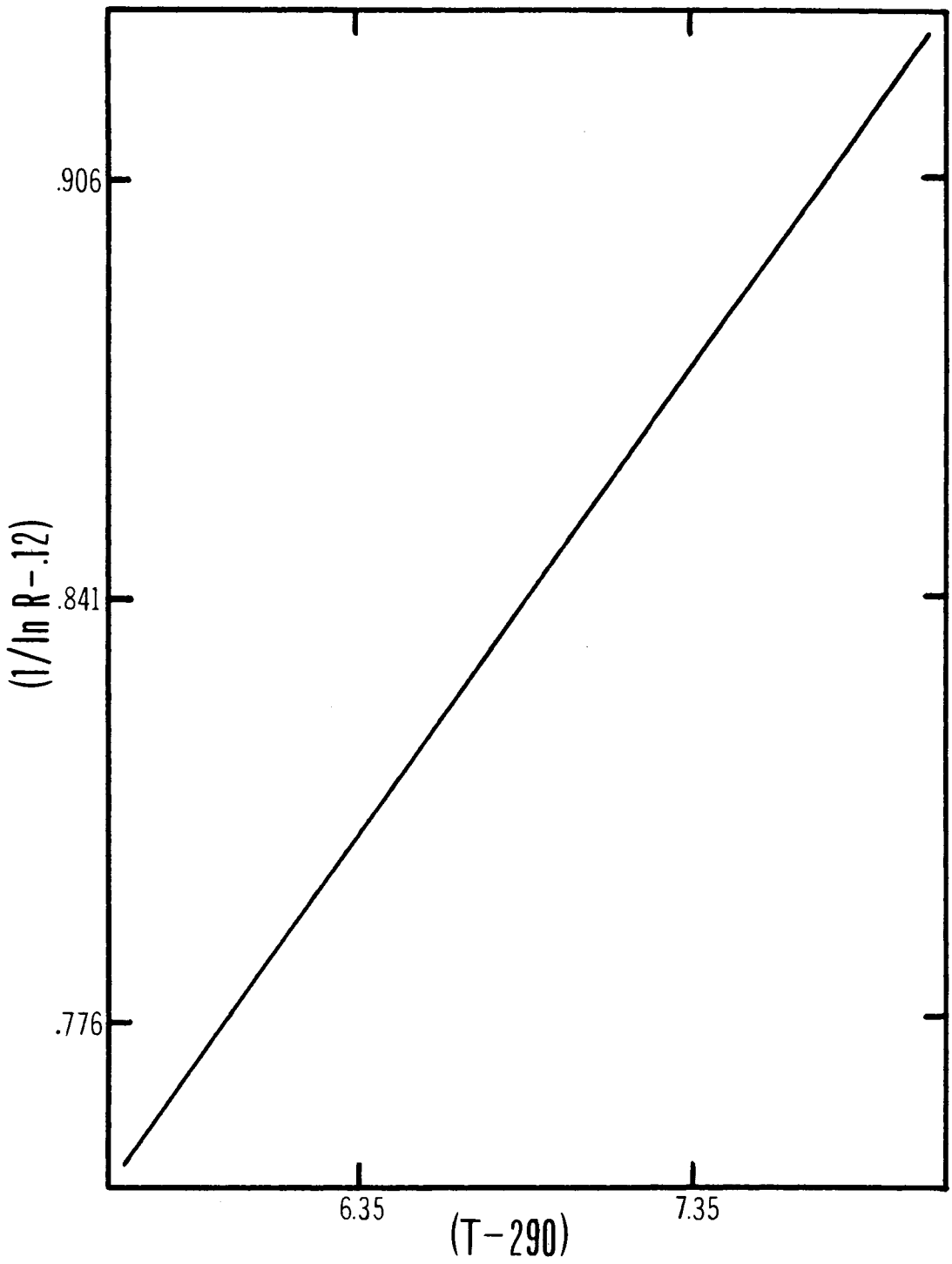

FIGURE 20: Thermistor calibration: plot of 1/lnR vs T.

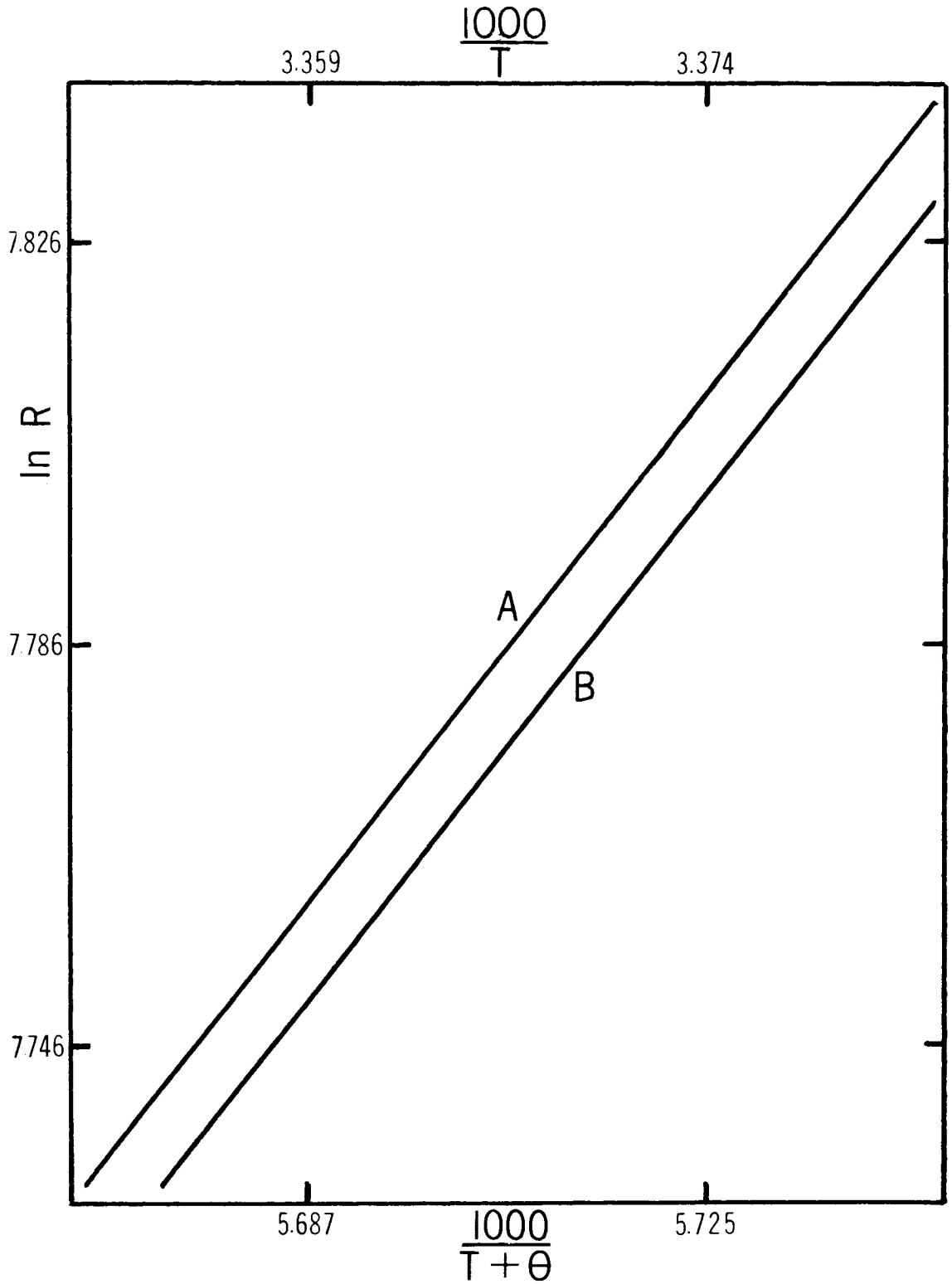

FIGURE 21: Thermistor calibration: plots of lnR vs 1/T, B, and lnR vs 1/(T+θ), A.

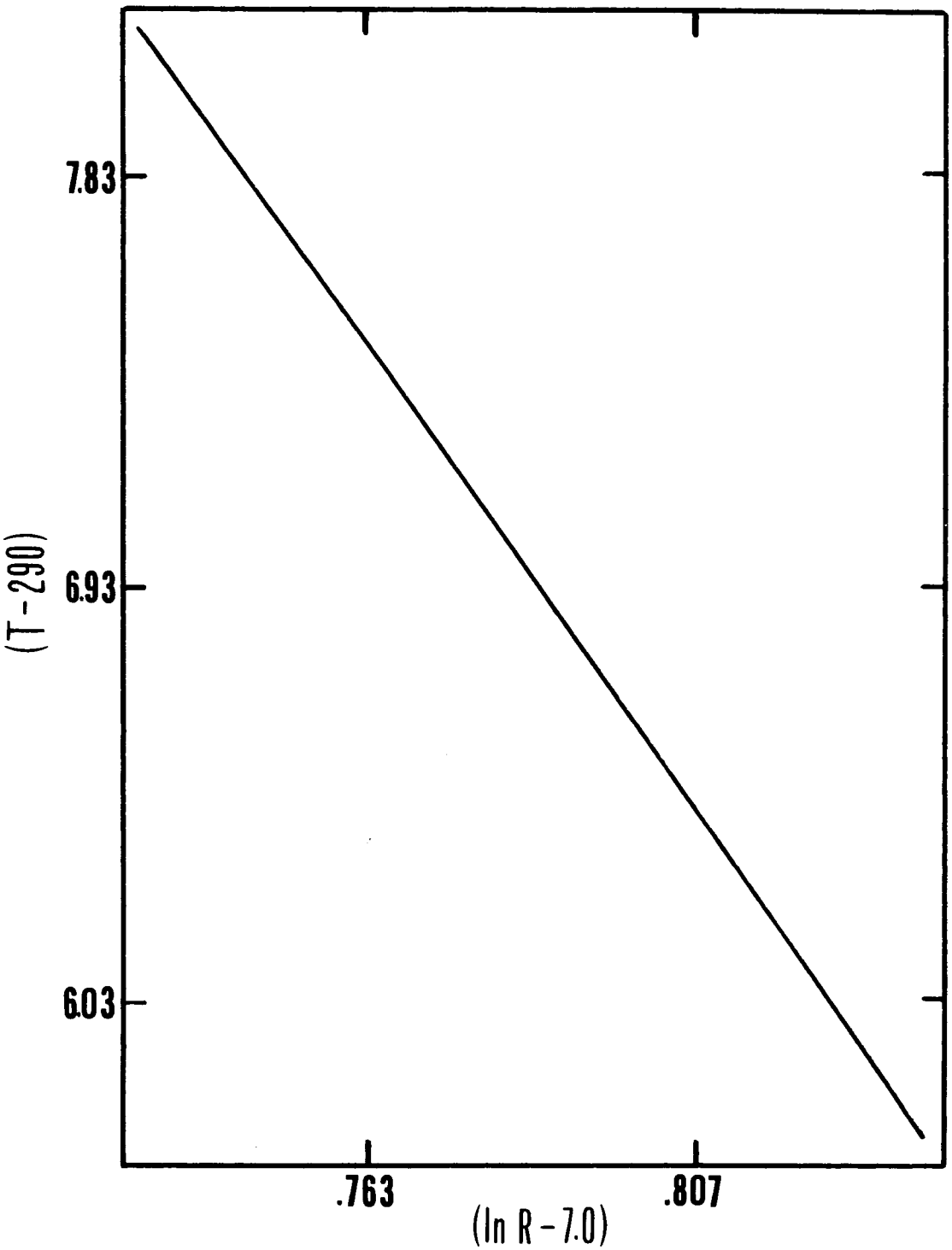

FIGURE 22: Thermistor calibration: plot of T vs lnR.

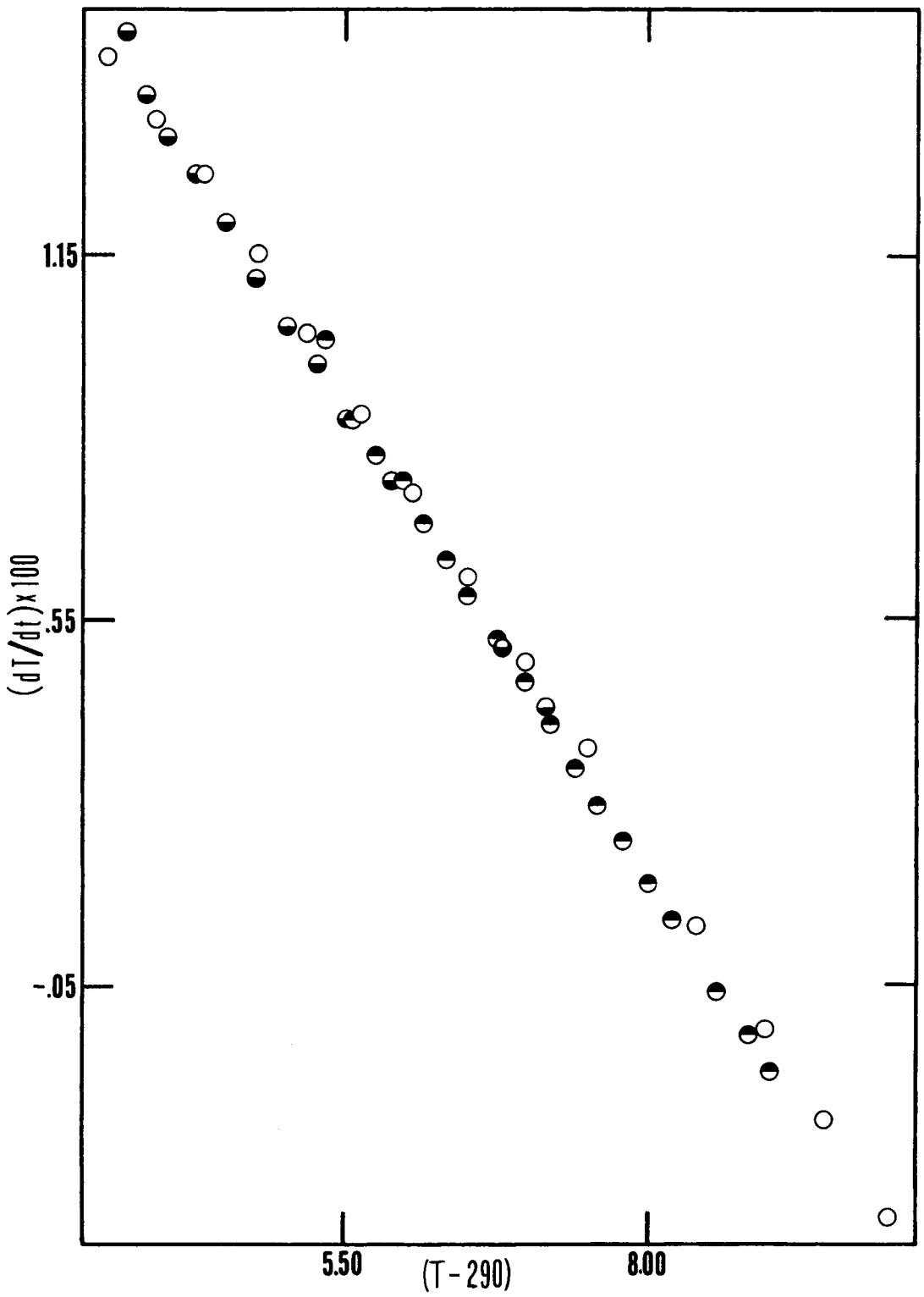

FIGURE 23: Characterization of the calorimeter: plot of dT/dt vs T.
O bomb rotating; ◐, ◑ bomb stationary.

TABLE 11

DATA FOR THE PLOT OF dT/dt vs T

Bomb Stationary				Bomb Rotating	
295.348-299.001		293.720-297.164		293.573-299.974	
$\frac{dT}{dt}(x10^3)$ (°K/min)	T(°K) (-290)	$\frac{dT}{dt}(x10^3)$	T(°K) (-290)	$\frac{dT}{dt}(x10^3)$	T(°K) (-290)
10.12	5.3488	15.05	3.720	14.74	3.573
8.787	5.579	14.07	3.880	13.69	3.960
8.255	5.763	13.42	4.041	12.84	4.363
7.780	5.981	12.78	4.285	11.53	4.778
7.052	6.160	11.98	4.528	10.24	5.198
6.541	6.341	11.05	4.774	8.943	5.627
5.924	6.519	10.28	5.026	7.638	6.070
5.214	6.759	9.690	5.279	6.188	6.519
4.469	6.978	8.761	5.539	4.805	6.976
3,833	7.192	7.805	5.887	3.392	7.497
3.125	7.401	5.098	6.792	.5320	8.409
2.551	7.584	4.109	7.164	-1.202	8.961
1.912	7.786			-2.672	9.446
1.236	8.000			-4.345	9.974
.5799	8.204				
.5554	8.572				
-1.315	8.825				
-1.859	9.001				
slope=$-3.007x10^{-3}$ std.dev.=$.1346x10^{-3}$		slope=$-3.191x10^{-3}$ std.dev.=$.1222x10^{-3}$		slope=$-3.094x10^{-3}$ std.dev.=$.2054x10^{-3}$	

Whether the bomb was or was not rotating, a linear relationship between dT/dt and T was found. A least squares treatment of the 3 sets of data gave the slopes listed in Table 11. Combining the 3 sets of data gave a slope of -3.06×10^{-3} min^{-1} and a standard deviation of 0.22×10^{-3}. Fitting polynomials of 2nd and 3rd degrees to the data resulted in no significant change in the standard deviation and thus also indicated a valid linear relationship. Therefore, it was assumed that equation [4] holds for this calorimeter for the temperature range used.

To make sure the rearranged form of equation [33] was valid, plots were also made of dT/dt vs (T_j-T). The same slope, and standard deviation were found in this case.

Also, due to the linearity of the plot of 1/lnR vs T, 1/lnR was used as a variable in place of T in the dT/dt vs T and dT/dt vs (T_j-T) plots. The same linearity was observed along with comparable standard deviations for the least squares treatment.

Since the validity of equation [4] had been established for the calorimeter, the calculation of the corrected temperature rise would involve the evaluation of the definite integral $\int_{t_b}^{t_e} T dt$ where t_b and t_e are the times at the start and finish respectively of the main period of the time-temperature curve for a combustion experiment. As no known relationship between time and temperature existed for the main period of a calorimeter experiment (14), an attempt

was made using the polynomial curve fitting program to approximate the curve. However, no success was achieved. Therefore, a numerical method was employed to evaluate the integral.

In order to test the validity of different numerical integration methods, two hyperbolas were employed which generated a curve (Figure 24) similar to the time-temperature curve in Figure 1. The equations used were

$$T = 296.0 - \frac{0.3}{t - 10.0} \qquad [5]$$

and

$$T = 298.0 - \frac{0.05}{t - 9.70} \qquad [6]$$

with the time ranging from 8 to 9.8 minutes for [5] and 9.8 to 12.2 for [6]. This would be the approximate time over which the maximum temperature rise in a combustion would occur.

Equations [46] and [47] in Chapter II as well as the integrals of polynomials of different degrees were tried as methods for integral solution. These methods are manifested in the subroutines G05TRP, G05ARA, and G05ACF respectively. Table 12 lists the calculated areas under the T vs t curve generated by equations [5] and [6] for different numbers of intervals taken over the time ranges already given. The temperature values were adjusted so that the first temperature was zero rather than 296.0 and thus reduced the effects of round-off error. Also listed is the actual area as calculated from the integrals $\int_{8.0}^{9.8} (296.0 - \frac{0.3}{t-10.0})dt$ and

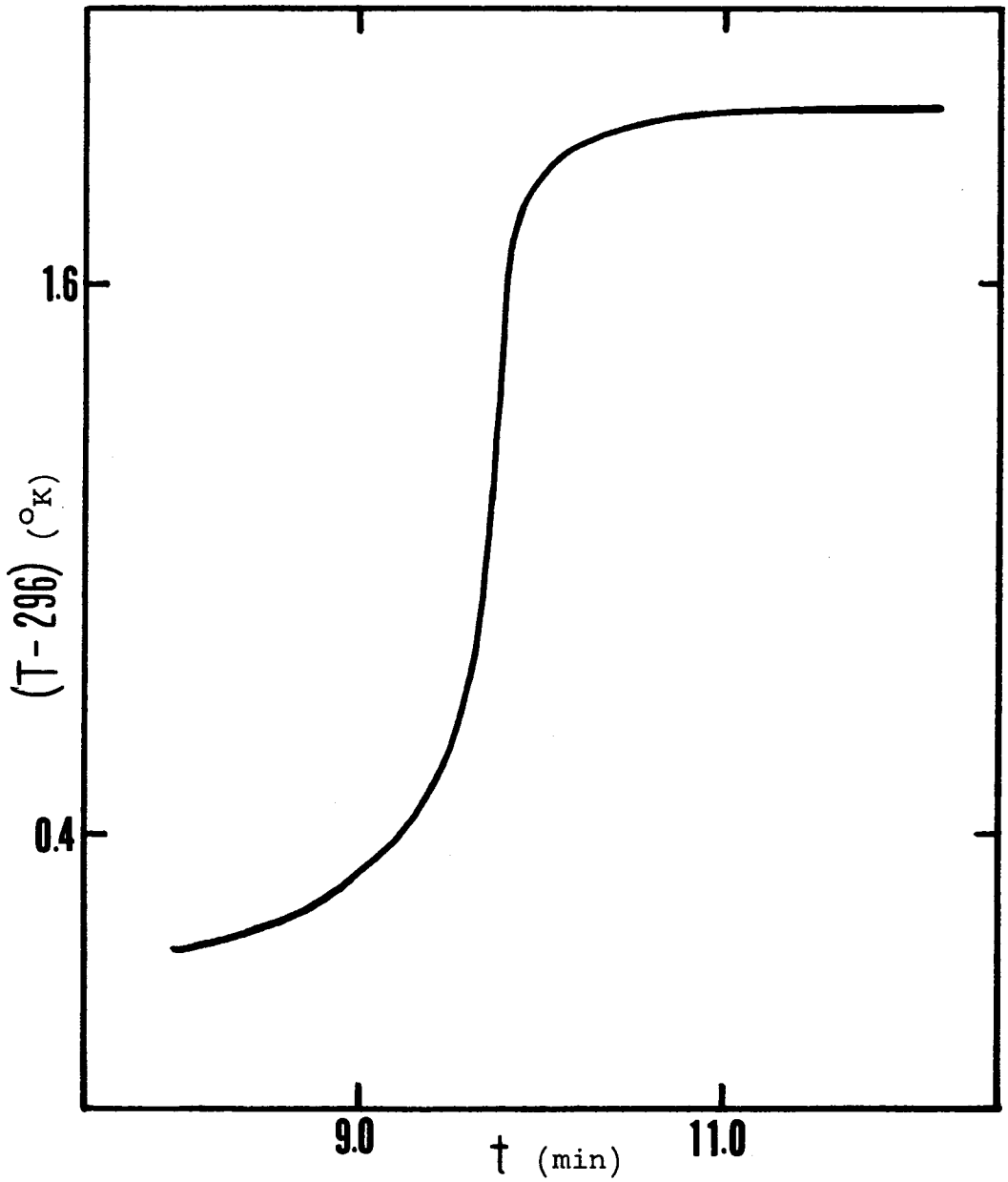

FIGURE 24: Test curve generated from two hyperbolas for evaluation of the best method of numerical integration.

$\int_{9.8}^{12.2} (298.0 - \frac{0.05}{t-9.70})dt$. The program for all these evaluations is listed in the appendix.

Reading across Table 12 are areas of the same magnitude. Reading down Table 12 are the area for the first time interval already mentioned, the area for the second time interval, and the total area respectively. Along with the total area is listed the total number of points used in the area calculation for each of the two time intervals. For these time ranges, 19 to 25 points represented about 0.1 minute time intervals. With the timing system used, it was possible to take readings as often as 0.05 minutes.

Examination of the areas shows that the numerical method based on equation [47] in Chapter II (G05ARA) approximates the real area best. For 0.1 minute intervals agreement is being reached in the 4th significant digit while for 0.05-0.07 minute intervals, agreement is achieved for 5 significant digits. The method as carried out in G05TRP gives values deviating less from the real values than the method in G05ARA for the total area, but this is due to the S-shape of the curve used. The error in calculating the first area is negated by the error in calculating the second area.

The method involving the use of the curve fit program should theoretically provide as good an answer as G05ARA. However, Table 12 shows this not to be the case. Doing the calculation in 16 digit arithmetic rather than 8 digit arithmetic gives exact agreement between areas found by employing

TABLE 12

RESULTS OF TESTS TO EVALUATE THE BEST METHOD OF NUMERICAL INTEGRATION

Number of Intervals	Areas Calculated by Subroutine (degree min)			Actual Area (degree min)
	G05ARA	G05TRP	G05ACF	
	.70253	.73904	.67259	.69077
	4.6214	4.5971	4.6242	4.6390
7	5.3240	5.3361	5.2968	5.3298
	.69174	.70062	.70888	.69077
	4.6362	4.6287	4.6137	4.6390
15	5.3280	5.3293	5.3226	5.3297
	.69097	.69483	.69869	.69076
	4.6381	4.6344	4.6307	4.6389
23	5.3291	5.3293	5.3294	5.3296
	.69083	.69297	.69509	.69077
	4.6387	4.6365	4.6342	4.6390
31	5.3295	5.3295	5.3293	5.3298
	.69080	.69230	.69377	.69077
	4.6388	4.6372	4.6356	4.6388
37	5.3296	5.3295	5.3294	5.3296

G05ARA and G05ACF. Therefore, it is just roundoff error giving the erroneous result.

While the calculation using equation [46] is limited to approximating the T vs t function with a polynomial of one degree less than the number of points used per interval (21), G05ACF can fit an mth degree polynomial to more than m + 1 points. However, attempts to fit 2nd degree polynomials to sets of 4 and 5 points gave poorer results than G05ARA even when done in 16 digit arithmetic. As a result of these investigations, the method based on Lagrangian interpolation (equation [46], Chapter II) was used in any subsequent numerical integrations of the T vs t curves.

The results of benzoic acid calibrations of the calorimetric system are listed in Table 13. The system to be defined by the energy equivalent was taken to be the calorimeter system with an empty bomb at the end of the combustion experiment. Therefore, suitable corrections were applied for the heat capacities of the products of benzoic acid combustion. Equation [4] was used to calculate the corrected temperature rise. The constants $(u + gT_j)$ and g were calculated for each run either by calculating the slopes and mean temperatures (subroutine G05LSQ in appendix) of the time-temperature readings in the initial or final periods, or calculating the temperature rise and value of the integral in the integrated form

$$T = (u + gT_j)\,\Delta t - g\int_{t_1}^{t_2} T\,dt$$

TABLE 13

DETERMINATION OF THE ENERGY EQUIVALENT OF THE CALORIMETER

Experiment	12	13	14	15	16	17	18	19
m(benzoic)(g)	1.11379	1.13973	1.07685	1.05096	1.09204	1.14376	1.16519	1.18506
$T_{corr}(^{o}K)$	1.6609	1.7031	1.6082	1.5691	1.6284	1.7049	1.7377	1.7681
q_i(cal)	2.65	2.62	2.62	2.72	2.62	2.69	2.80	2.69
q_n(cal)	3.98	3.67	3.14	1.42	1.31	3.52	1.26	1.83
q_{fuse}(cal)	7.59	18.63	23.00	17.71	10.35	6.44	10.35	18.63
C_{cf}	3.85	3.86	3.82	3.81	3.84	3.86	3.87	3.88
C_{sf}(cal/deg)	4241.7	4239.0	4244.7	4242.1	4242.0	4242.2	4241.1	4244.1
Average E_c	4242.1	standard deviation of the mean = $\pm$1.75						

for the initial and final periods. The result was two equations in two unknowns which were readily soluble. As both methods gave the same result, the first was used as it computed more rapidly. The constants were evaluated in this manner rather than using the values found by the previous dT/dt vs T studies, as the rate of stirring, while constant for long periods, would have to be adjusted occasionally due to a mechanical fault. Also, the heat capacity of the system would be different due to the presence of the particular combustant used, and thus the rate of heat exchange would differ slightly. From Table 14, however, it can be seen that the value of the constants in the combustion experiments differ only slightly from the values obtained from the dT/dt vs T studies.

The critical factor in the calculation of the correct temperature rise is the choice of the time at the end of the main period. This problem was solved by incorporating an iterative feature into the calibration program of evaluating ΔT over a time range judged to extend from the main period into the final period of the time-temperature readings. The point at which the end of the main period, t_e, (figure 1) was reached, the ΔT values would start to converge. This convergence is shown in Table 14 for runs 18 and 19.

Plots of the time-temperature data for runs 18 and 19 were made using the IBM 1627 Autoplotter. The scale used was 0.001° per 0.01 inch. Using these plots and the method of Dickinson as outlined by the Parr Instrument Company (16),

TABLE 14

CONVERGENCE OF VALUES IN THE CALIBRATION PROGRAM

Run	E_c (cal/°K)	$(u+gT_j)$	g	T_{corr} (°K)	T (°K)
	4388.52	.0224	-.0024	1.67935	.01188
	4339.38	.0234	-.0026	1.69836	.01217
	4292.39	.0242	-.0028	1.71693	.01293
	4270.07	.0245	-.0028	1.72590	.01363
	4261.57	.0248	-.0029	1.72934	.01407
	4253.56	.0250	-.0029	1.73259	.01469
	4248.32	.0251	-.0029	1.73472	.01545
	4245.40	.0252	-.0029	1.73592	.01619
	4243.08	.0252	-.0029	1.73687	.01718
	4241.86	.0253	-.0029	1.73736	.01862
	4241.27	.0253	-.0029	1.73761	.02031
	4241.15	.0253	-.0029	1.73765	.02221
	4240.97	.0253	-.0029	1.73773	.02406
	4240.88	.0253	-.0029	1.73777	.02596
	4240.83	.0253	-.0029	1.73778	.02789
	4240.72	.0253	-.0029	1.73783	.02978
	4240.67	.0253	-.0030	1.73785	.03169
	4240.85	.0253	-.0029	1.73778	.03370
	4240.64	.0253	-.0029	1.73786	.03556
	4240.76	.0253	-.0029	1.73782	.03754
	.974426E-01	12.566970E-01		10.350000E+00	00.00000
	4417.58	.0205	-.0022	1.69869	.01184
	4367.88	.0220	-.0024	1.71800	.01186
	4320.20	.0231	-.0026	1.73695	.01226
	4285.73	.0238	-.0027	1.75090	.01283
	4264.28	.0242	-.0028	1.75970	.01372
	4251.08	.0244	-.0028	1.76516	.01504
	4248.05	.0245	-.0029	1.76642	.01572
	4245.84	.0246	-.0029	1.76734	.01674
	4244.56	.0246	-.0029	1.76787	.01815
	4244.08	.0246	-.0029	1.76807	.01989
	4243.89	.0246	-.0029	1.76815	.02175
	4243.99	.0246	-.0029	1.76811	.02373
	4243.72	.0246	-.0029	1.76822	.02556
	4243.77	.0246	-.0029	1.76820	.02752
	4243.70	.0246	-.0029	1.76823	.02943
	4243.68	.0246	-.0029	1.76824	.03136
	4243.64	.0246	-.0029	1.76825	.03329
	4243.63	.0246	-.0029	1.76825	.03523
	4243.51	.0246	-.0029	1.76831	.03711
	4243.63	.0246	-.0029	1.76826	.03910

the corrected temperature rise was found. The values for runs 18 and 19 were 1.738° and 1.769° respectively. This compares well with the values of 1.7377 and 1.7683 found by the numerical method. However, the Parr value for run 19 varied between 1.767 and 1.771 depending on where the value of t_e was selected, that is, where the linear portion of the T vs t curve began, which indicated the end of the main period. The numerical method eliminates the need for this human judgment of the end of the main period.

Since five of the seven values of the energy equivalent of the calorimeter were within 1.1 kcal/degree of each other, it was felt that their average would give a truer value for the energy equivalent of the system. Using this value, 4241.8 ± .20 kcal/degree, the heats of combustion of the auxiliary materials were determined. The values are listed in Table 15.

In order to correctly evaluate the heat capacity term due to CO_2 in the products, the amount of CO_2 from the auxiliary material had to be estimated. The molecular formulas for Mylar and unmercerized cotton thread were taken from the paper of Good et al. (46). These formulas were $CH_{1.774}O_{0.887}$ and $C_{10}H_8O_4$ for the thread and Mylar respectively. The formula for the n-paraffin oil of $CH_{2.100}$ was determined by finding the amount of carbon dioxide formed on combustion of a known weight of oil by absorption of the CO_2 on Indicarb. A similar absorption for the thread showed the formula used to be essentially true for the thread.

TABLE 15

HEAT OF COMBUSTION OF AUXILIARY MATERIALS

	Thread				
Experiment	20	21	22	23	24
m(substance)(gm)	0.11075	0.12546	0.10680	0.14586	0.09614
m(benzoic)(gm)	0.00000	0.98472	0.95076	0.98189	0.98125
q_i(cal)	1.58	1.61	1.61	1.66	1.53
q_n(cal)	0.00	2.49	.856	1.54	1.57
C_{cf}(cal/deg)	2.31	3.83	3.81	3.86	3.82
E_c(cal/gm)	3935.4	4034.2	3112.0	4068.2	4037.4
	Mylar				
Experiment	25	27	28	30	31
m(substance)(gm)	0.30656	0.21829	0.22761	0.24406	0.15895
m(benzoic)(gm)	0.93940	0.86759	0.88470	0.84437	0.92295
m(thread)(gm)	0.00516	0.00404	0.00430	0.00509	0.00276
q_i	1.66	1.61	1.72	1.64	1.69
q_n	1.91	4.48	2.54	2.87	4.89
q_{thread}	20.87	16.34	17.39	20.59	11.16
C_{cf}	3.89	3.80	3.82	3.81	4.27
E_c	5376.9	5465.5	5465.4	5463.2	5458.0

TABLE 15 (cont'd)

Oil

Experiment	36	37	38
m(substance)(gm)	0.48660	0.56801	0.60465
m(thread)(gm)	0.00343	0.00330	0.00330
q_i	1.72	1.72	1.66
q_n	8.64	9.96	10.36
q_{thread}	13.87	13.34	13.34
C_{cf}	3.87	3.98	4.02
E_c(cal/gm)	11052.2	11043.7	11050.7
E_c(cal/gm)*	11048.7	11040.2	11047.2

* 1/lnR was used instead of T as the variable with time.

Five determinations of the heat of combustion of the thread were attempted but only three showed no carbon deposits. Of these three, two are within 3 cal/gm of each other while the 3rd is about 30 cal/gm higher than these two. The average of the lower two values, 4035.8 cal/gm is taken as the heat of combustion of the unmercerized cotton thread. The value from Good et al. (46) of 4050 cal/gm indicates this value may be too low. Due to the fact that never more than about 3 mg of thread would be used as a fuse in a combustion, the value of the heat of combustion doesn't need to be known to more than 3 significant figures.

Similarly, five determinations of the heat of combustion of Mylar were performed. While the scatter was not as bad as in the case of the thread, there was still several calories difference between four of the values and a much larger discrepancy with the fifth. However, the average of the four, 5463.3 cal/gm compares well with the value of Good et al. of 5476.1.

The paraffin oil combusted the most cleanly of the auxiliary materials. The three values show agreement within 9 cal/gm. The relatively large heat of combustion of 11048.9 cal/gm shows the high energy content of the oil due to the presence of only C-H and C-C linkages rather than carbon bonds to other elements.

As the variable 1/lnR had been shown to behave the same as T with time, the calibration calculations and the calculation of the heat of combustion of the oil were carried out

using 1/lnR in place of T. The results are shown in Table 15. As was done with T as the variable, the average of the four closest values, 58029 x 10^7 cal ohm, was used for the energy equivalent. The values of the heat of the combustion of the oil were 3.5 cal/gm lower in each case. This figure approaches the experimental uncertainty one would like for this type of work, 1 part in 10000 (8), as opposed to 3 parts in 10000 which the 3.5 figure represents. Therefore further work should be done with compounds of well characterized heats of combustion to see if 1/lnR is a substitute for T.

Two preliminary attempts were made to combust trimethylindium. The metal-alkyl was housed in a polyethylene bag as Mylar was attacked. Paraffin oil was the auxiliary combustant along with a cotton fuse. A 20% by weight hydrochloric acid solution was used as the bomb solution. In both cases very poor combustions resulted. In the one instance, bits of fused metal were stuck tightly to the platinum crucible and there was a fine suspension of a white material in the hydrochloric acid solution. In the other instance, a murky grey solution resulted along with soot deposits on the wall of the bomb. The grey colour of the solution was imparted by small sharp-looking particles. These particles were filtered off and attempts to dissolve them in various strengths of hydrochloric, nitric, and sulphuric acids failed. Some success was achieved using aqua regia but the practicality of this mixture as a bomb solution is nil. As a result of these preliminary combustions, it

would seem that the oxidative degradation of trimethylindium would not give any quantitative thermochemical data.

CHAPTER VI

Suggestions for Further Research

a) Trimethylindium

As an alternate to the combustion of trimethylindium, it might be possible to use the rotating bomb calorimeter as a reaction calorimeter. Trimethylaluminum was reacted with approximately 4N acetic acid in toluene solution in a rotating bomb calorimeter to give aluminum triacetate and methane (20). Small percentages of isobutene and hydrogen necessitated minor corrections for their conversion to methane. Sample size of trimethylaluminum was limited to less than 0.7 gm due to the formation of carbon and large quantities of unsaturated hydrocarbons. As trimethylindium is further down the aluminum subgroup in the periodic table, its comparable reactions are much less violent. Therefore, it should be possible to affect its reaction with acetic acid in toluene solution with less or no occurrence of side reactions. However, like trimethylaluminum, no thermochemical data for the triacetate is available and would require additional thermochemical studies (20) to realize a value for the heat of formation.

In the preliminary work done on the reaction calorimetry of trimethylindium in Chapter IV, the possibility of obtaining

100% reaction with halogens or aequeous solutions of mineral acids seems remote. However, the use, as above, of an organic solvent for a mineral acid might overcome the inability to achieve the clean reaction of the trimethylindium with the mineral acid. The value of the heat of formation of ($In_2(SO_4)_3$, c) is known (4), and the solubility of sulphuric acid in ethyl ether is quite sufficient to provide an excess of acid in ether solution (50). The idealized reaction would be

$$2In(CH_3)_3 + 3H_2SO_4 \longrightarrow In_2(SO_4)_3 + 6CH_4.$$

The heats of solution of sulphuric acid, indium sulfate, and methane in ethyl ether would have to be determined.

b) Trimethylthallium

Trimethylthallium is the only member of the last three elements in Group IIIB in the Periodic Table for which no thermochemical data is available. The degradative oxidation of trimethylthallium should provide an excellent means of determining its heat of formation, provided no insoluble problem of incomplete combustion arises. Both known oxides of thallium, Tl_2O, and Tl_2O_3 are quite soluble in aequeous solutions of hydrochloric, sulphuric, or nitric acids (51). In the case of the latter oxide, it also hydrolyses to the thallous salt (51). The values of the thermodynamic properties of ($TlNO_3$, c) are known (4), and thus the use of an acqueous nitric acid solution would allow the idealized oxidation of trimethylthallium to be referred to the solid

nitrate:

$$Tl(CH_3)_3,c + 5.5O_2,g + HNO_3 \cdot nH_2O \longrightarrow TlNO_3,c + 3CO_2 + 5H_2O.$$

The comparison experiment would involve the solution of $TlNO_3,c$ in the bomb solution along with the combustion of materials of known heat values to generate an equivalent amount of carbon dioxide as found for trimethylthallium.

If the trimethylthallium could not be oxidized completely, recourse to other reactions in the rotating bomb calorimeter would be available. As values for the heat of formation of thallous acetate, and thallous sulphate are listed (4), the methods already outlined for trimethylindium could be attempted.

c) Trimethylgallium

The value of the heat of formation of trimethylgallium has been reported twice (19,31), and the values are quite divergent, 14.5 kcal/mole and 17.6 kcal/mole respectively. Neither method involved the use of a rotating bomb calorimeter.

Conflicting reports appear for the solubility of the oxides Ga_2O, and Ga_2O_3 in aequeous sodium hydroxide solutions; one source gives an affirmative statement (52), while another denies the solubility if the oxides have been strongly heated (53). The only solution would be a trial combustion.

Failure of the oxidation procedure would not mean the end of further studies. The two reactions outlined for trimethylindium with acetic acid and sulphuric acid could be tried but in the case of acetic acid, the heat of formation of gallium acetate would also have to be determined.

APPENDIX

Computation of the Ethylbenzene Formed by Recombination of Benzyl and Methyl Radicals

The minimum detectable amount of ethane is about 4.00×10^{-6} moles. For a vessel volume of 150 cc, a contact time of 0.5 sec, and a time of ethylbenzene flow of 18 min, the concentration of ethane is

$$[C_2H_6] = \frac{4.00 \times 10^{-6} \times 0.5}{150 \times 18 \times 60} = 1.23 \times 10^{-11} \text{ moles/cc.}$$

From the work of Kominar, Jacko, and Price (25), the rate

$$2CH_3 \longrightarrow C_2H_6 \qquad [4]$$

$$CH_3 + C_6H_5CH_3 \longrightarrow CH_4 + C_6H_5CH_2 \qquad [3]$$

$$C_6H_5CH_2 + CH_3 \longrightarrow C_6H_5C_2H_5 \qquad [6]$$

of formation of ethylbenzene $= k_6[C_6H_5CH_2][CH_3]$, where $[CH_3] = \left(\frac{\text{rate of formation of } C_2H_6}{k_4}\right)^{1/2}$. The rate constant, k_4 is obtained from the Arrhenius plot for the pressure dependence of $k_3/k_4^{1/2}$ at the desired temperature (51). At 1000°K and 24.4 mm, $\log(k_3/k_4^{1/2})^{\infty} - \log(k_3/k_4^{1/2})^{24.4} = 0.61$ where the superscripts indicate the pressure in mm. Using the high pressure value (∞), $k_4 = 10^{13.4}$ (52), k_4 at 24.4 mm is $10^{12.2}$ as reaction [3] is pressure independent.

The benzyl radical is obtained from ethylbenzene from the reverse of reaction [6] and from reaction [3]. Therefore, using the representative value of 2.0×10^{-4} moles of methane produced,

$$[C_6H_5CH_2] = \frac{4.0 \times 10^{-4} \times 0.5}{150 \times 18 \times 60} = 1.23 \times 10^{-9} \text{ moles/cc.}$$

From Kominar, Jacko and Price (25), $k_6 = 10^{11.2}$. Therefore,

$$\text{moles ethylbenzene} = 18 \times 60 \times \text{rate of formation of ethylbenzene}$$
$$= 8.23 \times 10^{-7}$$

at 1000°K and 24.4 mm.

Derivation of Theta in the Relationship

$$\ln R = \frac{C}{T+\theta} + D$$

From the above relationship,

$$\ln R = \frac{DT + D\theta + C}{T + \theta} .$$

Therefore

$$\frac{1}{\ln R} = \frac{T + \theta}{DT + D\theta + C}$$

$$= \frac{T}{DT + D\theta + C} + \frac{\theta}{DT + D\theta + C}$$

$$= \frac{T}{DT + K} + \frac{\theta}{DT + K}$$

where $K = D\theta + C$. In a plot of $1/\ln R$ vs T, the slope $= \frac{1}{DT + K}$ and the y-intercept $= \frac{\theta}{DT + K}$. Therefore,

$$\theta = \frac{\text{y-intercept}}{\text{slope}} .$$

If the curve fit of $1/\ln R$ vs T is a polynomial of degree 2, for example,

$$\frac{1}{\ln R} = a_1 + a_2 T + a_3 T^2,$$

then $$\frac{d(1/\ln R)}{dT} = a_2 + 2a_3 T$$

and $$\theta = \frac{a_1}{a_2 + 2a_3 T} .$$

```
C                        PYROLYSIS OF ETHYLBENZENE
C      PROGRAM TO CALCULATE THE FIRST-ORDER RATE CONSTANTS AND THE EVALUATE THE
C      PRODUCT DATA
       DIMENSIONCMW(4),PG(4),HL(4),PT(4),HLS(4),DEN(4),GMOLE(4),CMOLE(4)
       DIMENSION SEN(4),SENS(4),ISEN(4),ISENS(4),IPT(4),AREA(4),AREAS(4)
       READ 100,(CMW(I),DEN(I),I=1,4),R
  100  FORMAT (4(F6.1,F6.3),F6.0)
       IRNO=0
    4  IF(IRNO-50) 2,52,52
   52  IF(IRNO-60) 53,53,2
   53  READ 107,IRNO,L,EBW,TOLW,PAVE,P,V,T,ITRUN,ITEB,PSGC,PCH,ITEXP,TOLK
      1,IPRT
  107  FORMAT (I2,I1,F6.4,4F6.2,F6.1,2I3,2F5.2,I5,E9.2,I3)
       PRT=IPRT
       GO TO 6
    2  READ 101,IRNO,L,EBW,TOLW,PAVE,P,V,T,ITRUN,ITEB,PSGC,PCH,ITEXP,TOLK
    6  READ 103,(PG(I),AREA(I),ISEN(I),AREAS(I),ISENS(I),IPT(I),I=1,4)
  103  FORMAT (2(1X,F4.2,F4.1,I2,F2.0,2I2),F4.2,F4.1,I2,F4.1,I2,I2,1X,F4.
      12,F4.1,I2,F2.0,2I2)
       DO 14 I=1,4
       SEN(I)=ISEN(I)
       PT(I)=IPT(I)
       SENS(I)=ISENS(I)
   14  CONTINUE
       EBMW=CMW(3)
       TMW=CMW(2)
       TRUN=ITRUN
       TEB=ITEB
       TEXP=ITEXP
       PCM=PAVE/7.5
       TLEB=(TEB*TOLW*EBMW)/(TRUN*EBW*TMW)
       IF(L-1) 10,20,20
   10  IF(IRNO-34) 11,11,12
   11  D=17.53
       GO TO 15
   12  D=13.67
       GO TO 15
   20  IF(IRNO-55) 21,21,22
   22  D=19.48
       GO TO 15
   21  D=22.784
   15  IF(TOLK) 37,38,37
   38  D=D*78.1/92.1
       TLEB=(TEB*TOLW*EBMW)/(TRUN*EBW*CMW(1))
   37  CT=(PAVE*TRUN*D)/(TOLW*TEXP)
       A=(P*V)/(T*R)
       EBN=EBW/EBMW
       B=(PCH*A)/PSGC
       IF(IRNO-51) 61,62,62
   62  IF(IRNO-61) 63,63,61
   63  C=(TOLK*TOLW*CT*(TEB+PRT))/(3.*TMW*TRUN)
       GO TO 66
   61  C=(TOLK*TOLW*CT*(TEB+3.))/(3.*TMW*TRUN)
   66  CHN=B-C
       EXPK=LOGF(EBN/(EBN-CHN))/CT
       ELOG=(LOGF(EXPK))/2.303
       PXET=1000./TEXP
       RNO=IRNO
       PUNCH 102,RNO,L,TEXP,TLEB,PCM,CT,EBN,CHN,EXPK,ELOG,PXET,C,DIFL
  102  FORMAT (F4.0,I2,F6.0,F5.0,F5.2,F6.3,3E9.2,2F6.3/2E9.2)
       IF(TOLK) 30,31,30
```

```
 31 READ 113,BENK
113 FORMAT (E9.2)
    H2C=TOLW*BENK*CT*(TEB+3.)/(TRUN*CMW(1))
    FTOL=1.-2.*H2C*CMW(1)/TOLW
 71 K=1
    GO TO 33
 30 H2C=2.*C
    FTOL=1.-(C+H2C)*CMW(2)/TOLW
 70 K=2
 33 FEB=1.-CHN*CMW(3)/EBW
 73 VLIQ=TOLW*FTOL/DEN(K)
    DO 24 I=1,4
    AREAS(I)=AREAS(3)
    SENS(I)=SENS(3)
    PT(I)=PT(3)
 24 CONTINUE
    DO 34 I=1,4
    GMOLE(I)=(PG(I)*A)/PSGC
    IF(AREAS(I)) 44,44,43
 44 AREAS(I)=1.
 43 CMOLE(I)=AREA(I)*SEN(I)*VLIQ*PT(I)*DEN(I)/(AREAS(I)*SENS(I)*1000.*
   1CMW(I))
 34 CONTINUE
    DIFL=EBN-CMOLE(3)
    FEBL=CMOLE(3)*CMW(3)/EBW
    BENEB=CMOLE(1)-C
    H2EB=GMOLE(2)-H2C
    IF(CMOLE(3)) 77,77,76
 77 EXKL=0.
    ELOGKL=1.
    GO TO 78
 76 EXKL=(LOG(EBN/CMOLE(3)))/CT
    ELOGKL=(LOG(EXKL))/2.303
 78 PUNCH 105,(GMOLE(I),I=1,3),(CMOLE(I),I=1,3)
105 FORMAT (6E9.2)
    PUNCH 115,H2EB,GMOLE(4),BENEB,CMOLE(4),EXKL,ELOGKL,FEB,FEBL,FTOL
115 FORMAT (5E9.2,4F6.3)
    H2EBR=H2EB/EBN
    CH4EB=CHN/EBN
    C2H4CH=GMOLE(4)/CHN
    STEB=CMOLE(4)/EBN
    H2CH4=H2EB/CHN
    C2H4EB=GMOLE(4)/EBN
    STYCH4=CMOLE(4)/CHN
    BENEBR=BENEB/EBN
    BENCH=BENEB/CHN
    PUNCH 109,H2EBR,CH4EB,C2H4EB,STEB,BENEBR,H2CH4,C2H4CH,STYCH4,BENCH
109 FORMAT (5E9.2/36X,4E9.2)
    GO TO 4
101 FORMAT (I3,I2,F6.4,4F6.2,F6.1,213,2F5.2,I5,E9.2)
    END
```

```
      SUBROUTINE G05CSP(NUMBER,M,MTOTAL)
C     WILLIAM CLARK))))))CHEMISTRY DEPARTMENT
C     PROGRAM TO FIT A POLYNOMIAL TO A SET OF DATA USING THE METHOD OF LEAST
C     SQUARES.  M IS THE DEGREE OF THE POLYNOMIAL, AND HAS A MAXIMUM VALUE OF 10
C     ONLY 199 POINTS CAN BE ENTERED. A BLANK CARD MUST SEPARATE SETS OF DATA
C     MTOTAL ALLOWS ONE TO TRY A RANGE OF POLYNOMIALS WHERE MTOTAL IS THE LOWEST
C     DEGREE AND M IS THE HIGHEST DEGREE. IF MTOTAL IS ZERO, ONLY A POLYNOMIAL
C     OF DEGREE M IS FITTED
      DIMENSION X(200),Y(200),A(11,11),B(11),C(11),P(20),NCOL(11)
      COMMON Y,X,B
      IF(MTOTAL) 7,7,8
    8 LIM=M
      DO 101 M=MTOTAL,LIM
    7 MX2=M*2
C     FINDING THE LARGEST AND SMALLEST ELEMENTS IN THE X AND Y ARRAYS
      IND=0
   26 YX1=Y(1)
      YN1=Y(1)
      XX1=X(1)
      XN1=X(1)
      DO 14 I=1,NUMBER
   16 IF(YN1-Y(I)) 18,18,17
   17 YN1=Y(I)
   18 IF(YX1-Y(I)) 20,19,19
   20 YX1=Y(I)
   19 IF(XN1-X(I))  21,21,22
   22 XN1=X(I)
   21 IF(XX1-X(I)) 23,14,14
   23 XX1=X(I)
   14 CONTINUE
      IF (IND) 46,46,44
C     NORMALIZING DATA AND TRANSPOSING COORDINATES
   46 TX=(XX1+XN1)/2.
      TY=(YX1+YN1)/2.
      DO 49 I=1,NUMBER
      X(I)=X(I)-TX
   49 Y(I)=Y(I)-TY
   34 IND=1
      GO TO 26
C     DETERMINING THE ELEMENT OF LARGEST MAGNITUDE
   44 IF(ABS(YX1)-ABS(YN1)) 24,25,25
   24 DY=ABS(YN1)
      GO TO 27
   25 DY=ABS(YX1)
   27 IF(ABS(XX1)-ABS(XN1)) 28,29,29
   28 DX=ABS(XN1)
      GO TO 30
   29 DX=ABS(XX1)
   30 DO 31 I=1,NUMBER
      X(I)=X(I)/DX
   31 Y(I)=Y(I)/DY
C     FORMING THE POWERS OF X AND STORING IN THE P ARRAY
      DO 33 I=1,MX2
      P(I)=0.
      DO 33 J=1,NUMBER
   33 P(I)=P(I)+X(J)**I
C     DEVELOPING COEFFICIENTS AND CONSTANTS FOR THE NORMAL EQUATIONS
      N=M+1
      DO 35 I=1,N
      NCOL(I)=I
      DO 35 J=1,N
```

```
      K=I+J-2
      IF(K) 39,39,38
   38 A(I,J)=P(K)
      GO TO 35
   39 A(1,1)=NUMBER
   35 CONTINUE
      B(1)=0.0
      DO 41 J=1,NUMBER
   41 B(1)=B(1)+Y(J)
      DO 42 I=2,N
      B(I)=0.0
      DO 42 J=1,NUMBER
   42 B(I)=B(I)+Y(J)*X(J)**(I-1)
C     DOING THE PIVOTAL CONDENSATION BY EXAMINING ALL ELEMENTS
      NM1=N-1
      DO 300 K=1,NM1
      KP1=K+1
      L=K
      LC=K
      DO 400 I=K,N
      DO 400 II=K,N
      IF(ABS(A(I,II))-ABS(A(L,LC))) 400,400,401
  401 L=I
      LC=II
  400 CONTINUE
      DI=0.
      IF(L-K) 501,501,405
  405 DO 410 J=K,N
      TEMP=A(K,J)
      A(K,J)=A(L,J)
  410 A(L,J)=TEMP
      TEMP=B(K)
      B(K)=B(L)
      B(L)=TEMP
      DI=DI+1.
  501 IF(LC-K) 500,500,406
  406 DO 411 J=K,N
      TEMP=A(J,K)
      A(J,K)=A(J,LC)
      A(J,LC)=TEMP
      ITEM=NCOL(K)
      NCOL(K)=NCOL(LC)
  411 NCOL(LC)=ITEM
      DI=DI+1.
C     BEGINNING ELIMINATION AND BACK SOLUTION
      IF(SENSE SWITCH 1) 417,500
  417 PUNCH 437,((A(IQ,JQ),JQ=1,10),IQ=1,10)
      PUNCH 437,(B(IQ),IQ=1,10)
  437 FORMAT (8E9.2)
      PUNCH 438,DI
  438 FORMAT (/I3/)
  500 DO 300 I=KP1,N
      FACTOR=A(I,K)/A(K,K)
      A(I,K)=0.0
      DO 301 J=KP1,N
  301 A(I,J)=A(I,J)-FACTOR*A(K,J)
  300 B(I)=B(I)-FACTOR*B(K)
      DET=1.
      DO 420 I=1,N
  420 DET=DET*A(I,I)
      ID=DI/2.
```

```
      DD=ID*2
      IF(DI-DD) 413,414,413
  413 DET=-DET
  414 CONTINUE
      PUNCH 426,DET
  426 FORMAT (/31HTHE VALUE OF THE DETERMINANT IS E16.8/)
      C(N)=B(N)/A(N,N)
      I=NM1
  710 IP1=I+1
      SUM=0.0
      DO 700 J=IP1,N
  700 SUM=SUM+A(I,J)*C(J)
      C(I)=(B(I)-SUM)/A(I,I)
      I=I-1
      IF(I) 800,800,710
C     CORRECTING THE SOLUTION VECTOR SO THAT THE X.S AGREE WITH THE INDICES
  800 DO 50 I=1,N
      K=NCOL(I)
   50 B(K)=C(I)
C     CORRECTING FOR EFFECTS OF NORMALIZING AND TRANSPOSING
      B(1)=B(1)*DY
      DO 54 I=1,M
   54 B(I+1)=B(I+1)*DY/(DX**I)
      IF(M-1) 99,99,92
   99 SUM=B(M)-B(N)*TX
      GO TO 95
   92 MM=M-1
      RK=M
      SUM=B(N)*RK
      DO 91 I=1,MM
      JJ=N-I
      RJ=JJ
      IF(I-1) 91,91,94
   94 SUM=RJ*B(JJ+1)-TX*SUM
   91 C(JJ)=B(JJ)-TX*SUM
      SUM=B(M)-TX*B(N)
      DO 97 J=1,MM
      JJ=M-J
   97 SUM=B(JJ)-TX*SUM
   95 C(1)=SUM+TY
      DO 98 I=1,M
   98 B(I)=C(I)
      DO 52 I=1,NUMBER
      X(I)=X(I)*DX
      Y(I)=Y(I)*DY
      X(I)=X(I)+TX
   52 Y(I)=Y(I)+TY
C     CALCULATING THE RESIDUALS USING HORNER.S METHOD OF POLYNOMIAL EVALUATION
      ADD=0.0
      MM=M-1
      BDD=0.0
  119 DO 56 I=1,NUMBER
      SUM=B(M)+X(I)*B(M+1)
      IF(M-1) 108,108,59
   59 DO 57 J=1,MM
      JJ=M-J
   57 SUM=B(JJ)+X(I)*SUM
  108 RES=SUM-Y(I)
      IF(BDD) 56,56,61
   61 IF(ABS(RES)-4.*RMSQ) 56,56,62
   62 PUNCH 63,I,I
```

```
   63 FORMAT (2HX(I4,4H),Y(I4,34H) IS TOO FAR OFF THE CURVE (STDEV))
   56 ADD=ADD+RES*RES
      IF(BDD) 116,116,58
  116 AD=NUMBER-1
      RMSQ=SQRT(ADD/AD)
      SQRES=ADD
      BDD=1.
      GO TO 119
C     EXAMINING THE RESIDUALS IN LIGHT OF THE ROOT MEAN SQUARE AND AVERAGE DEV.
   58 CONTINUE
      PUNCH 83,M
   83 FORMAT(//41HCOEFFICIENTS OF THE POLYNOMIAL OF DEGREE I3,4H ARE/)
      PUNCH 84,(B(I),I=1,N)
   84 FORMAT (5E14.7)
      PUNCH 85,RMSQ,SQRES
   85 FORMAT (/21HSTANDARD DEVIATION = E14.8/27HSUM OF RESIDUALS SQUARED
     1 = E14.8)
  101 CONTINUE
      M=0
      RETURN
      END
```

```
      SUBROUTINE G05PLT(YCOOR,XCOOR,IGRID,XL,IC,KONTRL,J,K)
C     G05PLT FINDS THE LIMITS FOR THE PLOTTER ROUTINE. DATA OUTSIDE THE DEFINED
C     LIMITS WILL BE REJECTED AND AN INDICATIVE MESSAGE PUNCHED.
C     G05PIT MUST BE CALLED BEFORE ANY DATA IS READ INTO THE CALLING PROGRAM.
C     IGRID ALLOMS THE CHOICE OF GRID TYPE, AND MAY BE1(OUTLINE ONLY), 101(COM-
C     PLETE GRID), OR 201(NO OUTLINE OR GRID)).
C     XL IS THE PHYSICAL LENGTH OF THE PLOT IN INCHES IN THE X DIRECTION
C     IC DETERMINES THE ACTION OF THE PEN IN PLOTTING
C     IC MAY BE 0, 9, 90, OR99 (SEE SHEET).
C     KONTRL DETERMINES THE INITIALIZATION PROCEDURE.
C     KONTRL = 1, ...GRID + PLOT + NO REINITIALIZATION
C     KONTRL = 2, ..........PLOT + NO REINITIALIZATION
C     KONTRL = 3, ...GRID + PLOT + REINITIALIZATION
C     KONTRL = 4, ..........PLOT + REINITIALIZATION
C     KONTRL = 1, OR 3 MUST BE IN THE FIRST CALL G05PLT STATEMENT.
C     SUBSEQUENT SETS OF DATA PLOTTED ON THE SAME GRID WILL BE DONE IN DIFFERENT
C     COLOURS, AND A MESSAGE RELATING COLOUR TO DATA PUNCHED.
      DIMENSION YCOOR(200),XCOOR(200)
      COMMON YCOOR,XCOOR
      GO TO (23,48,23,48),KONTRL
   23 YX=YCOOR(J)
      TYPE 29
   29 FORMAT (51HTURN ON THE PLOTTER PLEASE, ADJUST THE PEN, RESTART//)
      PAUSE
      YN=YCOOR(J)
      XX=XCOOR(J)
      XN=XCOOR(J)
      DO 61 I=1,200
C     THE POINT 0,0 IS IGNORED IN FINDING THE LIMITS OF THE PLOT.
      IF(ABS(YCOOR(I))+ABS(XCOOR(I))) 60,61,60
   60 IF(YX-YCOOR(I)) 62,63,63
   62 YX=YCOOR(I)
   63 IF(YN-YCOOR(I)) 64,64,65
   65 YN=YCOOR(I)
   64 IF(XX-XCOOR(I)) 66,67,67
   66 XX=XCOOR(I)
   67 IF(XN-XCOOR(I)) 61,61,68
   68 XN=XCOOR(I)
   61 CONTINUE
      YD=(YX-YN)/10.
      YX=YX+0.1*YD
      YN=YN-0.1*YD
      XD=(XX-XN)/XL
      XL=XL+0.2
      XX=XX+0.1*XD
      XN=XN-0.1*XD
      CALL PLOT(IGRID,XN,XX,XL,XD,YN,YX,10.2,YD)
      KOUNT=1
      PUNCH 45,YX,XX,YN,XN
   45 FORMAT (/32HTHE BOUNDS OF THE PLOT ARE YMAX=E11.4,7H, XMAX=E11.4/2
     16X,5HYMIN=E11.4,7H, XMIN=E11.4/)
      GO TO 47
   48 TYPE 50
   50 FORMAT (65HCHANGE THE PEN PLEASE, AND TYPE THE COLOUR CODE BEFORE
     1RESTARTING/52H.... 1 FOR RED, 2 FOR GREEN, 3 FOR BLUE, 4 FOR BLACK
     2)
      TYPE 52
   52 FORMAT (37HTHE FORMAT FOR THE COLOUR CODE IS I2.//)
      ACCEPT 51,KOLOUR
   51 FORMAT (I2)
      KOUNT=KOUNT+1
```

```
      GO TO (91,92,93,94),KOLOUR
   91 PUNCH 95,KOUNT,XCOOR(J),YCOOR(J)
      GO TO 47
   92 PUNCH 96,KOUNT,XCOOR(J),YCOOR(J)
      GO TO 47
   93 PUNCH 97,KOUNT,XCOOR(J),YCOOR(J)
      GO TO 47
   94 PUNCH 98,KOUNT,XCOOR(J),YCOOR(J)
   96 FORMAT (10HTHE NUMBERI2,27H SET OF DATA BEGINS WITH X=E11.4,4H, Y=
     1E11.4,14H AND IS GREEN.)
   97 FORMAT (10HTHE NUMBERI2,27H SET OF DATA BEGINS WITH X=E11.4,4H, Y=
     1E11.4,13H AND IS BLUE.)
   98 FORMAT (10HTHE NUMBERI2,27H SET OF DATA BEGINS WITH X=E11.4,4H, Y=
     1E11.4,14H AND IS BLACK.)
   95 FORMAT (10HTHE NUMBERI2,27H SET OF DATA BEGINS WITH X=E11.4,4H, Y=
     1E11.4,12H AND IS RED.)
   47 DO 39 I=J,K
      IF(YX-YCOOR(I)) 71,72,72
   72 IF(YN-YCOOR(I)) 73,73,71
   73 IF(XX-XCOOR(I)) 71,74,74
   74 IF(XN-XCOOR(I)) 75,75,71
   75 CALL PLOT (9,XCOOR(I),YCOOR(I))
      GO TO 39
   71 PUNCH 78,XCOOR(I),YCOOR(I)
   78 FORMAT (2HX=E11.4,4H, Y=E11.4,18H ARE OFF THE PLOT.)
   39 CONTINUE
      GO TO (81,81,82,82),KONTRL
   82 CALL PLOT(7)
   81 RETURN
      END



      SUBROUTINE G05PIT
C     THIS SUBROUTINE INITIALIZES THE CONTENTS OF X AND Y.
      DIMENSION X(200),Y(200)
      COMMON Y,X
      DO 606 I=1,200
      X(I)=0.
  606 Y(I)=0.
      RETURN
      END
```

```
C      PROGRAM TO TEST VARIOUS METHODS OF NUMERICAL INTEGRATION
C      CALCULATES A COMPLETE SET OF TEMPERATURE-TIME POINTS FOR THE MOST
C      CHANGING PART OF THE CURVE.  290 IS SUBTRACTED FROM EACH TEMPERATURE
       DIMENSION TEMP(200),TIME(200),A(2)
       DIMENSION AA(2),AC(2)
       DIMENSION AE(2)
       COMMON TEMP,TIME
       PUNCH 999
  999 FORMAT (14H$WILLIAM CLARK)
       DO 75 IM=3,4
       DO 75 KI=IM,4
       KZ=KI+1
       PUNCH 123,KZ,IM
  123 FORMAT (/32HNUMBER OF POINTS PER INTERVAL IS I2/22HORDER OF POLYNOM
      1IAL IS I2/)
       DO 75 I=KI,36,KI
       RI=I
       IR=I+1
       RA=1.8
       TIME(1)=8.0
       LM=0
       DO 95 IJ=1,2
       RJ=RA/RI
       TEMP(1)=296.0-0.3/(TIME(1)-10.0)
       TEMP(1)=TEMP(1)-296.
       DO 85 KJ=1,I
       KL=LM+KJ+1
       TIME(KJ+1)=TIME(KJ)+RJ
       IF(IJ-2) 67,68,68
   67 TEMP(KJ+1)=296.0-0.3/(TIME(KJ+1)-10.0)
       TEMP(KJ+1)=TEMP(KJ+1)-296.
       D=6.0
       E=0.3
       F=10.0
       GO TO 85
   68 TEMP(KJ+1)=298.0-0.05/(TIME(KJ+1)-9.70)
       TEMP(KJ+1)=TEMP(KJ+1)-296.
       D=8.0
       E=0.05
       F=9.70
   85 CONTINUE
       A(IJ)=G05ARA(TEMP,TIME,1,IR)
       AA(IJ)=G05TRP(TEMP,TIME,1,IR)
       AE(IJ)=G05ACF(1,IR,KI,IM)
       AC(IJ)=D*(TIME(IR)-TIME(1))-E*LOG((TIME(IR)-F)/(TIME(1)-F))
       AD=RA*6.
       AC(IJ)=AC(IJ)-AD
       RA=2.4
       TIME(1)=9.8
       LM=I
   95 CONTINUE
       SAS=A(1)+A(2)
       SACS=AC(1)+AC(2)
       SAAS=AA(1)+AA(2)
       SCS=AE(1)+AE(2)
       PUNCH 100,(A(N),AA(N),AE(N),AC(N),N=1,2)
  100 FORMAT (4X,4(1X,E15.8))
       PUNCH 101,IR,SAS,SAAS,SCS,SACS
  101 FORMAT (I4,4(1X,E15.8))
   75 CONTINUE
   19 CALL EXIT
       END
```

```
C      PROGRAM FOR CALIBRATING THE CALORIMETER AND CALCULATING THE HEATS OF
C      COMBUSTION OF THE AUXILIARY MATERIALS
C      NOTE**MM,IC,ID MUST BE ODD NUMBERS
C      WILLIAM CLARK   CHEMISTRY DEPARTMENT
       DIMENSION TEMP(200),TIME(200),QE(5,5)
       DIMENSION WAUX(3),EAUX(3),A(3),B(3),C(3),D(3),AUXN(3)
       COMMON TEMP,TIME,QE,NO,MO
       PRINT 80
    80 FORMAT (20X,26HSWILLIAM CLARK...CHEMISTRY//)
       READ 101,Z,R,DH2O,NO,MO,VBOM,CH2O,CO2,CCO2,CPT,EFUSE,EBENZ
       READ 104,(A(I),B(I),C(I),I=1,3)
   104 FORMAT (3F6.3)
    90 READ 102,IRUN,MM,IC,ID,WBENZ,WFUSE,WCRUC,WWIRE,VH2O,V1,PO2,VBASE,T
      1JACK
       READ 103, BASEN,(WAUX(I),I=1,3)
   103 FORMAT (4F8.5)
       READ 105,(EAUX(I),I=1,3)
   105 FORMAT (3F7.1)
       READ 209,(TIME(I),TEMP(I),I=1,MM)
C      CONVERSION OF RESISTANCE TO TEMPERATURE
   125 CALL G05CON(TEMP,MM)
       TMP=TEMP(1)
       DO 97 I=1,MM
    97 TEMP(I)=TEMP(I)-TMP
       PPO2=(14.7+PO2)/14.7
       WH2O=DH2O*VH2O
C      CALCULATION OF MINOR HEAT TERMS
       F=1.+(20.*(PPO2-30.)+42.*((WBENZ/VBOM)-3.)+30.*((WH2O/VBOM)-3.)-45
      1.*(TEMP(MM)-(8.0-TMP)))/(10.**6)
       EBENZC=EBENZ*F
       EIGN=(500.*V1*V1)/(4.184*10.**6)
       EACID=VBASE*BASEN*13.8
       DQ=WBENZ*EBENZC+EIGN+EACID+WFUSE*EFUSE
       EFU=WFUSE*EFUSE
C      CALCULATION OF MOLES OF PRODUCTS FROM BENZOIC ACID
       BEN=WBENZ/122.12
       O2NI=(PPO2*VBOM)/(0.082*(TEMP(IC)+290.))
       O2NF=O2NI-7.5*BEN
       CO2N=7.0*BEN
       H2ON=WH2O/18.016+3.*BEN
       PTN=(WCRUC+WWIRE)/195.09
       KONT=0
       DO 41 I=1,3
       IF(WAUX(I)) 41,41,42
    42 IF(EAUX(I)) 43,43,41
    43 KONT=I
       GO TO 46
    41 CONTINUE
C      CALCULATION OF MOLES OF PRODUCTS FROM THE AUXILIARY MATERIALS
    46 DO 30 I=1,3
       D(I)=A(I)+B(I)/4.-C(I)/2.
       AUXN(I)=WAUX(I)/(12.01*A(I)+1.008*B(I)+15.999*C(I))
       DQ=DQ+WAUX(I)*EAUX(I)
       CO2N=CO2N+AUXN(I)*A(I)
       O2NF=O2NF-AUXN(I)*D(I)
       H2ON=H2ON+AUXN(I)*B(I)/2.
    30 CONTINUE
       ETH=WAUX(1)*EAUX(1)
       IF(KONT) 71,72,71
    71 CSYS=4241.8
       CMEAS=CSYS+CH2 )*H2ON+CO2*O2NF+CCO2*CO2N+CPT*PTN
```

```
C       CALCULATION OF THE CORRECTED TEMPERTURE RISE
   72   DO 230 L=1,20
        JA=1
        IA=IC
        DO 120 I=1,2
        SLOPE=0.
        YINT=0.
        TAVE=0.
        CALL G05LSQ(TEMP,TIME,JA,IA,SLOPE,YINT,TAVE)
        QE(I,1)=1.
        QE(I,2)=TAVE
        QE(I,3)=SLOPE
        JA=ID
        IA=MM
  120   CONTINUE
        CALL G05SIM(QE,NO,MO)
        DELT=QE(1,1)*(TIME(ID)-TIME(IC))+QE(2,2)*G05ARA(TEMP,TIME,IC,ID)
        DELTC=TEMP(ID)-TEMP(IC)-DELT
        IF(KONT) 66,130,66
C       CALCULATION OF THE ENERGY EQUIVALENT OF THE CALORIMETER
  130   CMEAS=DQ/DELTC
   67   CSYS=CMEAS-CH2O*H2ON-CO2*O2NF-CCO2*CO2N-CPT*PTN
        PRINT 250,IRUN,CSYS,QE(1,1),QE(2,2),DELTC,DELT
  250   FORMAT (I4,5E13.7)
        GO TO 69
C       CALCULATION OF THE HEAT OF COMBUSTION OF AUXILIARY MATERIALS
   66   DQQ=CMEAS*DELTC
        EAUX(KONT)=(DQQ-DQ)/WAUX(KONT)
        PRINT 260,IRUN,EAUX(KONT),DELTC
  260   FORMAT (I3,F9.1,E16.8)
   69   ID=ID+2
  230   CONTINUE
        CPD=CSYS-CMEAS
        PRINT 262,EIGN,EACID,EFU,ETH,CPD
  262   FORMAT (/5E14.6/)
        GO TO 90
  101   FORMAT (E12.5,F9.5,F6.4,2I2,F5.3,F7.3,3F6.3,F4.1,F6.0)
  102   FORMAT (I3,I4,2I3,F8.5,F5.1,2F8.5,F5.2,2F5.0,F6.2,F8.3)
  209   FORMAT (5(F7.2,F7.1))
    3   CALL EXIT
        END



        SUBROUTINE G05CON(TEM,NN)
C       SUBPROGRAM FOR CONVERSION OF RESISTANCE TO TEEMPERATURE
        DIMENSION TEM(200)
        DO 22 I=1,NN
        XC=(ALOG(TEM(I))*10.)-77.8
        TEM(I)=1.6578123+2.5536824*XC+.0011885630*XC*XC
        TEM(I)=((10.**5)/(TEM(I)+335.))-290.
   22   CONTINUE
        RETURN
        END
```

```
      FUNCTION G05ARA(TE,TI,N,NM)
C     SUBPROGRAM FOR FINDING AREA UNDER CURVE USING LAGRANGIAN FORMULA
      DIMENSION TE(200),TI(200)
      MM=NM-2
      G05ARA=0.0
      DO 40 J=N,MM,2
      D=(TE(J)*(3.*TI(J+1)-2.*TI(J)-TI(J+2)))/((TI(J)-TI(J+1))*(TI(J)-TI
     1(J+2)))
      E=(TE(J+1)*(TI(J)-TI(J+2)))/((TI(J+1)-TI(J))*(TI(J+1)-TI(J+2)))
      F=(TE(J+2)*(2.*TI(J+2)+TI(J)-3.*TI(J+1)))/((TI(J+2)-TI(J))*(TI(J+2
     1)-TI(J+1)))
      TDT=(TI(J+2)-TI(J))*(TI(J+2)-TI(J))*(D+E+F)/6.
      G05ARA=G05ARA+TDT
   40 CONTINUE
      RETURN
      END


      FUNCTION G05TRP(TE,TI,N,NM)
      DIMENSION TE(200),TI(200)
      COMMON TE,TI
      MM=NM-1
      G05TRP=0.0
      DO 41 J=N,MM
      TDT=(TI(J+1)-TI(J))*TE(J)+0.5*(TI(J+1)-TI(J))*(TE(J+1)-TE(J))
      G05TRP=G05TRP+TDT
   41 CONTINUE
      RETURN
      END


      FUNCTION G05ACF(N,NM,NO,NP)
C     SUBPROGRAM TO FIND THE AREA UNDER A CURVE WHICH IS A POLYNOMIAL CURVE FIT.
C     OF 3 TO 5 EXPERIMENTAL POINTS.
C     NP IS THE ORDER OF THE POLYNOMIAL, AND IS LESS THAN OR EQUAL TO NO
C     NO+1 IS THE NUMBER OF POINTS CONSIDERED PER STEP
C     N AND NM ARE THE LIMITS OF THE EXPERIMENTAL DATA TO BE PROCESSED
      DIMENSION TE(200),TI(200),TEA(5),TIA(5),SOLN(5)
      COMMON TE,TI
      MO=NO+1
      MM=NM-NO
      MP=NP+1
      G05ACF=0.0
      DO 40 J=N,MM,NO
      DO 44 K=1,MO
      KK=J+K-1
      TIA(K)=TI(KK)
   44 TEA(K)=TE(KK)
      CALL G05CFP(TIA,TEA,SOLN,MO,NP)
      TOTAL=0.
      DO 46 L=1,MP
      FL=L
      TOTAL=TOTAL+SOLN(L)*(TIA(MO)**L-TIA(1)**L)/FL
   46 CONTINUE
      G05ACF=G05ACF+TOTAL
   40 CONTINUE
      RETURN
      END
```

```
      SUBROUTINE G05SIM(Q,NP,MP)
C     SUBROUTINE FOR SOLUTION OF SIMULTANEOUS LINEAR EQUATIONS
      DIMENSION TX(200),TY(200),Q(5,5)
      Q(2,2)=(Q(2,3)*Q(1,1)-Q(1,3)*Q(2,1))/(Q(2,2)*Q(1,1)-Q(1,2)*Q(2,1))
      Q(1,1)=(Q(1,3)-Q(1,2)*Q(2,2))/Q(1,1)
      RETURN
      END



      SUBROUTINE G05LSQ(YYY,XXX,IH,II,SLP,YNT,YAVE)
C     SUBROUTINE TO DO LEAST SQUARES ANALYSIS ON LINEAR RELATIONSHIP
      DIMENSION YYY(200),XXX(200)
      SUMX=0.
      SUMY=0.
      DO 8 IG=IH,II
      SUMY=SUMY+YYY(IG)
      SUMX=SUMX+XXX(IG)
    8 CONTINUE
      XII=II+1-IH
      YAVE=SUMY/XII
      SX=0.
      SY=0.
      SXY=0.
      SXSQ=0.
      DO 7 IE=IH,II
      SX=SX+XXX(IE)
      SY=SY+YYY(IE)
      SXY=SXY+XXX(IE)*YYY(IE)
      SXSQ=SXSQ+XXX(IE)*XXX(IE)
    7 CONTINUE
      XII=II+1-IH
      SLP=(SX*SY-XII*SXY)/(SX*SX-XII*SXSQ)
      YNT=(SX*SXY-SXSQ*SY)/(SX*SX-XII*SXSQ)
      RETURN
      END
```

REFERENCES

1. T. L. Cottrell. The Strengths of Chemical Bonds. 2nd Edition. Butterworths Scientific Publications, London. 1958.

2. M. Szwarc. Chemical Reviews, 47, 75 (1950).

3. M. G. Evans. Proc. Roy. Soc. A207, 1 (1951).

4. Selected values of chemical thermodynamic properties. Natl. Bur. Std. U. S. Tech. Notes, No. 270-3 (1968).

5. M. Szwarc. Proc. Roy. Soc. A207, 5 (1951).

6. A. F. Trotman-Dickenson. Ann. Rep. Chem. Soc. 55, 36 (1958).

7. C.T. Mortimer. Reaction Heats and Bond Strengths. Pergamon Press, London. 1962.

8. Frederick D. Rossini. In "Experimental Thermochemistry." Vol. I. Edited by Frederick D. Rossini. Interscience Publishers, New York. 1956.

9. A. F. Trotman-Dickenson. Gas Kinetics. Butterworths Scientific Publications, London. 1955.

10. S. J. Price. Private Communication.

11. S. J. Price. Can. J. Chem. 40, 1310 (1962).

12. Guy Waddington. In "Experimental Thermochemistry." Vol. II. Edited by H. A. Skinner. Interscience Publishers, New York. 1962.

13. W. D. Good and D. W. Scott. In "Experimental Thermochemistry." Vol. II. Edited by H. A. Skinner. Interscience Publishers, New York. 1962.

14. J. Coops, R. S. Jessup, and K. Van Nes. In "Experimental Thermochemistry." Vol. I. Edited by Frederick D. Rossini. Interscience Publishers, New York. 1956.

15. D. W. Scott, W. D. Good, and Guy Waddington. J. Phys. Chem. 60, 1090 (1956).

16. Technical Manual no. 130. Parr Instrument Co. (1960).

17. H. A. Skinner, J. M. Sturtevant, and Stig Sunner. In "Experimental Thermochemistry." Vol. II. Edited by H. A. Skinner. Interscience Publishers, New York. 1962.

18. F. Daniels et al. Experimental Physical Chemistry. 6th Edition. McGraw-Hill Book Co. Inc., New York. 1962.

19. P. A. Fowell and C. T. Mortimer. J. Chem. Soc. 3734 (1958).

20. C. T. Mortimer and P. W. Sellers. J. Chem. Soc. 1978 (1963).

21. I. S. Sokolnikoff and R. M. Redheffer. Mathematics of Physics and Modern Engineering. McGraw-Hill Book Company, Inc., New York. 1958.

22. Daniel D. McCracken and William S. Dorn. Numerical Methods and Fortran Programming. John Wiley and Sons, Inc., New York. 1964.

23. M. Szwarc. J. Chem. Phys. 17, 431 (1949).

24. G. L. Estaban, J. A. Kerr, and A. F. Trotman-Dickenson. J. Chem. Soc. 3873 (1963).

25. R. J. Kominar, M. G. Jacko, and S. J. Price. Can. J. Chem. 45, 575 (1967).

26. Alan S. Rodgers, David M. Golden, and Sidney W. Benson. J. Am. Chem. Soc. 89, 4578 (1967).

27. M. J. Krech. Ph.D. Thesis. University of Windsor. 1964.

28. L. M. Dennis, R. W. Work, E. G. Rochow, and E. M. Charmot. J. Am. Chem. Soc. 56, 1047 (1934).

29. F. E. Bartell and R. M. Suggitt. J. Phys. Chem. 58, 36 (1954).

30. W. D. Clark and S. J. W. Price. Can. J. Chem. 46, 1633 (1968).

31. L. H. Long and J. F. Sackman. Trans. Far. Soc. 54, 1797 (1958).

32. M. G. Jacko and S. J. W. Price. Can. J. Chem. 41, 1560 (1963).

33. M. G. Jacko and S. J. Price. Can. J. Chem. 42, 1198 (1964).

34. P. Fowell, J. R. Lacher, and J. D. Park. Trans. Faraday Soc. 61, 1324 (1965).

35. A. B. Littlewood. Gas Chromatography. Academic Press, New York. 1962.

36. P. A. F. White and S. E. Smith. Inert Atmospheres. Butterworths Scientific Publications, London. 1962.

37. R. H. Harrison. J. Sci. Inst. 29, 295 (1952).

38. William Goode. Thermodynamics Section, U. S. Bureau of Mines. Private Communication.

39. W. D. Good, D. W. Scott, J. L. Lacina and J. P. McCullough. J. Phys. Chem. 63, 1139 (1959).

40. H. Flaschka and H. Abdine. Chemist-Analyst. 45, 58 (1956).

41. H. A. Skinner. In "Advances in Organometallic Chemistry." Vol. 2. Edited by F. G. A. Stone and Robert West. Academic Press, N. Y. 1964.

42. P. W. Selle rs and C. T. Mortimer. J. Chem. Soc. 1965 (1964).

43. E. R. Lippincott and M. C. Tobin. J. Amer. Chem. Soc. 75, 4141 (1953).

44. G. Bosson, F. Gutmann, and L. M. Simmons. J. Appl. Phys. 21, 1267 (1950).

45. H. O. Pritchard and H. A. Skinner. J. Chem. Soc. 272 (1950).

46. W. D. Good, D. R. Donslin, D. W. Scott, Ann George, J. L. Lacina, J. P. Dawson, and Guy Waddington. J. Phys. Chem. 63, 1133 (1959).

47. Solubilities of Organic Compounds. Atherton Seidell Editor. Vol. II. 3rd Edition. Dan Van Nostrand Co. Inc., N. Y. 1941.

48. Encyclopedia of Chemical Reactions. Edited by C. A. Jacobsen. Vol. VII. Reinhold Publishing Corp., N. Y. 1958.

49. Handbook of Chemistry and Physics, 47th Edition (1966-1967). The Chem. Rubber Co., Cleveland, Ohio.

50. Treatise on Inorganic and Theoretical Chemistry. Edited by J. W. Mellor. Vol. V. Longmans, Green, and Co., London. 1956.

51. R. J. Kominar. Ph.D. Thesis. University of Windsor. 1968.

52. A. Shepp. J. Chem. Phys. 24, 939 (1956).

VITA AUCTORIS

Born:

August 11, 1941; Windsor, Ontario, Canada.
Son of Mr. William and Mrs. Irene Kennedy.

Primary Schools:

Wescott, Mayfair, and John Ross Schools, Windsor, Ontario, Canada.

Secondary School:

Patterson Collegiate Institute, Windsor, Ontario, Canada.
Academic Course: 1955 - 1960.

University:

University of Windsor, Windsor, Ontario, Canada.
1960 - 1964. Degree: Bachelor of Science in Honours Chemistry awarded in 1964.

University of Windsor, Windsor, Ontario, Canada.
1964 - 1968. Research and teaching assistant.

Awards:

1964: Board of Governors Medal.
1964: National Research Council of Canada Bursary.
1965 - 1968: National Research Council of Canada Studentship.

Publication:

Determination of the Heat of Formation of Trimethyl Indium and Calculation of the Mean In-CH_3 Bond Dissociation Energy, Canadian Journal of Chemistry, 46, 1633 (1968).

Professional Society:

Chemical Institute of Canada: Student Member.

Marital Status:

Married June 4, 1966, to Kathleen Joyce Thornton.
One child: Derek Andrew.